NEUROBEHAVIOURAL AND NEUROHISTOLOGICAL EFFECTS OF *Nigella sativa* AFTER NEUROTOXICANT TOLUENE ADMINISTRATION IN MICE

NUR LISA BINTI MOHD YUSOFF

FACULTY OF SCIENCE
UNIVERSITI MALAYA
KUALA LUMPUR

2022

NEUROBEHAVIOURAL AND NEUROHISTOLOGICAL EFFECTS OF Nigella sativa AFTER NEUROTOXICANT TOLUENE ADMINISTRATION IN MICE

NUR LISA BINTI MOHD YUSOFF

DISSERTATION SUBMITTED IN FULFILMENT OF THE REQUIREMENTS FOR THE DEGREE OF MASTER OF SCIENCE

INSTITUTE OF BIOLOGICAL SCIENCES
FACULTY OF SCIENCE
UNIVERSITI MALAYA
KUALA LUMPUR

2022

UNIVERSITI MALAYA ORIGINAL LITERARY WORK DECLARATION

Name of Candidate: NUR LISA BINTI MOHD YUSOFF

Matric No: 17058840/3

Name of Degree: MASTERS OF SCIENCE

Title of Dissertation ("this Work"):

NEUROBEHAVIOURAL AND NEUROHISTOLOGICAL EFFECTS OF

Nigella sativa AFTER NEUROTOXICANT TOLUENE ADMINISTRATION IN

MICE Field of Study: NEUROSCIENCE

I do solemnly and sincerely declare that:

- (1) I am the sole author/writer of this Work;
- (2) This Work is original;
- (3) Any use of any work in which copyright exists was done by way of fair dealing and for permitted purposes and any excerpt or extract from, or reference to or reproduction of any copyright work has been disclosed expressly and sufficiently and the title of the Work and its authorship have been acknowledged in this Work;
- (4) I do not have any actual knowledge nor do I ought reasonably to know that the making of this work constitutes an infringement of any copyright work;
- (5) I hereby assign all and every rights in the copyright to this Work to the University of Malaya ("UM"), who henceforth shall be owner of the copyright in this Work and that any reproduction or use in any form or by any means whatsoever is prohibited without the written consent of UM having been first had and obtained;
- (6) I am fully aware that if in the course of making this Work I have infringed any copyright whether intentionally or otherwise, I may be subject to legal action or any other action as may be determined by UM.

Candidate's Signature	Date: 6/2/2022
Subscribed and solemnly declared before,	
Witness's Signature	Date: 6/2/2022
Name:	
Designation:	

NEUROBEHAVIOURAL AND NEUROHISTOLOGICAL EFFECTS OF Nigella sativa AFTER NEUROTOXICANT TOLUENE ADMINISTRATION IN MICE

ABSTRACT

Humans are readily exposed to the environmental pollutant toluene, commonly in small amount, e.g., from daily household products, petroleum, and occupational settings. Reports showed that toluene toxicity is detrimental to human physiological systems, especially the central nervous system (CNS). Hence, the intensive search for substances that can offer neuroprotection, ideally, sourced from the natural product, considering it to be less costly and possibly with less side effects. One such candidate is the Nigella sativa (NS), a traditionally consumed natural supplement, also known to have antioxidant properties and the potentials for neuroprotective effects. The current study aimed to investigate NS protective potentials from neurobehavioural aspect through recognition memory and neurohistological aspect of hippocampal region of mice exposed to toluene. The study consisted of three main experiments: Experiment 1 (preliminary toluene toxicity test), Experiment 2 (preliminary Novel Object Recognition (NOR) behavioural test), and Experiment 3 (NS neuroprotective test). Experiment 1 and 2 were conducted to determine the toluene dosage capable of causing the highest abnormalities in the brain of the experimental animals as well as its consequent effects on learning and behaviour. From the two preliminary tests, 500 mg/kg toluene caused the most recognition memory impairment in NOR and demonstrated smaller hippocampal neuron size in mice brain. Adult male ICR mice (8 weeks old) were used in this study. For all three tests, corn oil was used as the control. In the NS neuroprotective test, treatments were conducted for 14 consecutive days. Mice were orally supplemented from day 1 and continued until day 14 with three different forms of NS: NS seeds (NSS), NS oil (NSO), and its selected bioactive NS constituent,

thymoquinone (TQ). Toluene was intraperitoneally injected (i.p.) in mice starting from day 7 until day 14. Following the treatments, NOR test was conducted, and mice were intracardially perfused. Brain was collected, histologically processed and Nissl stained with Cresyl Violet dye. Brain gross morphology was measured, and then somatic size and shape of hippocampal CA1 pyramidal neurons were quantified according to specific morphometric parameters. Results from the current study showed that toluene had the tendency to reduce recognition memory performance of mice and somatic size of hippocampal CA1 pyramidal neurons. Contradictorily, the other treatments, especially involving TQ, NSO, and NSS improved the mice recognition memory and somatic size of hippocampal CA1 pyramidal neurons. Meanwhile, brain morphology and somatic shape of hippocampal CA1 pyramidal neurons showed no significant differences between all NS treatment groups. The key findings from the current study concluded that 500 mg/kg toluene could cause impairment, while NS induced improvement of mice neurobehavioural performance and neurohistological brain and neuronal structure, though not significantly.

Keywords: Toluene, *Nigella sativa*, recognition memory, brain morphology, somatic morphometry

KESAN Nigella sativa TERHADAP TINGKAH LAKU SARAF DAN HISTOLOGI SARAF SELEPAS PEMBERIAN AGEN NEUROTOKSIK TOLUENA KEPADA MENCIT

ABSTRAK

Manusia mudah terdedah kepada toluena pencemar alam sekitar, lazimnya dalam jumlah kecil, contohnya dari produk harian isi rumah, petroleum, dan persekitaran pekerjaan. Kajian melaporkan ketoksikan toluena adalah merbahaya kepada sistem fisiologi manusia, terutamanya sistem saraf pusat. Justeru, pencarian intensif bahan-bahan yang boleh menawarkan perlindungan kepada sistem saraf, yang idealnya berasal daripada produk semulajadi, memandangkan ia kurang mahal dan berkemungkinan mempunyai kurang kesan sampingan. Salah satu calon ialah Nigella sativa (NS), satu suplemen semula jadi yang digunakan secara tradisional, juga diketahui mempunyai ciri antioksida serta berpotensi melindungi sistem saraf. Kajian semasa ini bertujuan untuk mengkaji potensi perlindungan NS dari aspek tingkah laku saraf melalui ingatan pengecaman dan histologi saraf kawasan hipokampus dalam mencit yang terdedah kepada toluena. Kajian ini terdiri daripada tiga eksperimen utama: Eksperimen 1 (ujian rintis ketoksikan toluene), Eksperimen 2 (ujian rintis tingkah laku Pengecaman Objek Novel (Novel Object Recognition, NOR)), dan Eksperimen 3 (ujian perlindungan saraf NS). Eksperimen 1 dan 2 dijalankan untuk menentukan dos toluena yang mampu mengakibatan keabnormalan tertinggi pada otak haiwan kajian serta mempunyai kesan selanjutnya terhadap pembelajaran dan tingkah laku. Daripada kedua-dua ujian rintis tersebut, 500 mg/kg toluena mengakibatkan penjejasan paling teruk ingatan pengecaman NOR dan mempamerkan saiz neuron hipokampus yang lebih kecil dalam otak mencit. Mencit ICR jantan dewasa (umur 8 minggu) digunakan dalam kajian ini. Untuk ketiga-tiga ujian, minyak jagung digunakan sebagai kawalan. Untuk ujian perlindungan saraf NS, rawatan dijalankan selama 14 hari berturut-turut. Mencit diberikan suplemen oral dari hari 1 dan diteruskan sehingga hari 14 dengan tiga jenis NS yang berbeza: Biji NS (NS seeds, NSS), minyak NS (NS oil, NSO), dan thymoquinone (TQ) iaitu konstituen bioaktif terpilih NS. Toluena disuntik secara intraperitoneal (i.p.) kepada mencit bermula hari 7 sehingga hari 14. Berikutan rawatan, ujian NOR dijalankan dan perfusi intrakardiak dilakukan ke atas mencit. Otak dikumpulkan, diproses secara histologi dan diwarnai dengan kaedah pewarnaan Nissl menggunakan pewarna Cresyl Violet. Morfologi umum otak diukur, dan kemudian saiz dan bentuk soma CA1 neuron piramid hipokampus dikuantifikasi mengikut parameter morfometrik yang spesifik. Keputusan daripada kajian semasa ini menunjukkan bahawa toluena mempunyai kecenderungan mengurangkan prestasi ingatan pengecaman mencit dan saiz soma CA1 neuron piramid hipokampus. Sebaliknya, rawatan-rawatan yang lain, terutamanya melibatkan TQ, NSO, dan NSS menambahbaik ingatan pengecaman mencit dan saiz soma neuron piramid hipokampus CA1. Sementara itu, morfologi otak dan bentuk soma neuron piramid hipokampus CA1 tidak menunjukkan perbezaan signifikan antara semua kumpulan rawatan NS. Dapatan utama daripada kajian semasa ini merumuskan bahawa 500 mg/kg toluene merosakkan, dan NS menambahbaikkan, meskipun tidak secara signifikan, prestasi tingkah laku saraf dan histologi saraf otak dan struktur neuron.

Kata kunci: Toluena, Nigella sativa, ingatan pengecaman, morfologi otak, morfometri soma

ACKNOWLEDGEMENTS

First and foremost, I would like to express my sincerest gratitude to my supervisors, Dr. Sheena Yin Xin Tiong and Assoc. Prof. Dr. Durriyyah Sharifah Hasan Adli, who has supported me throughout my entire graduate study. This dissertation would not have been possible without their great mentorship and training. Their knowledge, diligence, persistence, patience, and encouragement have been with me during the whole dissertation.

My deepest appreciation goes to my dearest husband, Izzat Iskandar, for his persistent support, encouragement, and unwavering love. His support, both physically and emotionally, along with his help in taking care of our little beloved son enabled me to gracefully hold the role of both a wife and a student. And to our little munchkin, Ammar Iskandar, for becoming his mama's greatest motivation in completing this dissertation.

To my parents Mohd Yusoff and Siti Katijah, I cannot thank them enough for raising me up and educating me with their endless caring love. And to my siblings, Iliyana, Shaira, Izz, Hannah, Haikal, for encouraging and supporting me to pursue my studies. My heartful thanks also goes to my family in-law for always offering help whenever needed, and for caring and accepting me as their own.

I would also like to thank my NeuroRG lab members and lab staffs who had helped and motivated me during my graduate study. I would like to acknowledge our funding sources from the Fundamental Research Grant Scheme (FRGS) FP039-2015A and FP120-2020. Finally, I am eternally grateful for the love, guidance and mostly the prayers from family and friends throughout this small journey of mine, particularly during those challenging moments. Without the support I have received, this dissertation would never have been accomplished.

TABLE OF CONTENTS

ORI	GINAL LITERARY WORK DECLARATION	ii
ABS	STRACT	iii
ABS	TRAK	v
ACF	KNOWLEDGEMENTS	vii
TAB	BLE OF CONTENTS	viii
LIST	Γ OF FIGURES	xiii
LIST	Γ OF TABLES	xvii
LIST	Γ OF SYMBOLS AND ABBREVIATIONS	xix
LIST	Γ OF APPENDICES	XXV
CHA	APTER 1: INTRODUCTION	1
1.1	Background of study	1
1.2	Central nervous system (CNS) and the brain	2
1.3	Medial temporal lobe and memory	4
1.4	Hippocampus	6
	1.4.1 Hippocampal CA1 pyramidal neurons	8
1.5	Recognition memory	9
	1.5.1 Behavioural Novel Object Recognition (NOR) test	10
1.6	Toluene	14
	1.6.1 Toxicokinetics of toluene	15
1.7	Approach against toluene-induced negative effects	18
	1.7.1 Nigella sativa	19
1.8	Rationale of the study	21

1.9	Research questions				
1.10	Objectiv	ves of study	23		
СНА	PTER 2	: LITERATURE REVIEW	24		
2.1	Object 1	recognition memory and hippocampus	24		
	2.1.1	Variation of behavioural Novel Object Recognition (NOR) test	25		
2.2	Effects	of toluene on the nervous system	27		
	2.2.1	Potential mechanisms of toluene toxicity on the CNS	31		
2.3	Effects	of NS on memory and the nervous system	33		
2.4	Effects	of TQ on memory and the nervous system	38		
	2.4.1	In vivo studies on the effects of TQ on nervous system	38		
	2.4.2	<i>In vitro</i> studies on the effects of TQ on nervous system	41		
СНА	PTER 3	: MATERIALS AND METHOD	48		
3.1	Experin	nental design	48		
	3.1.1	Preliminary test 1: Toluene toxicity test	49		
	3.1.2	Preliminary test 2: Novel Object Recognition test	49		
	3.1.3	Test 3: Nigella sativa (NS) neuroprotective test	50		
3.2	Animal	care and maintenance	51		
3.3	Body w	eight monitoring	52		
3.4	Treatme	ent administration	53		
	3.4.1	Oral gavage/ Force feeding	53		
	3.4.2	Intraperitoneal injection	53		
3.5	Treatme	ent solution preparation	54		

	3.5.1	Corn oil	55
	3.5.2	Toluene	55
	3.5.3	Nigella sativa seeds (NSS)	55
	3.5.4	Nigella sativa oil (NSO)	55
	3.5.5	Thymoquinone (TQ)	55
3.6	Novel C	Object Recognition (NOR) test	57
	3.6.1	Task protocol	57
	3.6.2	Apparatus	60
	3.6.3	Structural objects	62
	3.6.4	Behavioural analysis	63
3.7	Histolog	gical processing of brain and other vital organs	66
	3.7.1	Intracardiac perfusion	68
	3.7.2	Dissection and sample abstraction	69
	3.7.3	Measurement of brain gross morphology	70
	3.7.4	Dehydration	70
	3.7.5	Clearing	70
	3.7.6	Paraffin infiltration	71
	3.7.7	Embedding	72
	3.7.8	Sectioning	74
	3.7.9	Mounting of sections onto microscope slides	74
	3.7.10	Staining	75
	3.7.11	Mounting of coverslip onto tissue sections	76
3.8	Morpho	metric analysis of neuronal soma	78
	3.8.1	Image acquisition	78

	3.8.2	Image processing	80
3.9	Statistic	cal analysis	80
CHA	APTER 4	4: RESULTS	81
4.1	Prelimi	nary test 1: Toluene toxicity test	81
	4.1.1	Brain hippocampal histopathology	81
	4.1.2	Liver histopathology	84
	4.1.3	Kidney histopathology	87
	4.1.4	Heart histopathology	90
4.2	Prelimi	nary test 2: Novel object recognition (NOR) test	93
	4.2.1	Memory performance in NOR test	93
	4.2.2	Brain CA1 hippocampal histopathology	97
4.3	Nigella	sativa (NS) neuroprotective test	100
	4.3.1	Novel object recognition (NOR) test	100
	4.3.2	Gross morphology measurements of brain	104
	4.3.3	Morphometric analysis of hippocampal CA1 pyramidal neurons	107
CHA	APTER 5	5 : DISCUSSION	115
5.1	Effects	of TOL, NSS, NSO and TQ treatments on memory	115
	5.1.1	Effects of TOL treatment	115
	5.1.2	Effects of NS supplementations	118
5.2	Effects	of TOL, NSS, NSO and TQ treatments on brain morphology	122
	5.2.1	Effects of TOL treatment	122
	5.2.2	Effects of NS supplementations	124

	ERENC	TES	1
CHA	APTER (5 : CONCLUSION	1
	5.5.5	Morphometric analysis	1
	5.5.4	Histology	1
	5.5.3	Novel object recognition (NOR) behavioural test	-
	5.5.2	Toluene administration in animals	-
	5.5.1	NS supplementations	
5.5	Limitat	ions and suggestions for future studies	-
5.4	Potenti	al mechanisms of Nigella sativa effects on the CNS	
	5.3.2	Effects of NS supplementations	
	5.3.1	Effects of TOL treatment	
5.3		of TOL, NSS, NSO and TQ treatments on morphometric properties of gramidal neurons	

LIST OF FIGURES

Figure 1.1	:	Different lobes of the brain. Taken from Raslau et al. (2014)	3
Figure 1.2	:	Anatomy of the medial temporal lobe structures. Taken from Raslau et al. (2015)	5
Figure 1.3	:	Coronal section of mouse brain with hippocampus structure. (a) Drawing with labelled brain areas, (b) Nissl-stained brain areas. Both images taken from Paxinos and Franklin (2001)	7
Figure 1.4	:	Schematic diagram of a transverse slice through the hippocampus of mouse showing the DG fields, CA3, and CA1. Taken from Vago et al. (2014)	7
Figure 1.5	:	Schematic illustrations of various object recognition memory tests. Adapted from Kinnavane et al. (2015)	13
Figure 1.6	:	Chemical structure of toluene	14
Figure 1.7	:	Proposed pathways of toluene metabolism. Taken from Wang (2017)	17
Figure 1.8	:	Chemical structures of thymoquinone (2-isopropyl-5-methyl-1,4 benzoquinone). Taken from Al-Majed et al. (2006)	19
Figure 3.1	:	General overview of research methodology	48
Figure 3.2	:	Animals in labeled cages	52
Figure 3.3	:	Animals were weighed daily before treatment administration	52
Figure 3.4	:	Oral administration using a feeding needle	53
Figure 3.5	:	Intraperitoneal administration	54
Figure 3.6	:	Nigella sativa (NS) supplementations	56
Figure 3.7	:	Novel Object Recognition (NOR) test	59
Figure 3.8	:	Schematic diagram of the apparatus	60
Figure 3.9	:	Video camera set up for recording during the Phase 3 (test phase) of NOR test. (a) Front view (b) Top view	61

Figure 3.10	:	Structural objects made up of blocks that were used in the Novel Object Recognition (NOR) test. (a) Front view of structural objects (b) Top view of structural objects	(2
Figure 3.11	:	Examples of results generated by the OptiMouse semiautomatic analysis behavioural tracking software. (a) Distance travelled by mouse during test phase. (b) Positions of mouse nose in the arena during test phase.	62
Figure 3.12	:	Examples of results generated as histograms from data by OptiMouse semiautomatic analysis. a) Nose zone preference during test phase. (b) Number of visits of mouse nose in each zone during test phase.	65
Figure 3.13	:	Setup of apparatus for intracardiac perfusion	68
Figure 3.14	:	Brain and other vital organs kept in 10% formalin solution	69
Figure 3.15	:	Gross morphology measurements of whole brain structure	69
Figure 3.16	:	Embedded tissues in solidified paraffin.	71
Figure 3.17	:	Tissue sectioning using a rotary microtome	73
Figure 3.18	:	Hematoxylin and eosin (H&E) staining solution step	75
Figure 3.19	:	Nissl staining solution step	76
Figure 3.20	:	Overview of steps and solutions in histological processing	77
Figure 3.21	:	Image acquisition of hippocampal CA1 region of brain tissue sample	79
Figure 4.1	:	Photomicrographs of hippocampus sections stained with H&E at 100× magnification for (a) control, (b) 100 mg/kg toluene, (c) 300 mg/kg toluene, and (d) 500 mg/kg toluene experimental groups, respectively	82
Figure 4.2	:	Photomicrographs of hippocampus sections stained with H&E at 400× magnification for (a) control, (b) 100 mg/kg toluene, (c) 300 mg/kg toluene, and (d) 500 mg/kg toluene experimental groups, respectively	83
Figure 4.3	:	Photomicrographs of liver sections stained with H&E at 100× magnification for (a) control, (b) 100 mg/kg toluene, (c) 300 mg/kg toluene, and (d) 500 mg/kg toluene experimental groups	85

Figure 4.4	:	Photomicrographs of liver sections stained with H&E at 400× magnification for (a) control, (b) 100 mg/kg toluene, (c) 300 mg/kg toluene, and (d) 500 mg/kg toluene experimental groups	86
Figure 4.5	:	Photomicrographs of kidney sections stained with H&E at $100 \times$ magnification for (a) control, (b) 100 mg/kg toluene, (c) 300 mg/kg toluene, and (d) 500 mg/kg toluene experimental groups	88
Figure 4.6	:	Photomicrographs of kidney sections stained with H&E at $400\times$ magnification for (a) control, (b) 100 mg/kg toluene, (c) 300 mg/kg toluene, and (d) 500 mg/kg toluene experimental groups	89
Figure 4.7	:	Photomicrographs of heart sections stained with H&E at $100\times$ magnification for (a) control, (b) 100 mg/kg toluene, (c) 300 mg/kg toluene, and (d) 500 mg/kg toluene experimental groups	91
Figure 4.8	:	Photomicrographs of heart sections stained with H&E at $400\times$ magnification for (a) control, (b) 100 mg/kg toluene, (c) 300 mg/kg toluene, and (d) 500 mg/kg toluene experimental groups	92
Figure 4.9	:	Percentage of novel and familiar object preference during test session.	94
Figure 4.10	:	Discrimination index (DI) during test session	94
Figure 4.11	:	Percentage of novel and familiar object preference during test session.	95
Figure 4.12	:	Discrimination index (DI) during test session	96
Figure 4.13	:	Photomicrographs of hippocampal CA1 pyramidal neurons stained with H&E at 200× magnification for (a) control (CO), (b) 100 mg/kg toluene, (c) 300 mg/kg toluene, and (d) 500 mg/kg toluene experimental groups.	98
Figure 4.14	:	Photomicrographs of hippocampal CA1 pyramidal neurons stained with H&E at 200× magnification for (a) control (CO), (b) NSS, (c) NSO, and (d) TQ experimental groups	99
Figure 4.15	:	Percentage of novel and familiar object preference during test session.	101
Figure 4.16	:	Discrimination index (DI) during test session	102
Figure 4.17	:	Nose position track of mouse from each group during test session. F- familiar structural object, N- novel structural object	103
Figure 4.18	:	Mean weight of mouse brain.	104

Figure 4.19	:	Mean length and width of mouse brain	105
Figure 4.20	:	Mouse brain showing different gross anatomical parts (1) olfactory bulb, (2) telencephalon, (3) cerebellum, and (4) medulla oblongata. (a) Lateral view of mouse brain. (b) Dorsal view of mouse brain. (c) Schematic diagram of mouse brain showing measurements parameters.	106
Figure 4.21	:	Photomicrograph of hippocampus of right brain hemisphere analysed in this study. ($40 \times$ magnification, $500 \mu m$ calibration)	107
Figure 4.22	:	Photomicrograph of hippocampal CA1 pyramidal cell layer analysed in this study. (200× magnification, 100 μ m calibration)	108
Figure 4.23	:	Mean somatic area of CA1 pyramidal neurons	110
Figure 4.24	:	Mean somatic perimeter of CA1 pyramidal neurons	111
Figure 4.25	:	Mean somatic circularity of CA1 pyramidal neurons	112
Figure 4.26	:	Mean somatic aspect ratio of CA1 pyramidal neurons	113
Figure 4.27	:	Mean somatic roundness of CA1 pyramidal neurons	114
Figure 5.1	:	Hydrolysis of acetylcholine (ACh) to choline and acetate via acetylcholinesterase (AChE) activity. Adapted from Taqui et al. (2022)	121
Figure 5.2	:	TQ redox cycle for antioxidant or pro-oxidant potential. Taken from Younus (2018)	131
Figure 5.3	:	Glymphatic system and blood-brain barrier. Taken from Presta et al. (2018)	133

LIST OF TABLES

Table 2.1	:	Studies on the protective effects of NS against neurotoxicity	36
Table 2.2	:	In vivo studies on the protective effects of TQ against neurotoxicity	44
Table 2.3	:	In vitro studies on the protective effects of TQ against neurotoxicity	46
Table 3.1	:	Grouping, type of treatments and dosage	49
Table 3.2	:	Grouping, type of treatment, dosage, and route of administration	50
Table 3.3	:	Grouping and type of treatment.	51
Table 4.1	:	Mean squares from ANOVA for novel object preference of mice treated with CO and TOL treatment groups	93
Table 4.2	:	Mean squares from ANOVA for discrimination index of mice treated with CO and TOL treatment groups	93
Table 4.3	:	Mean squares from ANOVA for novel object preference of mice treated with CO, NSS, NSO and TQ treatment groups	95
Table 4.4	:	Mean squares from ANOVA for discrimination index of mice treated with CO, NSS, NSO and TQ treatment groups	96
Table 4.5	:	Mean squares from ANOVA for novel object preference of mice treated with CO, TOL and NS treatment groups	101
Table 4.6	:	Mean squares from ANOVA for familiar object preference of mice treated with CO, TOL and NS treatment groups	101
Table 4.7	:	Mean squares from ANOVA for weight of mice brain treated with CO, TOL and NS treatment groups	104
Table 4.8	:	Mean squares from ANOVA for length of mice brain treated with CO, TOL and NS treatment groups	105
Table 4.9	:	Mean squares from ANOVA for width of mice brain treated with CO, TOL and NS treatment groups	105
Table 4.10	:	Mean squares from ANOVA for somatic area of CA1 pyramidal neurons of mice treated with CO, TOL and NS treatment groups	109
Table 4.11	:	Mean squares from ANOVA for somatic perimeter of CA1 pyramidal neurons of mice treated with CO, TOL and NS treatment groups	111

Table 4.12	:	Mean squares from ANOVA for somatic circularity of CA1 pyramidal neurons of mice treated with CO, TOL and NS treatment groups	112
Table 4.13	:	Mean squares from ANOVA for somatic aspect ratio of CA1 pyramidal neurons of mice treated with CO, TOL and NS treatment groups.	113
Table 4.14	:	Mean squares from ANOVA for somatic roundness of CA1 pyramidal neurons of mice treated with CO, TOL and NS treatment groups	114

LIST OF SYMBOLS AND ABBREVIATIONS

 αSN : α -synuclein

 μM : micrometer

AlCl₃ : aluminium chloride

Ca²⁺ : calcium

cm : centimeter

H₂O₂ : hydrogen peroxide

mg/kg : milligram per kilogram

nM : nanometer

Na+-K+-ATPase : sodium potassium atpase

 O_2^- : superoxide anion

OH : hydroxyl radicals

2D : two-dimensional

5-HT : serotonin

6-OHDA : 6-hydroxy dopamine

 $A\beta$: amyloid beta

Aβ1-42 : amyloid beta-protein 1-42

ACGIH : American Conference of Governmental Industrial Hygienist

Ach : acetylcholine

AChE : acetylcholinesterase

ACR : acrylamide

AD : Alzheimer's disease

ADME : absorption, distribution, metabolism, and excretion

ANMAF : neuronal morphology analysis framework

APP : amyloid precursor protein

AQP4 : astrocyte aquaporin 4

As : arsenic

ATSDR : Agency for Toxic Substances and Disease Registry

BAX : BCL2-associated x protein

BBB : Blood-brain barrier

BCL2 : B-cell lymphoma 2

BDNF : brain-derived neurotrophic factor

BTEX : benzene, toluene, ethylbenzene, and xylene

CA : cornu ammonis

CAT : catalase

CCL5 : chemokine ligand 5

CNN : convolutional neural networks

CNS : central nervous system

CREB : cAmp-Response Element-Binding Protein

CO : corn oil

COMT : catechol-O-methyltransferase

CPu : caudate putamen

CSF : cerebrospinal fluid

CTE : chronic toxic encephalopathy

D-gal : D-galactose

DA : dopamine

DCX : doublecortin

DG : dentate gyrus

DNA : deoxyribonucleic acid

DNMS : delayed nonmatching-to-sample

DS : difference score

DWH : deepwater horizon

EAE : experimental autoimmune encephalomyelitis

EF1 : elongation factor 1

EU : European Union

GAPDH : glyceraldehyde 3-phosphate dehydrogenase

GFAP : glial fibrillary acidic protein

GPx : glutathione peroxidase

GR : glutathione reductase

GSH : glutathione

GSH-Px : glutathione peroxidase

GST : glutathione-s-transferase

hiPSC : human induced pluripotent stem cells

IC : insular cortex

ICR : Institute of Cancer Research

IL : interleukin

iNOS : inducible nitric oxide synthase

IS : interstitial solute

ISF : interstitial fluid

I/R : ischemia-reperfusion

LDH : lactate dehydrogenase

LPS/IFNy : lipopolysaccharide interferon gamma

MAO : monoamine oxidase

MCAO : middle cerebral artery occlusion

MDA : malondialdehyde

mPFC : medial prefrontal cortex

MEP : motor evoked potential

MeCP2 : methyl-CPG-binding protein 2

mRNA : messenger ribonucleic acid

MWM : Morris Water Maze

NADH : reduced nicotinamide adenine dinucleotide

NADPH : nicotinamide adenine dinucleotide phosphate

NE : norepinephrine

NGF : nerve growth factor

NINDS : National Institute of Neurological Disorders and Stroke

NMDA : n-methyl-d-aspartate

NO : nitric oxide

NOR : novel object recognition

NOS : nitric oxide synthase

NQO1 : NADPH quinone oxidoreductase-1

NRG4 : neuregulin-4

NS : Nigella sativa

NSO : Nigella sativa oil

NSS : Nigella sativa seed

PARP1 : poly (ADP-ribose) polymerase 1

PAT : passive avoidance task

PD : Parkinson's disease

PKB : protein kinase b

PNI : peripheral nerve injury

PNS : peripheral nervous system

ppm : parts per million

PRDX : peroxiredoxin

PRh : perirhinal cortex

PTGS : prostaglandin-endoperoxide synthase

PTZ : pentylenetetrazole

PVS : perivenous space

RAM : radial arm maze

ROS : reactive oxygen species

SAI : short-latency afferent inhibition

SC : Schwann cells

SCOEL : Scientific Committee on Occupational Exposure Limit

SOD : superoxide dismutase

SXRN : sulfiredoxin

TAC : total antioxidant capacity

TBARS : thiobarbituric acid reactive substance

TBI : traumatic brain injury

tDCS : transcranial direct current stimulation

TNF α : tumor necrosis factor alpha

TXNIP : thioredoxin-interacting protein

UBIQ-RD : NADH ubiquinone reductase

UDP : uridine diphosphate

US EPA : United States Environmental Protection Agency

VOC : volatile organic compound

WHO : World Health Organization

LIST OF APPENDICES

Appendix A	: Animal ethics approval	165
Appendix B	: Preparation of treatment solution: Toluene	166
Appendix C	: Preparation of treatment solution: Nigella sativa seeds (NSS)	166
Appendix D	: Preparation of treatment solution: Nigella sativa oil (NSO)	
Appendix E	: Preparation of treatment solution: Thymoguinone (TO)	167

CHAPTER 1: INTRODUCTION

1.1 Background of study

Air pollution exposure has been proven to cause negative impacts on human health. According to the World Health Organization (WHO), exposure to air pollution causes an estimated 7 million deaths worldwide annually (World Health Organization, 2021). Approximately 4.2 million premature deaths worldwide per year in 2016 were reported due to outdoor air pollution, while 3.8 million premature deaths a year were reported due to indoor air pollution (World Health Organization, 2018). Besides respiratory and cardiovascular diseases (Brucker et al., 2020), recent studies indicated that the central nervous system (CNS) has also become a significant target of air pollution (Costa et al., 2020, 2019). In recent years, mounting evidence from epidemiological studies demonstrated the correlation between air pollution and neurodevelopmental and neurodegenerative diseases.

Exposure to volatile pollutants in the air poses threat to the well-being of the community especially in inevitable occupational settings and daily exposure to various household products. Indoor air pollution particularly has become a growing public concern since the concentration of volatile organic compounds (VOCs) were reported to be higher indoors than outdoors. In addition, people especially in the developed countries spend up to 90% of their time indoors (Sarkhosh et al., 2012). The United States Environmental Protection Agency (US EPA) classified air pollutants into primary or secondary pollutants, and VOCs such as benzene, toluene, ethylbenzene, and xylene, all four collectively referred to as BTEX, were included as primary pollutants (Baghani et al., 2019).

A study on ambient BTEX levels over urban, suburban and rural areas in Malaysia showed that toluene was the most abundant organic air pollutant (Hamid et al., 2019). Another study conducted in Serdang, Selangor also manifested that toluene concentration was the highest in the selected indoor and outdoor sites (Abd Hamid et al., 2017). Toluene was detected in consumer products such as shoe polish, leather cleaners, lead in mechanical pencils, whiteout, glues, highlighters (Ehsanifar et al., 2019; Moro et al., 2012), in newly renovated houses (Du et al., 2014), and petrol service stations (Edokpolo et al., 2014).

Exposure to toluene is known to have harmful effects on the CNS and peripheral nervous system (PNS), even at low concentrations (Hopf et al., 2012; Latif et al., 2019). Interference with cognitive performance and working memory (Yavari et al., 2018), difficulty to concentrate and becoming easily irritable (Tualeka et al., 2019), nausea, and peripheral neuropathy (Thetkathuek et al., 2015) were reported among workers exposed to toluene. Cellular and animal studies suggested that toluene modulates neurotransmitter ion-activated channels and causes alteration of gene transcriptions in pathways associated with synaptic plasticity of the nervous system (Yavari et al., 2018).

1.2 Central nervous system (CNS) and the brain

The CNS comprises the brain and the spinal cord. The brain is contained within the cranial cavity of the skull, and the spinal cord is the extension of nervous tissue contained within the vertebral cavity of the vertebral column (Jacobson & Marcus, 2008). The brain is a complex organ that controls body activities. It receives information from the external stimuli through sensory nerves, integrates and processes the information, and sends signals to the body via motor nerves (Taylor et al., 2019).

The brain is surrounded and protected by cerebrospinal fluid and three (3) layers of meninges namely the dura mater, arachnoid mater, and pia mater. The human brain is divided into three (3) principal morphological divisions: cerebrum, cerebellum, and brainstem (Figure 1.1). The cerebrum is the largest portion of the brain and controls most of the brain's activities. It is divided into two hemispheres, which each consists of an outer layer grey matter called the cerebral cortex and the inner layer white matter (Taylor et al., 2019). The cerebrum is further divided into four (4) lobes of different specific functions: frontal, parietal, temporal, and occipital lobes (Figure 1.1) (Ludwig & Varacallo, 2018; Raslau et al., 2014).

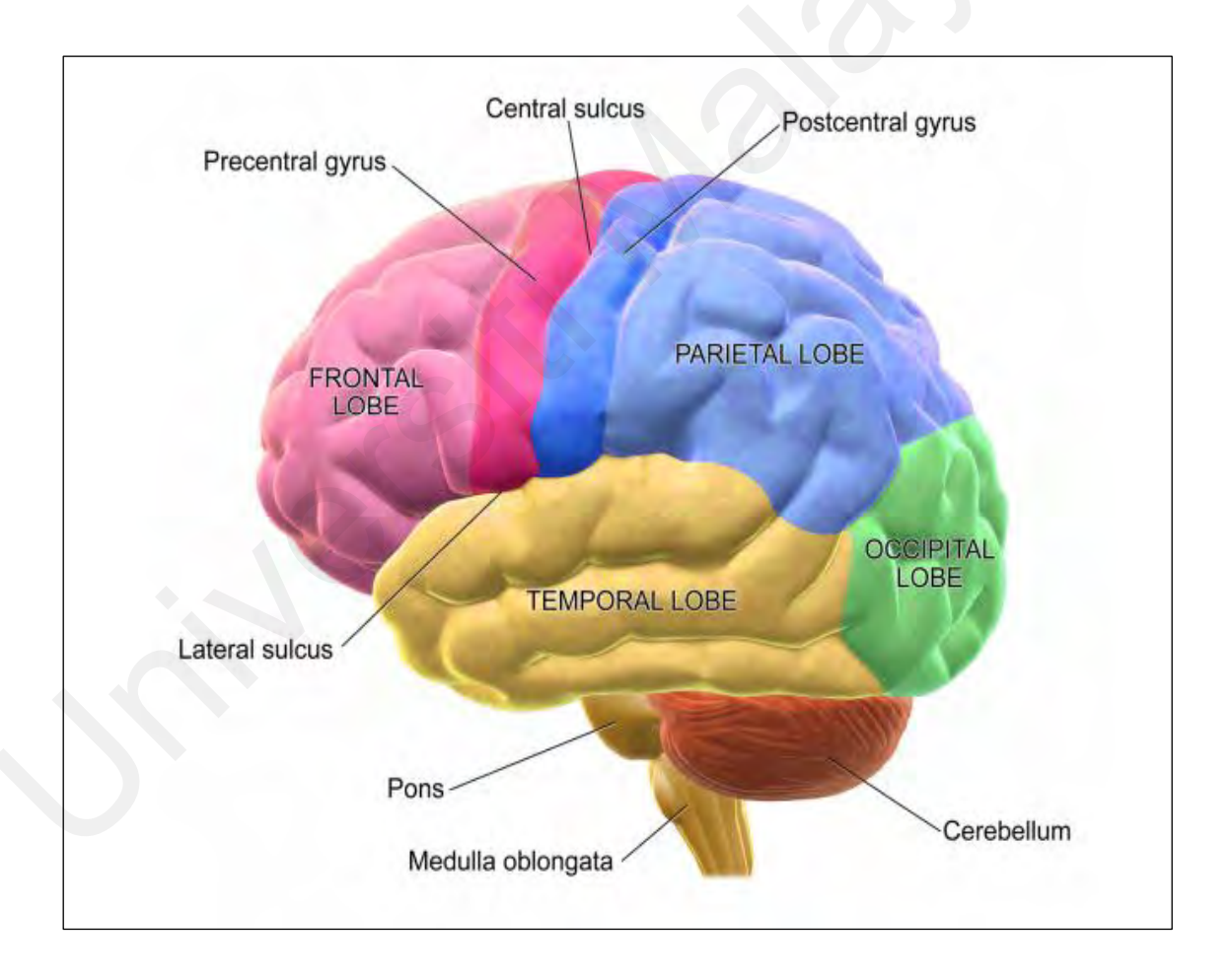


Figure 1.1: Different lobes of the brain. Taken from Raslau et al. (2014).

The frontal lobe, the largest lobe of the brain, is the most rostral part of the hemispheres. It is associated with prospective memory which involves planning and executive functions, motor performance, personality and social behaviour, speech, and language. The parietal lobe lies posterior to the frontal lobe and superior (towards dorsal) to the temporal lobe. It functions in the processing of proprioceptive and tactile stimuli, spatial orientation, and attentiveness towards the environment. The occipital lobe, the smallest lobe of the brain, is at the most caudal/posterior part of the brain. It contains the primary visual cortex and visual association areas; thus, its primary function is in visual processing and interpretation. The temporal lobe is located posterior to the frontal lobe and inferior (towards ventral) to the parietal lobe. It is involved in auditory perception, sound interpretation, understanding of visual perception and facial expressions, and speech. The medial surface of the temporal lobe is essential to declarative memory, which includes semantic memory, recognition memory, and episodic memory (Jawabri & Sharma, 2019).

1.3 Medial temporal lobe and memory

Memory is the ability to encode new information acquired by the sensory stimuli, store and consolidate it within the neural networks, and retrieve it when required (Crowley et al., 2019; Jawabri & Cascella, 2020). The medial temporal lobe and structures underneath it plays an essential role in memory processing, primarily declarative memory. It consists of the hippocampus, amygdala, and the adjacent entorhinal, perirhinal and parahippocampal cortices (Figure 1.2) (Kern et al., 2017). They act as the temporary storage of information before finally being deposited at the neocortex level of the brain (Feigin et al., 2017).

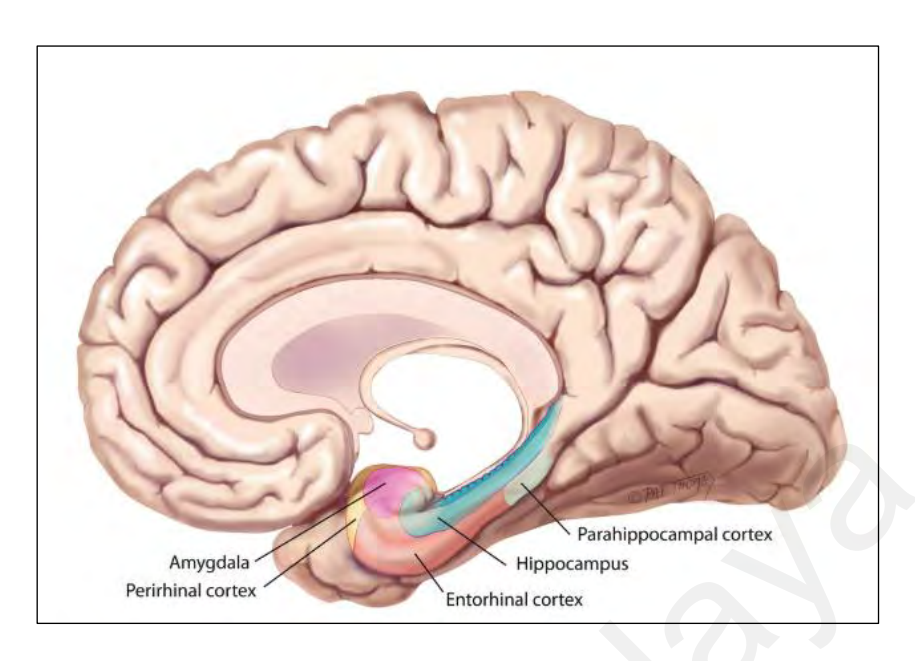


Figure 1.2: Anatomy of the medial temporal lobe structures. Taken from Raslau et al. (2015).

As proposed by Atkinson and Shiffrin in 1968, memory is substantially classified into sensory memory, short-term memory, and long-term memory (Camina & Güell, 2017; Jawabri & Cascella, 2020). Sensory memory stores the information received from the outside world, allowing it to be accessed in the future. Meanwhile, short-term memory differs from long-term memory in terms of duration and capacity (Cowan et al., 2008). Short-term memory refers to small amount of information processed by the brain and only available within a short time, from few seconds to minutes. On the contrary, long-term memory refers to larger amount of information stored for a longer period, from days to months to even years. Long-term memory can further be classified into two (2) major types, whether retrieved consciously (explicit memory) or unconsciously (implicit memory) (Camina & Güell, 2017).

Explicit memory, also known as declarative memory, refers to memories that are intentionally recalled, such as events (episodic memory) and facts (semantic memory) (Raslau et al., 2015). Meanwhile, implicit memory or nondeclarative memory concerns with

the automatic recall of memories that do not require any conscious effort. For example, skills of playing piano (procedural memory) and salivating when thinking of food (conditioning memory) (García-Lázaro et al., 2012; Raslau et al., 2015).

1.4 Hippocampus

Hippocampus is a small but complex brain structure located within the temporal lobe and makes up part of the limbic system, which is functionally related to emotion (Ahmad & Nameer, 2009). The structure of the hippocampus has been extensively studied and its role in declarative memory is well-defined (Anand & Dhikav, 2012; Meira et al., 2018). Hippocampus comprises two (2) parts: (i) the cornu Ammonis (CA) or also named as hippocampus proper, and (ii) the dentate gyrus (DG). The position of the CA and DG bear a resemblance to two interlocking, U-shaped laminae, one attaching into the other (Figure 1.3) (Wible, 2013).

Based on histology, CA has four (4) subdivisions which were previously named by Lorento de Nero (1934) as CA1, CA2, CA3 and CA4 (Figure 1.4). The DG is narrow, concaves dorsally and covers the CA4 segment. It has a simpler structure compared to the CA. The CA1 principally consists of pyramidal neurons that plays a vital role in the matching and mismatching of information received from CA3 (Anand & Dhikav, 2012). CA1 and CA3 have specific roles in memory, where pattern completion and one-trial contextual learning involves CA3 while temporal association memory involves CA1. CA2 is a small area and to date, only little information is known about its role in declarative memory (Meira et al., 2018).

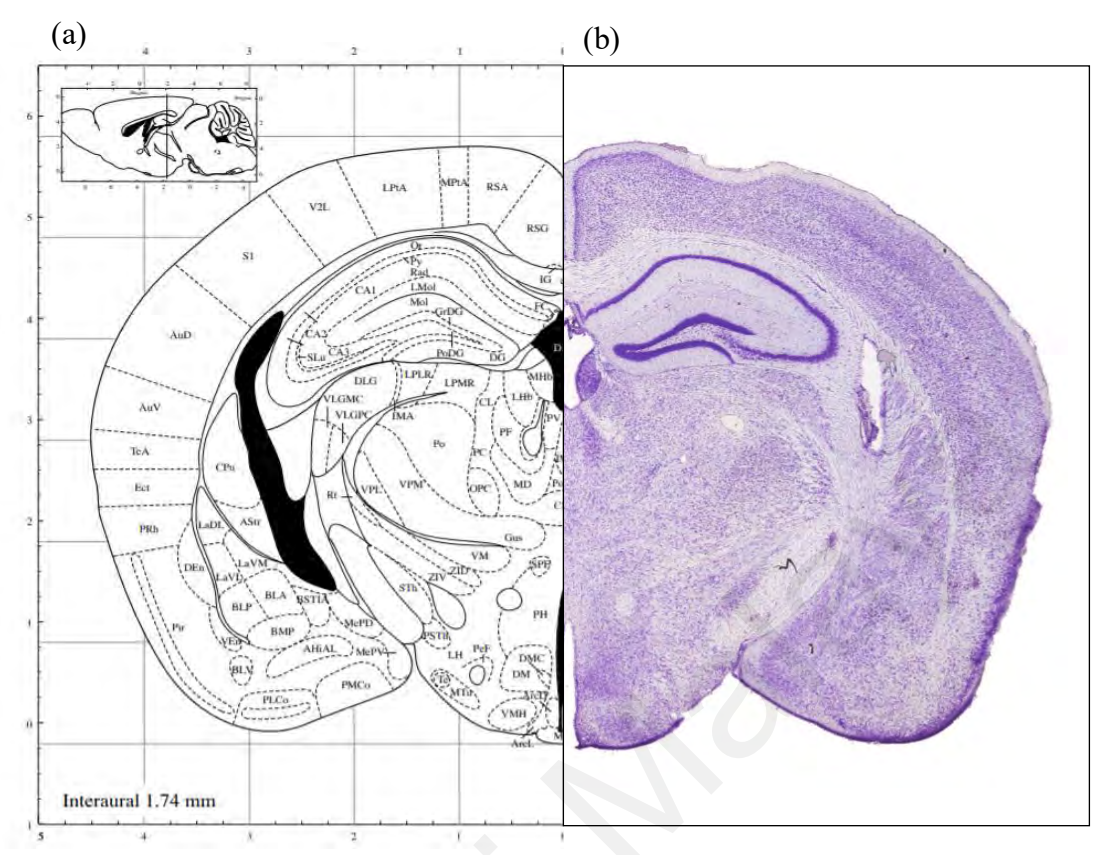


Figure 1.3: Coronal section of mouse brain with hippocampus structure. (a) Drawing with labelled brain areas, (b) Nissl-stained brain areas. Both images taken from Paxinos and Franklin (2001).

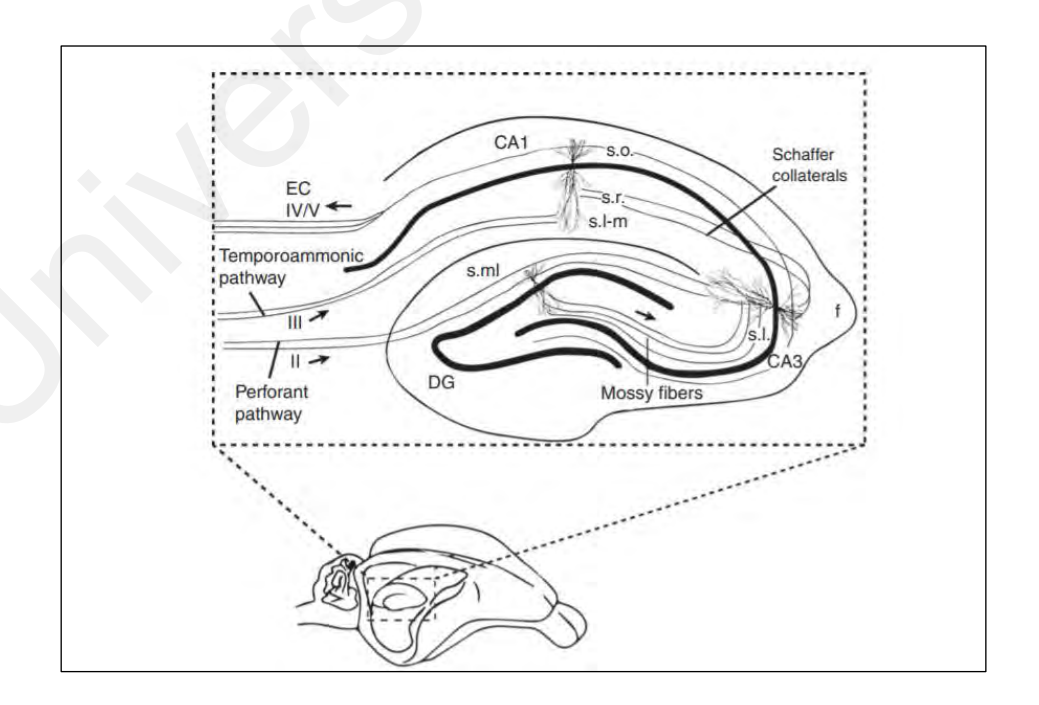


Figure 1.4: Schematic diagram of a transverse slice through the hippocampus of mouse showing the DG fields, CA3, and CA1. Taken from Vago et al. (2014).

1.4.1 Hippocampal CA1 pyramidal neurons

Neurons are the fundamental structural and functional unit of the nervous system. They are the cells of communication in the brain. Neurons conduct many actions that express useful information from sensory receptors and translate them into movement, imagery, and memory (Benavides-Piccione et al., 2020). They use electrical impulses and chemical signals to convey information between different areas of the brain, and between the brain and the rest of the whole nervous system (National Institute of Neurological Disorders and Stroke (NINDS), 2015). Neurons have various extension length, shape, and size. Each neuron consists of three basic structural features, which are soma or cell body and two extensions namely dendrites and axon.

Soma is the central structure of a neuron. The predominant internal operations and functioning of neurons lie in the soma. It acts as the chemical integrator of the neuron that functions in assimilating incoming information received from a broad range of signals that may come from other neurons, environment, chemicals, hormones, light, drugs, and other types of stimuli.

Subcellular organelles that are crucial for the processing of information are all located in the cell body. The organelles include nucleus, Golgi apparatus, rough endoplasmic reticulum, smooth endoplasmic reticulum, mitochondria, and lysosomes. Nucleus contains the neurons' genetic information in deoxyribonucleic acid (DNA), directs protein synthesis and holds the task of manufacturing all the other organelles.

Pyramidal cells found in the CA1 region of the hippocampus are the main structural feature that are accountable for memory and learning, and is most susceptible to oxidative insult (El-Safti et al., 2017). They are morphologically pyramidal in shape, as hinted by its

name. They generally have soma with a triangular pyramidal-like shape, a large, singular dendrite that bifurcates from the peak of the pyramidal soma and many shorter dendritic branches that originates extensively from the base of the pyramid (Magee & Cook, 2000).

1.5 Recognition memory

Recognition memory is an essential part of the episodic declarative memory, which refers to the capacity to judge a previously encountered item as familiar. According to Morillas et al. (2017), recognition memory is defined as "the ability to know that something has been previously experienced". This ability to call on a particular personal history and to access the experiences and episodes of a lifetime defines the identity of an individual (Vogel-Cierna & Wood, 2015); hence, plays an undeniably significant role in life.

Recognition memory comprises two (2) components: (i) familiarity, and (ii) recollection. Familiarity is simply knowing that an item has been previously encountered. Meanwhile, recollection is a longer process, where the brain collects and retrieves specific information and details regarding the presented item.

There are two different views on the mechanisms underlying recognition memory. Firstly, recognition memory has been widely suggested to involve two different structures in the medial temporal lobe that mediate two distinct processes. The structures involved are the hippocampus and the perirhinal cortex (PRh). The hippocampus is the brain region responsible for recollection, particularly associated with the 'remembering' part of recognition memory while the PRh plays a role in familiarity, particularly associated with the 'knowing' part of recognition memory. In conclusion, the first view imposes a dual-process model where the recognition processes are functionally and anatomically distinct (Ameen-Ali et al., 2015).

Secondly, recognition memory is a single process that depends on the integrity of both the hippocampus and its adjacent PRh (Ameen-Ali et al., 2015). Recognition memory comprises only one component which is familiarity. The 'knowing' part of recognition memory reflects a much weaker memory while the 'remembering' part reflects a stronger memory. In summary, the second view suggests that recognition memory is a single-process model that primarily depends on the strength of the memory itself; in terms of encoding, storage, and retrieval.

Previous studies have shown that learning and memory formation of object recognition are dependent on multiple brain regions (Tanimizu et al., 2017, 2018), mainly the medial temporal lobe structures (Carlini, 2011; Yi et al., 2016). The integrity of the medial temporal lobe is important for the recognition of prior occurrence (Jeneson et al., 2010; Vogel-Cierna & Wood, 2015). However, the participation of the hippocampus and PRh regions in recognition memory are still extensively studied. Scientists are only convinced on the involvement of PRh whereas a consensus has yet to be achieved on the involvement of hippocampus in recognition memory (Vogel-Cierna & Wood, 2015).

1.5.1 Behavioural Novel Object Recognition (NOR) test

Novel Object Recognition (NOR) is the most widely used behavioural test to evaluate recognition memory in rodent models. Behavioural testing for recognition memory was first developed in 1975. Mishkin and Delacuor introduced a rewarded forced-choice test called delayed nonmatching-to-sample (DNMS) test for monkeys. DNMS utilized monkey's innate preference for novelty, but with rapid training to select a novel object over a familiar object. The monkeys were allowed to explore an object A during sample phase. After a delay, the monkeys were then allowed to explore two objects, the familiar object A and a novel object

B during test phase. If object B which was the non-matching object to the familiar sample object was chosen, the monkeys would be rewarded with food.

Later in 1985, Y-shaped maze was introduced by Aggleton to determine the effectiveness of DNMS on rodents. In the test, rats were placed and exposed to one object in arm 1 of the Y-shaped maze, and were expected to choose the novel object placed in arm 2 instead of the same familiar object placed in arm 3. Similar to the DNMS test on monkeys, rats were rewarded if they selected the novel object. Since this test employs the running recognition protocol, multiple trials per session can be conducted without any animal handling.

Over the years, in 1988, the first recognition test DNMS task, was supplanted by the spontaneous object recognition test or more commonly known as novel object recognition (NOR) test (Figure 1.5) (Kinnavane et al., 2015). NOR was originally developed for use on rats by Ennaceur and Delacour, but later adapted for use on mice (Lueptow, 2017; Mugwagwa et al., 2015; Vogel-Cierna & Wood, 2015). It has been suggested that NOR has the most resemblance to recognition memory tests for humans (Balderas et al., 2013, 2012). Based on observations from previous studies that demonstrated the preference of rats and hamsters towards novelty over familiarity, Ennaceur and Delacour showed that after given ample time to explore object A in an open rectangular arena, rats preferentially spent more time exploring novel object B over a duplicate of object A when placed in the same arena again. Spontaneous preference for novelty was the only fundamental of this test, with no training and reward motivation nor punishment required.

Mumby and his colleagues later introduced another non-matching task for rats in 1990. The test was conducted in a shuttle box with a central holding area. The left end of the box was the sample area while the right end was the test area. Familiarization phase was carried

out when rats were allowed to run from the central area to the left end and explore an object A. After that, rats were allowed to run from the central area to the right end where the familiar object A and novel object B were placed. Similar to the DNMS and Y-shaped maze tests, rats were only rewarded if the novel object B was selected.

The advantage of NOR test is that it does not require external stimuli and relies primarily on the innate preference of rodents to explore a novel object in a familiar environment (Leger et al., 2013). It does not require the involvement of any emotional or motivational reinforcers (Dere et al., 2007). Besides that, NOR is not dependent upon the encoding and retrieval of emotionally aversive and inherently stressful training events. It is not stressful to the rodents, therefore false-positives due to stress hormone-modulated memory performance can be avoided (Vogel-Cierna & Wood, 2015). It reflects the typical day-to-day experiences or memories most affected in human disease. The preference towards exploring the novel object reflects the use of learning and recognition memory (Leger et al., 2013).

NOR is a very simple test and comprises at least three phases only to be completed: habituation, training, and test phases. Studies have shown that the habituation period prior to training and test phases is essential for the formation of memory. Habituation to the task area and to the procedure minimizes stress and prevents any potential neophobic reactions from the rodents, hence encourages them to explore the objects (Leger et al., 2013). Better discrimination index and significantly longer exploration period of novel over familiar object in habituated mice suggested that habituation to the task area allowed formation of object recognition memory (Tanimizu et al., 2018).

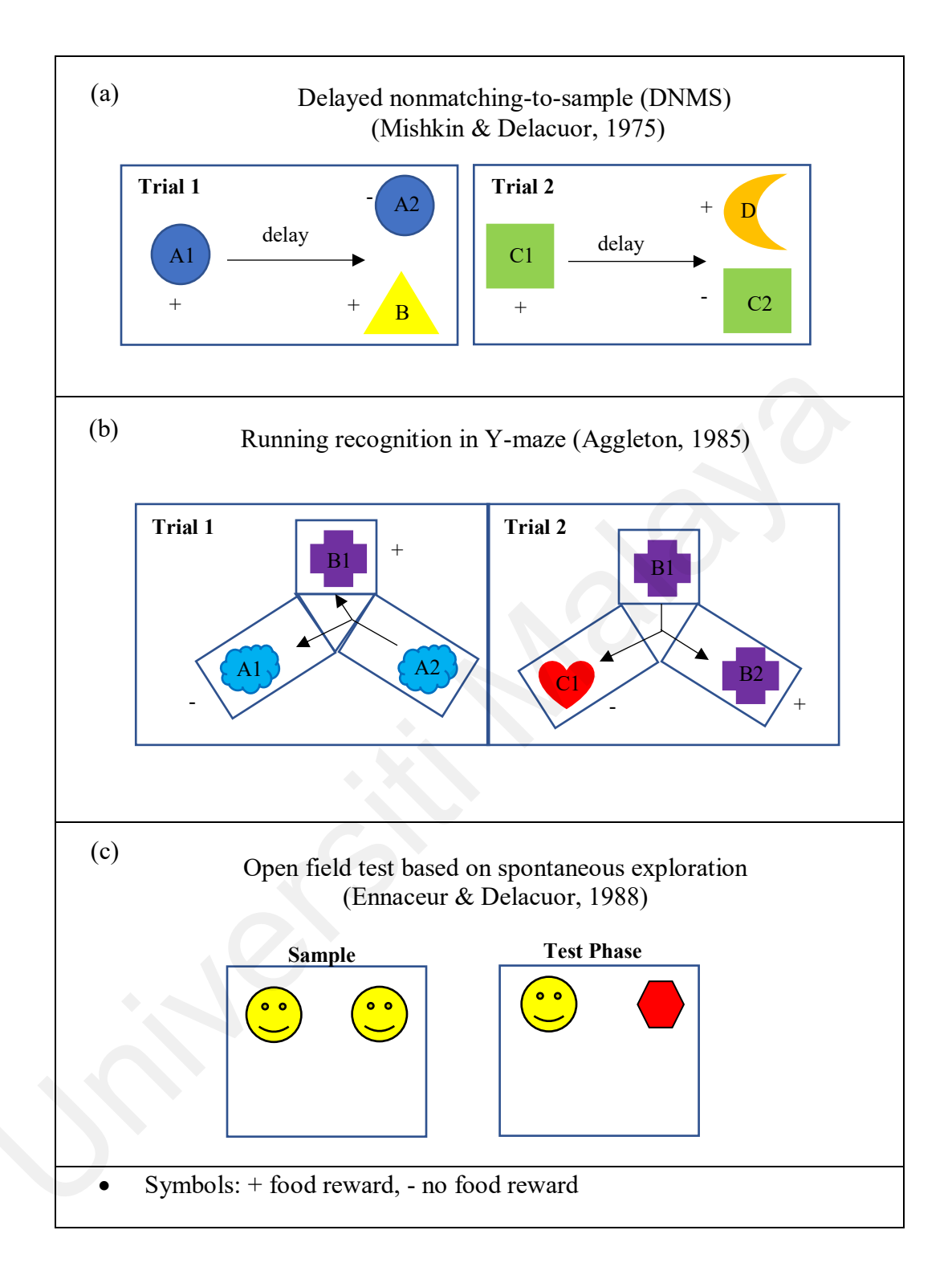


Figure 1.5: Schematic illustrations of various object recognition memory tests. Adapted from Kinnavane et al. (2015).

1.6 Toluene

Toluene (Chemical formula: C₆H₅CH₃) is a clear and colourless liquid with a sweet, pungent odour. Toluene occurs naturally in tolu tree and in crude oil (Agency for Toxic Substances and Disease Registry (ATSDR), 2015). It is an organic compound (Figure 1.6) with high volatile pressure and is insoluble in water. Also known as toluol, methylbenzene, and phenyl methane, toluene is a solvent commonly used in various commercial and household products such as paint, adhesives, printing inks and cleaning agents (Wang, 2017; Wang et al., 2014). Besides that, toluene is widely used in numerous industrial processes such as plastic manufacturing and petrol production (Cruz et al., 2019).

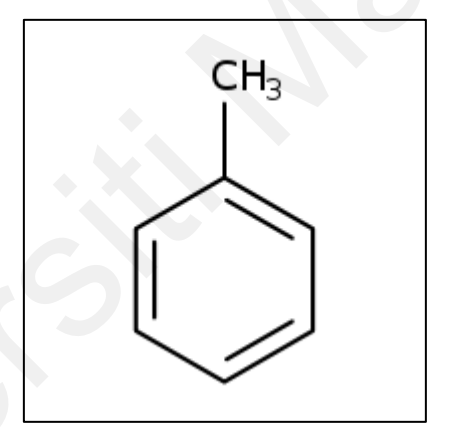


Figure 1.6: Chemical structure of toluene (TOL formula: C₆H₅CH₃)

Toluene can enter the body via ingestion, skin contact and inhalation (Tualeka et al., 2019). However, since toluene evaporates easily into the air, absorption via the gastrointestinal tract and skin, is less unlikely to occur. Toluene may also enter the soil and groundwater in cases of large toluene spills or in areas with heavy use and production of it (ATSDR, 2015). Humans are readily exposed to low concentration of toluene by inhaling it from household products, cigarette smoke and petroleum. The dominant source of toluene

exposure in ambient air is from automobile emission (Hamid et al., 2019), as expected to be found at oil gas stations.

High concentration of toluene exposure involves occupational exposure in workplaces such as printing industries (Marganda & Ashar, 2018), photocopy centers (Sarkhosh et al., 2012), and oil refineries (Hopf et al., 2012), because workers are exposed to it for several hours a day, five days a week (Cruz et al., 2014). The Scientific Committee on Occupational Exposure Limit (SCOEL) in the European Union (EU) and the American Conference of Governmental Industrial Hygienist (ACGIH) has set the toluene occupational exposure limit to 50 ppm and 20 ppm respectively (Hopf et al., 2012). Besides industry workers, cases of voluntary inhalation of toluene-based products for recreational drug abuse as occurring in Malaysia, also involves high and concentrated exposure to humans (Rahim Yacob et al., 2012).

1.6.1 Toxicokinetics of toluene

Toxicokinetics refers to the absorption, distribution, metabolism, and excretion, as a whole known as ADME of a toxicant in an organism (Gupta et al., 2011). Since inhalation is the primary route of toluene exposure, absorption of toluene occurs primarily through the respiratory tract. This is followed by gastrointestinal tract and at a lesser extent through skin (Cruz et al., 2014; Wang, 2017; WHO Regional Office for Europe, Copenhagen, Denmark, 2000). However, toluene toxicity after skin contact is uncommon due to the slow rate of dermal absorption (ATSDR, 2004).

After absorption, level of toluene rapidly increases in the systemic circulation, and it gets distributed throughout the body (Wang, 2017). Toluene is lipophilic; hence, it is distributed quickly to highly perfused and lipid-rich organs such as brain, liver, and kidney. Toluene's

high affinity for lipids enables it to easily cross the blood brain barrier (Cruz et al., 2014) and may result in CNS toxic effects only within minutes after the exposure (ATSDR, 2004). Available clinical studies reported that toluene accumulated the most in the brain following inhalation exposure, and in the liver following oral exposure (United States Environmental Protection Agency, 2005). Besides that, transplacental transfer has also been reported (Cruz et al., 2014; WHO Regional Office for Europe, Copenhagen, Denmark, 2000).

Toluene metabolism is depicted in Figure 1.7. It is metabolized mainly in the liver, by cytochrome P-450 enzymes. As the methyl group in toluene is hydroxylated, it forms benzyl alcohol before oxidized to benzoic acid. About 70-80% of toluene in humans is converted to benzoic acid (WHO Regional Office for Europe, Copenhagen, Denmark, 2000). Upon conjugation with glycine, most of the benzoic acid later forms the major metabolite, hippuric acid. A small portion of the benzoic acid conjugates with uridine diphosphate (UDP)-glycuronate to form acyl-glucuronide. Other minor metabolites include *ortho*- and *para*-creso may conjugate with sulfates and glucuronides and form S-benzyl-N-acetyl-L-cysteine, a minor metabolite specific for toluene exposure. Most of the metabolized toluene is excreted as hippuric acid in urine (Cruz et al., 2014). Meanwhile, the remaining toluene, approximately 7-20%, is mostly excreted in expired air, unchanged (Wang, 2017; WHO Regional Office for Europe, Copenhagen, Denmark, 2000).

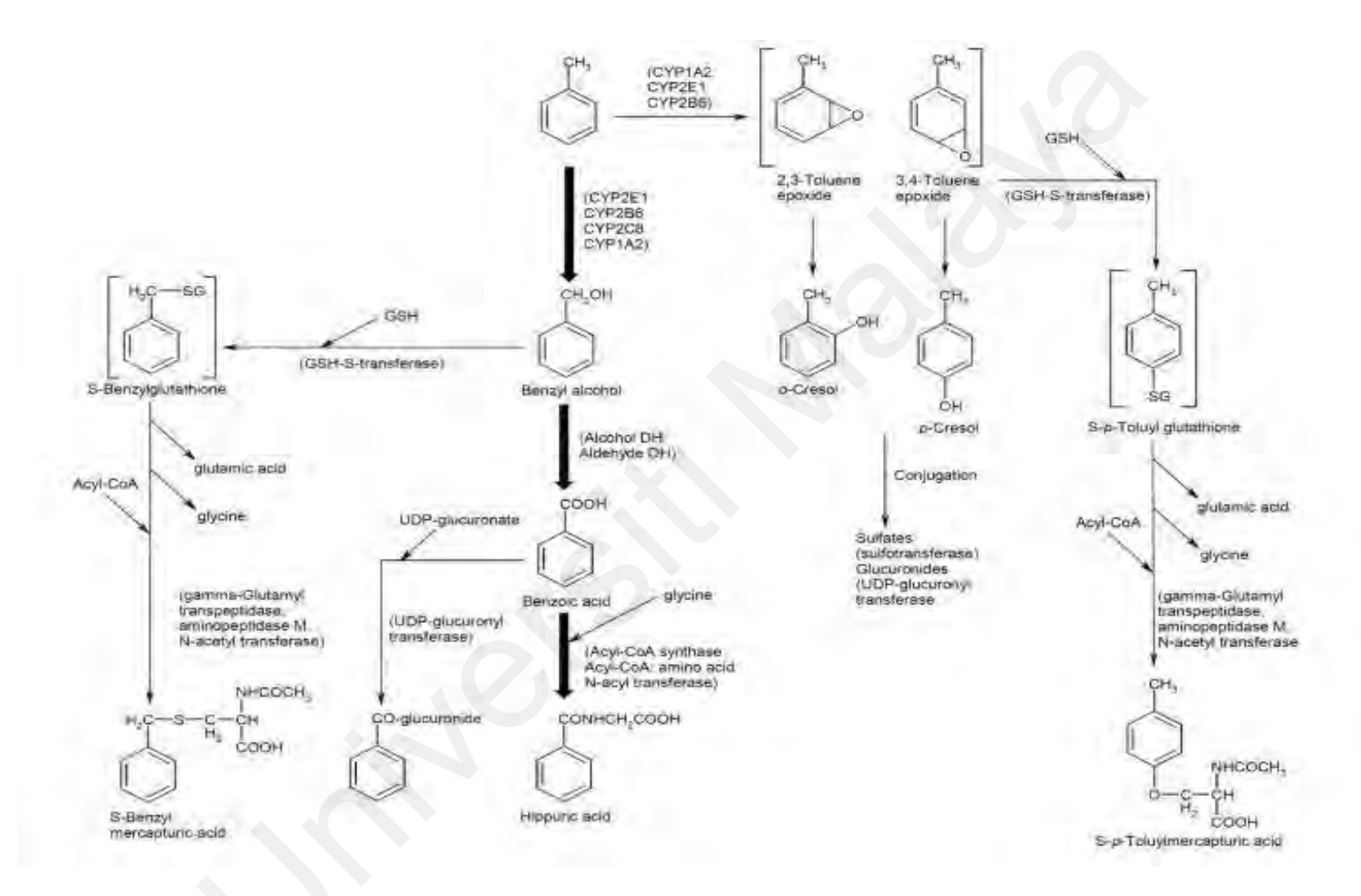


Figure 1.7: Proposed pathways of toluene metabolism. Taken from Wang (2017).

1.7 Approach against toluene-induced negative effects

As previously mentioned, the application of toluene is widespread in both industrial settings and consumer products. Although known to have neurotoxicant effects on the CNS, acute and chronic exposure to toluene in both home and occupational settings still commonly occur. As defined by the ATSDR and the Department of Health, New York State, acute exposure refers to contact with a substance that happens once or for a short period of time, which may last a few seconds, hours or at least up to 14 days. On the contrary, chronic exposure refers to contact with a substance that happens for a long period of time, from months till over a year time. Notably, studies have highlighted the toxic effects of toluene, that has deteriorating health effects in humans ranging from neurologic changes (Kao et al., 2014; Thetkathuek et al., 2015; Werder et al., 2019) to genetic abnormalities (Braunscheidel et al., 2019; Dick et al., 2021; Soares et al., 2020a). Hence, efforts are ongoing to protect CNS from its damaging effects. Despite the advanced achievements in the modern medical system, traditional and complementary medicines are continuously practiced (Azaizeh et al., 2010). In fact, more than 80% of the worldwide population relies on traditional medicines as a method of healthcare (Ekor, 2014) and the use of it has shown a significant growth since the early 1990s (Yamasaki, 2014). Therefore, a therapeutic approach, grounded in basic science, is studied to protect, and treat humankind from toluene-induced negative effects. Consumption of the beneficial medicinal plant *Nigella sativa* is the approach of this present study.

1.7.1 Nigella sativa

Nigella sativa (NS) is a widely used medicinal traditional plant and considered as one of the greatest healing medicines in the Islamic literature (Sahak et al., 2016). It is commonly known as black seed in English and Al-Habba Al-Sauda or Al-Habba Al-Baraka in Arabic, often found in the Mediterranean countries, Western Asia, Middle East, and Eastern Europe (Khazdair et al., 2019). It is known to have antibacterial, antifungal, antioxidant, antidiabetic, and anticancer properties (Beheshti et al., 2016). Its properties could probably be due to the oil found in the middle of the seed and/or the seed structure, itself (Sahak et al., 2016).

Chemical compositions of NS include thymoquinone (Alhebshi et al., 2014; Beheshti et al., 2016), thymohydroquinone, dithymoquinone, p-cymene, carvacrol, 4-terpinol, t-anethol, and thymol (Ahmad et al., 2013). Isoquinoline alkaloids and pyrazol alkaloid are the two different types of alkaloids present in the black seed. Figure 1.8 shows the chemical structure of thymoquinone (TQ).

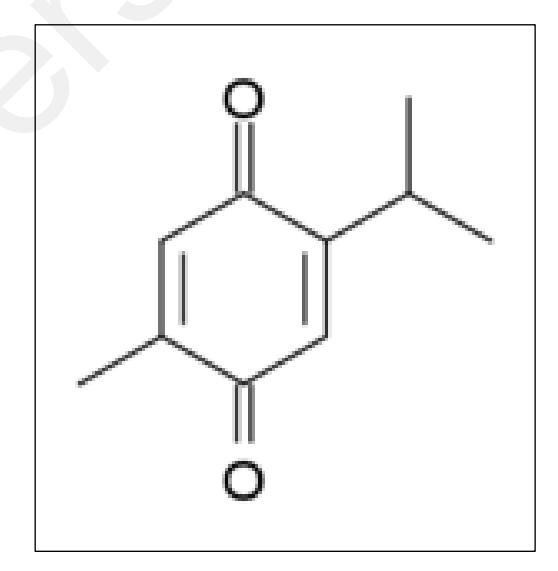


Figure 1.8: Chemical structures of thymoquinone (2-isopropyl-5-methyl-1,4 benzoquinone). Taken from Al-Majed et al. (2006).

Besides that, NS contains optimum amounts of proteins, carbohydrates, fat, crude fiber, and total ash as well as vitamins and minerals. Oil rich in unsaturated fatty acids predominantly linoleic acid, oleic acid, eicosadienoic acid and dihomolinoleic acid are also reported to be part of its oil constituents. For saturated fatty acids such as palmitic and stearic acids, the amounts are reported to be slightly lesser (Ahmad et al., 2013). Carbohydrates include glucose, xylose, rhamnose, and arabinose while the examples of vitamins are thiamine, riboflavin, pyridoxine, niacin, and folic acid. Aside from that, NS is also a source of calcium, potassium, iron, and flavonoids (El-Naggar et al., 2010).

NSS contains amino acids, proteins, carbohydrates, a small number of essential oils (0.4–1.49%), about 30–45% fixed oils and various concentration of other bioactive molecules. These compounds consist of alkaloids, fatty acids, polyphenols, phytosterols, terpenes and terpenoids, and others. Terpenes and terpenoids are the highest constituent of NSS metabolites. TQ is also the most prominent content of both volatile and fixed oil of NS seeds (Balbaa et al., 2021; Hossain et al., 2021).

1.8 Rationale of the study

Nervous system is among the main affected organ systems of toluene (Agency for Toxic Substances and Disease Registry, 2011). Negative alterations in learning and memory of both humans and animals after inhalation of low concentration of toluene has been reported (Win-Shwe & Fujimaki, 2011). The only study on the effects of Nigella sativa after toluene exposure has been conducted by Kanter (2008). However, comparison on the effects of Nigella sativa oil, seeds and its main bioactive constituent, thymoquinone against toluene toxicity has not been studied. In addition, according to the WHO Regional from Europe, Copenhagen, Denmark (2000), most of the studies that have been conducted on toluene employed exposure concentrations that far exceed the normal working environment exposure to humans, thus they relate best to cases of toluene abuse. Therefore, since humans are commonly exposed to low toluene exposure in their daily lives, this current study will be able to provide information on the effects, if any, of low concentration of toluene exposure, on both neurobehavioural and neurohistological aspects. Since Kanter (2008) reported on morphologic improvements of the hippocampus structure in rats treated with NS and its derived thymoquinone after chronic toluene exposure, this study expects to observe the neuroprotective effects of NS against low concentration of toluene administration. This was subsequent to the establishment that NS has antioxidant and neuroprotective properties (Sahak et al., 2016).

1.9 Research questions

In line with the rationale of the study, the research questions of the study are as follow:

- 1) What are the behavioural consequences in terms of recognition memory performance, of low toluene administration on mice?
- 2) Does low toluene administration affects the brain morphology of mice?
- 3) How does the administration of toluene affect the morphometric properties of pyramidal hippocampal neurons in the mice' brain?
- 4) Does NS seeds, oil, and thymoquinone treatment exert positive changes on the memory performance of the toluene-treated mice?
- 5) Does NS seeds, oil, and thymoquinone have neuroprotective effects on the brain morphology and morphometry of hippocampal neurons in mice co-treated with both toluene and NS?
- 6) Are there any differences in behavioural and histological effects of the three NS substances; seeds, oil, and thymoquinone, after toluene administration in mice?

1.10 Objectives of study

The general objective of the study is to evaluate the neuroprotective effects of various components of NS (e.g., seeds, oil, and selected constituent) against neurotoxicant toluene in mice. Specifically, the objectives of this study are as follows:

- 1) To evaluate the effects of toluene and/or NS related supplementations on mouse recognition memory by Novel Object Recognition (NOR) test.
- To investigate morphological changes (if any) in mouse brain treated with toluene and/or NS related supplementations.
- 3) To evaluate morphometric changes (if any) of hippocampal CA1 pyramidal neurons in mice treated with toluene and/or NS related supplementations.

CHAPTER 2: LITERATURE REVIEW

2.1 Object recognition memory and hippocampus

Hippocampus is known as the main brain structure that is involved in learning and memory (Cohen et al., 2020; Dekeyzer et al., 2017; Hales et al., 2015; Kim et al., 2014). Previous researches have shown that it is also responsible in the regulation of emotional behaviour as well as in motor-control and hypothalamic functions. In addition, hippocampus prominent role in creating episodic memory and spatial memory in animals has also been studied (Bird, 2017; Cohen et al., 2013; Takehara-Nishiuchi, 2021).

Study using immunohistochemistry results in c-fos expression, a marker for the detection of neuronal activities during a physiological response. This finding demonstrated a strong correlation between the hippocampus, insular cortex (IC), PRh and medial prefrontal cortex (mPFC) during the NOR test. Thus, it is suggested that all four structures, including the hippocampus, are required for the consolidation of object recognition memory (Tanimizu et al., 2018).

In a study by Cohen and colleagues (2013), inactivation of the mouse hippocampus for 20 minutes prior to the sample session in NOR test prevented encoding and/or consolidation of object memory. Hippocampal glutamate level showed an increase during the mouse's exploration activity in the NOR test, as well as its hippocampal CA1 neuronal cells firing rates in response to the objects. In another study on Institute of Cancer Research (ICR) mice, hippocampal lesions caused a significant lower exploration time during habituation phase in the NOR test compared to its control group. Preference for novel object was also significantly reduced in hippocampal-lesioned mice (Yi et al., 2017). These findings suggest the relevance

of hippocampus for adaptation to novel environments, thus, manifests that hippocampus is important in object recognition memory.

Muscimol is a potent GABA_A receptor agonist and partial GABA_{A- ρ} receptor agonist, known to inhibit memory retention. Pre-test muscimol inactivation of CA1 neurons in the dorsal hippocampus of mice caused an increase of exploration time in the NOR arena during the habituation phase and a decrease in preference towards novel object during the test phase (Cohen & Stackman, 2015). Another study on muscimol inactivation of the dorsal hippocampus region in rats also demonstrated impairment of visual discrimination of two-dimensional (2D) objects (Levcik et al., 2018). This suggests a hinder in the memory retrieval of the arena and the objects in mice, thus proves that hippocampus plays a crucial part in recognition memory.

2.1.1 Variation of behavioural Novel Object Recognition (NOR) test

Despite having basic procedures, only little consistency among NOR task procedures have been noted. These inconsistencies have made it difficult for direct comparisons between the different studies to be done.

One of the major variants among NOR protocols is the different habituation and familiarization exploration period. Some studies performed 3 days of habituation phase, where rodents were exposed to the open field twice a day, 3 or 5 minutes per each session (Reger et al., 2009) or for 2 days (You et al., 2019). Another variation is the involvement of a single 5-min exposure only (Mesa-Gresa et al., 2013), or a criterion of 20 seconds with a maximal time of 10 min to reach the criterion (Lueptow, 2017).

Another variable that usually differs among studies is the exploration period during test phase. In the original protocol for rats, a minimal of 20 seconds exploration time for both objects during the test phase was used. However, the current most used way to determine the recognition memory performance of rodents is to measure exploration period at a fixed 3- or 5-minutes period (Leger et al., 2013).

The open field/arena itself is another factor that influences differences of recognition memory performance in the NOR test. Different studies have used different sizes, shapes, and materials of the arena. Some were square, circular, or rectangular in shape. Kalueff and team (2006) demonstrated that mice's exploratory behaviour is not influenced by the different shapes of open field. On the contrary, Lueptow (2017) reported that circular open fields are more suitable for anxious mice as square arenas may make them to just sit in the corners.

Furthermore, objects used in the familiarization and test phases play an important role in rodents' exploratory behaviour. Parameters that should be taken into consideration before choosing the objects are colour, texture, height, and shape. Objects that provide rodents the possibility to climb over induce them higher interest to explore the objects even without any habituation (Leger et al., 2013). However, a too big and tall object should be avoided so as not to create fear response from the rodents (Vogel-Cierna & Wood, 2015). Selected objects must not be visualized as being very similar to one another as to make them easily differentiated by the rodents. However, both objects must have a certain level of similar complexity to avoid induced object preference that may cause biasness in the results obtained later (Lueptow, 2017).

General state of animals also affects their exploratory behaviour. Since NOR relies on the innate preference of animals, any condition that may impede their exploratory behaviour may generate false-positive results. Among the most crucial parameter that must be well monitored is animal stress. Rodents are considered as social species; hence, should be grouphoused unless required otherwise for study purposes. Social isolation caused social stress in rats; thus, resulted in impaired memory performance in the NOR test (Famitafreshi & Karimian, 2018). Familiarization to the handling of experimenters reduces novelty-induced stress in rodents. Therefore, it is essential for the rodents to be consistently accustomed to the experimenter before the study begins (Vogel-Cierna & Wood, 2015). Timing of the test is also important as exploratory behaviour of animals may vary according to their circadian rhythms and light cycle. Besides that, the testing room condition in terms of its odour and noise must also not generate stress to the animals.

Lastly, the most efficient method to assess exploratory behaviour of animals is still debated. However, majority of previous studies scored object exploration whenever the animal sniffed or touched the object within a distance of 2 cm or less. Chewing, climbing over, or leaning on the object is not accounted as explorative behaviour, unless accompanied with a nose-directing behaviour towards the object. Data collection is either conducted manually or by using a software. If collected manually, experimenter must be blinded to the treatment groups. If collected and analyzed using software, a video camera is usually placed above the arena for direct video recording (Leger et al., 2013).

2.2 Effects of toluene on the nervous system

Previous studies have reported extensive toxic effects of toluene exposure on the nervous system. Lin et al. (2010) reported a decrease in brain weight, memory impairments, and

reduced level of social interactions in adolescent mice exposed to acute concentration of toluene. Reduced brain weight may result from the interference of toluene in the nervous system development, since the neuronal cells in the hippocampus and cerebellum were observed to be slightly shrunken. Laio and his colleagues (2019) reported that comet assay results revealed that acute exposure of toluene induced significant levels of DNA damages in the hippocampus, cerebellum, and cortex regions of the brain in a dose-dependent manner. Brain-derived neurotrophic factor (BDNF) expression also showed a slight decrease in the toluene-exposed hippocampus.

A study on rabbits by Demir et al. (2017) demonstrated that toluene resulted in severe structural damage of hippocampal and cortical neuronal cells as well as abnormal malformations of nuclei structure in the oligodendrocyte cells. Besides cell disruption, toluene also altered protein levels in the brain. The tumor necrosis factor alpha (TNF-alpha) levels increased significantly while the dopamine, nerve growth factor (NGF), and glial fibrillary acidic protein (GFAP) levels manifested a significant decrease. Astrocyte activation and gliosis also occurred densely. In another study on male Sprague Dawley rats, 7000 parts per million (ppm) of toluene exposure resulted in moderate abnormal respiration rate, inactive behaviour, prone position, and irregular gait. The single toluene exposure reduced markers of hippocampal neurogenesis. The number of Ki-67-positive cells, a marker of cell proliferation, and doublecortin (DCX)-positive cells, a protein important for the migration and proliferation of neurons, were notably decreased after toluene exposure (Yoon et al., 2016).

In male adolescent Wistar rats that were exposed to increasing amounts of toluene from 500 to 8000 ppm, toluene blocked the N-methyl-D-aspartate (NMDA) and inhibited the neuronal nicotinic acetylcholine receptors resulting in a change of behavioural performance.

The study demonstrated that the highest concentration of toluene increased anxiety in rats, indicated by an increase in burying behaviour latency and a significant decrease in the total time of social interaction. Toluene caused damage of motor coordination in the rotarod test. Besides neurobehavioural changes, an increase in dopamine levels in the mesolimbic system were also noted (Armenta-Reséndiz et al., 2019).

Other relevant literature has demonstrated similar results on the alteration of neurochemical balance by toluene, which consequently affects behavioural performances. Apawu et al. (2015) reported that extracellular dopamine in the caudate putamen (CPu) of mice significantly escalated after toluene exposure. Locomotor activity of the mice also increased during the first 15 minutes, when exposed to 4000 and 8000 ppm of toluene. Conversely, at the highest toluene exposure of 8000 ppm, subdued locomotor activity was observed exhibiting little to no movements during the second 15 minutes of exposure.

Studies have shown that toluene causes impairments in learning and memory performance. (Callan et al., 2017) reported that rats prenatally exposed to toluene took a longer time to find the platform and exhibited significantly elevated cumulative distances from the platform in the Morris Water Maze (MWM) test, as compared to the control group. Rats exposed to an increasing concentration of toluene depicted a significant decrease in latency to cross through the gates between the compartments in the passive avoidance task (PAT), in a concentration-dependent manner (Cruz et al., 2019).

Another study on the effects of toluene exposure in rats manifested brain oxidative stress and tissue damage. Lipid peroxidation increased as stipulated by the increment of malondialdehyde (MDA) level (Abdel-salam et al., 2021; Sahindokuyucu-Kocasarı et al., 2021). Oxidative stress marker nitric oxide (NO) (Abdel-salam et al., 2020) increased while

antioxidant enzymes glutathione (GSH) and glutathione peroxidase (GSH-Px) decreased (Sahindokuyucu-Kocasarı et al., 2021). Histopathological damage on the brain were indicated by neuron degeneration in the cerebral cortex and significant vacuolation of hippocampal neurons. Besides that, edema and focal background hemorrhage were also observed (Abdel-salam et al., 2021, 2020).

Apart from literature on animals, case studies on humans concerning toluene toxicity have also been reported. In 2019, Werder and his colleagues conducted a study on the Gulf coast residents who were briefly exposed to BTEX during the 2010 Deepwater Horizon (DWH) oil spill disaster. Results showed that half of the participants experienced at least one of the neurologic symptoms listed and toluene exposure was linked to increasing peripheral nervous system (PNS) symptoms. PNS symptoms include tingling and numbness in the extremities, blurred vision, and stumbling while walking.

Toluene has always been one of the main organic solvents used in paint and thinner. A study on a 59-year-old man who worked as a shipyard painter for 20 years reported that he encountered several neurotoxicity syndromes. Firstly, he had a severe neuropsychological damage indicated by his bad performance in the neuropsychological tests. He also suffered extreme disability to focus, memorize and execute cognitive tasks, besides having an immensely low recall and recognition memory (Seo & Kim, 2018). In another case study on a 50-year-old Belgian woman who worked at a paintbrush manufactory for more than 20 years, similar complications were observed. She suffered acute solvent intoxication symptoms such as intense headaches, fatigue, irritability, feeling of drunkenness, sleeping disturbances, and nausea. She also experienced seizures before referred to a neurologist and diagnosed with chronic toxic encephalopathy (CTE) (Van Hooste, 2017).

A clinical study by Yavari et al. (2018) demonstrated that 200 ppm of toluene exposure resulted in the suppressant of neuroplasticity induced by anodal transcranial direct current stimulation (tDCS). Toluene also caused a reduction in intracortical facilitation and an increment in the inhibition of the transcranial magnetic stimulation motor evoked potential (MEP) in the short-latency afferent inhibition (SAI) measure. However, motor learning performance of participants were not affected as manifested in the motor sequence learning task, the serial reaction time task.

2.2.1 Potential mechanisms of toluene toxicity on the CNS

The exact mechanism of action of toluene toxicity have yet to be determined. However, substantial studies have reported on the possible mechanisms of it. Demir et al. (2017) suggested that toluene interacts with proteins and induces changes in the lipid structure of cell wall due to its lipophilic property. As the lipid structure is altered, the membrane fluidity increases, thus results in a significant elevation of the Na/K-ATPase activity. Sodium-potassium pump is essential for proper electrolyte balance in the body, which is very important for neuronal signaling in the nervous system.

The upsetting of the membrane integrity induces oxidative stress (Chew et al., 2020). Besides causing disturbance in the Na/K-ATPase activity, toluene exerts part of its toxicity via oxidative stress (Páez-Martínez et al., 2020). Toluene generates the build-up of cellular reactive oxygen species (ROS), and the organelle that is essentially responsible for this is the mitochondria (Chew et al., 2020). Toluene instigates modulation in cellular bioenergetics and modification of gene transcripts essential for the mitochondrial structure and function (Yavari et al., 2018). The imbalance of oxygen radicals causes DNA damage (Laio et al., 2019), protein oxidation and lipid peroxidation (Chew et al., 2020) that results in tissue damage.

When the damage is beyond repair, apoptotic pathway is activated and thus apoptosis occurs (Chew et al., 2020; Demir et al., 2017). Persistent oxidative stress accelerates neurotoxicity. Brain regions preferably affected by toluene includes white matter structures, periventricular regions, and subcortical region (Van Hooste, 2017).

Toluene affects the CNS by altering neutrophin-related genes and signaling pathways (Laio et al., 2019). NMDA receptor, a glutamate receptor and ion channel located in the neurons, have been reported to be the main molecular target of toluene (Cruz et al., 2020). Toluene acts as an antagonist where it blocks and inhibits the action of NMDA receptor in a non-competitive manner (Armenta-Reséndiz et al., 2019; Callan et al., 2016; Cruz et al., 2020; Gülşen et al., 2016). However, on some specific NMDA receptors in certain brain regions, a different effect of toluene has been proposed.

Montez et al. (2017) reported that toluene enhanced the function of NMDA receptors in the hippocampus. Similar findings were also presented in the prefrontal cortex and nucleus accumbens. Repeated toluene exposure increased the expression of GluN1 and GluN2B sub-receptor proteins (Callan et al., 2016). GluN1 is the major subunit of glutamate receptor associated with synaptic plasticity while GluN2B is the receptor related to neurodegenerative diseases. The overactivation of these NMDA receptors leads to high calcium (Ca²⁺) intake. Consequently, excessive concentration of the intracellular Ca²⁺ activates the mechanism of neuronal cell death (Schreiber et al., 2019). An interference to the calcium homeostasis may also disturb the control of neurotransmitter release, neurogenesis, and neuronal plasticity activities (Chew et al., 2020). In addition, alterations in NMDA receptors leads to overactivation of glutamatergic synapses which are important for learning and memory and when disrupted, may generate neurological or neurodegenerative diseases (Costa et al., 2020).

Several studies have also shown that high dose of toluene affects the GABAergic, glutamatergic, serotonergic, and dopaminergic pathways (Demir et al., 2107). However, its effects on the CNS may be inhibitory or excitatory (Van Hooste, 2017). In the mesolimbic system, toluene acts as a positive allosteric agonist at GABAA receptor, glycine and 5-HT₃ ionotropic receptors. In contrast, it inhibits neuronal nicotinic acetylcholine receptors and blocks sodium, calcium, and potassium channels (Cruz et al, 2019; Cruz, 2020).

Dopamine (DA) levels in the mesolimbic system are enhanced after toluene exposure (Cruz et al, 2019; Callan et al., 2016). This DA enhancement has been suggested to be the factor of increased locomotor activity during toluene exposure (Callan et al., 2016). However, in other regions of the brain, DA metabolism may be temporarily hampered due to the disruption of monoamine oxidase (MAO) or catechol-omethyltransferase (COMT) (Bowen et al., 2017). Demir et al. (2017) demonstrated that toluene binds to GABA receptor thus increases cholinergic activity. On the other hand, it inhibits the GABAA receptor and causes a reduction in the hippocampal excitability (Callan et al., 2016).

2.3 Effects of NS on memory and the nervous system

Studies on the potentials of NS in memory enhancement has been extensively studied (Table 2.1). Administration of *Nigella sativa* oil (NSO) reduced oxidative stress in D-galactose-induced aging mice. NSO attenuated oxidative stress biomarker MDA, B-cell lymphoma 2 (BCL2), BCL2-associated X protein (BAX), and caspase-3 levels, and augmented GSH level in brain (Shahroudi et al., 2017). Following scopolamine administration, *Nigella sativa* oil (NSO) improved memory performance of rats in T-maze alteration task and NOR test. Brain MDA and TNF-α contents decreased while GSH level increased (El-Marasy et al., 2012). Since the risk of Alzheimer's disease (AD) has been

reported to increase by 45-90% in Type 2 diabetes mellitus, a study on diabetic rats showed that NSO treated groups had increased antioxidant levels and decreased oxidative stress markers in the brain (Balbaa et al., 2017).

Experimental autoimmune encephalomyelitis (EAE) induction is the animal model of multiple sclerosis in rodents. Multiple sclerosis is known to be the most significant demyelinating and immune-mediated CNS neurodegenerative disease in young adults. Rats orally administered with water suspension of grinded NS seeds showed reduced histopathological observations in the brainstem. Reactive astrogliosis in cerebellar medullary and expression of astrocytes were low, and partial to complete remyelination in medulla and cerebellum were observed (Noor et al., 2015). Another study on EAE induction also reported that NS suppressed inflammation and enhanced remyelination in the hippocampus of treated rats (Fahmy et al., 2014).

Rats supplemented with hydro-alcoholic extract of NS showed improvements in their learning and memory performance, as observed in PAT and MWM test. Biochemical assessments also revealed a decrease in the hippocampal MDA level of NS-treated rats (Beheshti et al., 2017). Intraperitoneal administration of 400 mg/kg of NS ethanolic extract for 5 days demonstrated memory enhancement in pentylenetetrazole (PTZ)-induced epileptic rats. An increase in time latency for entering dark compartment after receiving shock was observed in PAT. Latency to onset of seizure also increased and production of dark neurons in hippocampus were notably prevented in NS treated groups (Vafaee et al., 2015).

Exposure to lead, a heavy metal and potent environmental toxicant, can cause damages to the CNS, most prominently via oxidative stress. Administration of NS ethanolic extract has been proven to reverse the known effects of lead by promoting antioxidant marker superoxide

dismutase 1 (SOD1), Peroxiredoxin-6 (PRDX6) and amyloid precursor protein (APP) 695 and impeding APP770 expression, as well as enhancing cell viability in the cortex and hippocampus regions of the brain (Butt et al., 2018). Besides lead, toluene is also an environmental pollutant known to cause significant deterioration to the CNS. Co-administration of NS extract and toluene exposure once daily for 12 weeks reduced the intensity of neuronal changes and immunoreactivity of degenerating neurons in the frontal cortex, hippocampus, and brainstem of rats (Kanter, 2008a, 2008b).

Cerebral ischemia or stroke is similarly known as "brain attack". Stroke occurs when there is cessation of blood flow to the brain that eventually will lead to cell death due to deprivation of oxygen (National Stroke Association, 2019). Intraperitoneal administration of 50 mg/kg of NS extract in stroke model of rats prevented intracellular edema of interneurons and decreased the incidence of edematous astrocytes (Hobbenaghi et al., 2014). Another study on middle cerebral artery occlusion (MCAO) model presented comparable decrease in level of thiobarbituric acid reactive substance (TBARS), increase in levels of GSH, superoxide dismutase (SOD) and catalase levels. Locomotor activity and grip strength of NS treated rats also showed significant improvements (Akhtar et al., 2013).

Table 2.1: Studies on the protective effects of NS against neurotoxicity

Toxicant	NS component	NS dosage	Animal model	Neuroprotective effects	Reference
D-galactose	NS oil	0.1, 0.2, 0.5 ml/kg	Male Razi mice	↑ GSH content in brain ↓ MDA, BAX, BCL2 and caspase3 levels in brain	Shahroudi et al., 2017
EAE induction	Water suspension of grinded NS seeds	2.8 g/kg	Female Wistar rats	Remyelination in medulla and cerebellum † GSH and \ MDA levels in cerebellum \ reactive astrogliosis and expression in cerebellar modullary \ histopathological observations in brainstem	Noor et al., 2015; Fahmy et al., 2014
Global cerebral ischemia-reperfusion injury	NS extract	1, 10, 50 mg/kg	Male and female albino Wistar rats	Prevent intracellular edema of interneurons in 50 mg/kg ↓ edematous astrocytes in 50 mg/kg	Hobbenaghi et al., 2014)
Lead	Ethanolic extract	250 & 500 mg/kg	Female and male Balb/c mice	Dose-dependent inhibition of free radicals Enhanced cell viability ↑ SOD1 and PRDX6 expression ↓ APP770 and APP695 expression	Butt et al., 2018
MCAO model	Petroleum and ether extracts	400mg/kg	Albino Wistar rats	↑ locomotor counts and grip strength ↑ GSH, SOD, catalase levels ↓ TBARS level and infarct volume	Akhtar et al., 2013)

Table 2.1, continued

Toxicant	NS component	NS dosage	Animal model	Neuroprotective effects	Reference
Pentylenetetrazole (PTZ)	Ethanolic extract	100, 200, 400 mg/kg	Wistar rats	Prevented production of dark neurons in hippocampus † latency to onset of seizure † time latency to enter dark compartment (PAT test) ↓ seizure score	Vafaee et al., 2015
Scopolamine	NS oil	1 mg/kg	Male albino Wistar rats	Significantly discriminated novel object in NOR test ↑ correct trials in T-maze alteration task ↑ GSH levels in brain ↓ MDA levels TNF-α content in brain	El-Marasy et al., 2012
Toluene	NS extract	400 mg/kg 50 mg/kg	Male albino Wistar rats	Absence of distorted nerve cells and dark stained nucleus ↓ intensity of neuronal changes ↓ immunoreactivity of degenerating neurons ↓ severity of nucleic and cytoplasmic degeneration ↓ dilataion of endoplasmic reticulum, mitochondrial	Kanter, 2008a, 2008b
Type 2 diabetes mellitus (T2DM)	NS oil	2.0 ml/kg	Male albino Wistar rats	↑ GSH, GPx, GST and SOD levels in brain ↑ BDNF, SIRT1, ADAM10 and miRNAs ↓ TBARS, NO and XO levels in brain ↓ TNF-α, IL-6, IL-1β and iNOS brain and levels ↓ AChE activity, AGE and Aβ-42 levels in brain ↓ APP, BACE1, RAGEs, p53, NF-κBp65 expression	Balbaa et al., 2017

2.4 Effects of TQ on memory and the nervous system

Effects of TQ to mitigate cell and neurotoxicity have been proven in several recent studies, through both *in vivo* and *in vitro* studies. Despite known for its neuroprotective effects, NS is less studied in recent in vitro studies. More focus is given on the effects of TQ, most probably due to it being known as one of the most abundant bioactive constituents of NS. Table 2.2 depicts *in vivo* studies that reported neuroprotective effects of thymoquinone on brain development and behavioural performance of animal models. Table 2.3 depicts *in vitro* studies that reported neuroprotective effects of thymoquinone in different types of cell lines.

2.4.1 In vivo studies on the effects of TQ on nervous system

A study by Khan and his colleagues (2015) showed that 30 mg/kg of TQ reversed the expression of alcohol-induced behavioural sensitization in mice by reducing its hyperlocomotion. Besides that, TQ also showed positive antioxidant effects in Wistar rats exposed to arsenic. Administration of 10 mg/kg arsenic for 8 days (Firdaus et al., 2018) and 20 mg/kg arsenic for 21 days (Kassab & El-Hennamy, 2017) caused an elevation of ROS. However, TQ treatment caused a decrease in intracellular ROS levels and oxidative stress markers such as MDA (Firdaus et al., 2018; Kassab & El-Hennamy, 2017), and a significant increase in antioxidant enzymes which include catalase (CAT), SOD, glutathione peroxidase (GPx) and glutathione reductase (GR) (Firdaus et al., 2018). Levels of norepinephrine (NE), DA and serotonin (5-HT) neurotransmitters and Na+-K+-ATPase in brain also increased (Kassab & El-Hennamy, 2017).

Supplementation of TQ for 11 days could suppress the intensity of acrylamide (ACR)-induced neuropathic syndromes in rats, as the animals showed better performance in gait score behavioural test. In addition, TQ showed antioxidant properties as proven by a decrease

in MDA and increase in GSH levels in rats' sciatic nerves (Tabeshpour et al., 2019). Another study on rats exposed to ACR has also reported that rats administered with 2.5, 5, and 10 mg/kg TQ had dose-dependent improvement in severe gait abnormalities. Reduced levels of MDA were also observed in 5 and 10 mg/kg TQ groups (Mehri et al., 2014).

Pretreatment of TQ to rats with spinal cord ischemia-reperfusion (I/R) injury minimized the severity of hindlimb motor dysfunction, proven by better angles in inclined-plane test. Oxidative stress markers and antioxidant levels in the spinal cord tissue decreased and increased, respectively. Pathological scores of spinal cord samples of TQ treated rats were also lower as compared to the untreated group (Gökce et al., 2016). Oral administration of TQ for 28 days reduced oxidative stress induced by imidacloprid in mice, as evidenced by slight histopathological changes followed by reduced MDA and enhanced CAT levels in the brain (Ince et al., 2013).

Six weeks of TQ oral administration in Sprague-Dawley rats exposed to titanium dioxide nanoparticles showed no brain lesions (Hassanein & El-Amir, 2017). Another study manifested the role of TQ in improving the prognosis of lead-induced brain damage in Sprague-Dawley rats, by decreasing the incidence of lead-induced brain lesions (Radad et al., 2014). Kanter (2008a) investigated on the protective effects of TQ against chronic toluene exposure, and TQ was proven to ameliorate neurodegeneration in the hippocampus. Absence of distorted nerve cells and dark stained nucleus reduced severity of neuronal changes and nucleic and immunoreactivity of degenerating neurons were reported (Kanter, 2008a).

Neurotoxic effects of 6-hydroxy dopamine (6-OHDA), a neurotoxin known to trigger degeneration of dopaminergic neurons and induce parkinsonism in rodents, could be improved by pretreatment of TQ. Less significant rotations in the apomorphine-induced

rotations were observed while loss of substantia nigra pars compacta neurons were prevented. Reduced MDA level in brain was also reported (Sedaghat et al., 2014). It is well known that glutamate is a primary neurotransmitter that plays a role in learning and memory. However, overstimulaton of glutamatergic receptors provokes neuronal apoptosis that leads to many neuropathological conditions including Alzheimer's disease (AD) and Parkinson's disease (PD). Oral administration of TQ in male albino rats improved spatial memory performance, as proven in Y-maze and MWM behavioural tests (Fouad et al., 2018).

D-galactose (D-gal) and aluminium chloride (AlCl₃) when chronically administered together, have been proven to induce learning and memory impairment as well as neurodegeneration in rats (Abulfadl et al., 2018). However, TQ treatment demonstrated improvements in their spatial memory performance in the MWM test. Biochemical analysis of brain tissue also showed reduced levels of MDA and NO oxidative stress markers, increased levels of antioxidants SOD and total antioxidant capacity (TAC) and increased levels of BDNF and BCL2. In addition, TQ treatment marked reduced level of brain TNF-α immunoreactivity.

Prolonged morphine administration is known to induce dependence and tolerance. Pretreatment of TQ was shown to inhibit the development of tolerance towards morphine analgesia. Decreased oxidative stress in the brain was also reported, as evidenced by marked decrease in the MDA concentration and in GSH level and GSH-Px brain activities (Abdel-Zaher et al., 2017, 2013). Furthermore, in another study using rat model of traumatic brain injury (TBI), less degenerative changes in the cytoplasm and nucleus of brain neuronal cells were observed in TQ-treated groups. Rats treated with TQ showed higher neuron densities in the contralateral hippocampal regions and lesser oxidative DNA damage as compared to the untreated rats (Gülşen et al., 2016).

2.4.2 *In vitro* studies on the effects of TQ on nervous system

It has been reported that TQ inhibited spontaneous aggregation and neurotoxicity of amyloid beta-protein 1-42 (Aβ1-42), a protein type which is usually accumulated in AD, in primary hippocampal and cortical neurons. As a result, neuronal cell death significantly decreased (Alhebshi et al., 2014). A similar study against Aβ1-42 neurotoxicity in human induced pluripotent stem cells (hiPSC)-derived cholinergic neurons also demonstrated antioxidant effects of TQ. Cell viability and caspase 3/7 activities were restored to control level, antioxidant enzyme GSH and synaptic vesicles recycling activity increased, and hydrogen peroxide (H₂O₂) level decreased (Alhibshi et al., 2019).

Treatment with 0.1 and 1 μM TQ reduced lactate dehydrogenase (LDH) activity in primary cultured cerebellar granule neurons exposed to β-amyloid (Ismail et al., 2013). Level of condensed chromatin, free radicals and caspase3 activity were also reduced. Consequently, intact cell bodies, neurite network and cell viability were notably preserved. Besides that, TQ also proved to restore cell viability and protect cells against damage in SH-SY5Y human neuroblastoma cells against H₂O₂ toxicity. Antioxidant capacity of TQ was demonstrated by an increase of SOD1, SOD2 and catalase antioxidant genes, decrease of ROS, and reduce of necrotic and apoptotic cells (Ismail et al., 2016).

Studies on SH-SY5Y human neuroblastoma cells and prenatal rat cortical neurons proved that TQ has dose-dependent protective effects against arsenic (As) and ethanol toxicity, respectively. In both studies, TQ significantly decreased cytotoxicity and ROS levels. TQ also successfully restored mitochondrial membrane potential (Firdaus et al., 2019; Ullah et al., 2012). Anti-apoptotic effects of TQ were proven by the decline of BAX protein expression and cleaved poly (ADP-ribose) polymerase 1 (PARP1), and increased levels of

BCL2 markers (Firdaus et al., 2019). Elevation of cytosolic free Ca²⁺ concentration, release of cytochrome-c into cytosol, apoptotic cell death, cleaved PARP-1 level, and caspase-3 activation were attenuated in TQ-treated cells (Ullah et al., 2012).

Neuroinflammation and microglial activation generates ROS production which induce neurodegeneration such as shown in AD and Parkinson's Disease (PD). A study on lipopolysaccharide interferon gamma (LPS/IFNγ) activated BV-2 murine microglial cells proved the ability of TQ to significantly reduce NO and H₂O₂ levels in cells exposed to LPS/IFNγ or H₂O₂. Antioxidant effects of TQ were manifested, as evidenced by an increase in the levels of antioxidants GSH and SOD, downregulation of C-C, chemokine ligand 5 (CCL5), nitric oxide synthase (NOS) 2, prostaglandin-endoperoxide synthase (PTGS) and thioredoxin-interacting protein (TXNIP) pro-oxidant genes, and upregulation of peroxiredoxin 1 (PRDX1) and sulfiredoxin 1 (SXRN1) antioxidant genes (Cobourne-Duval et al., 2016).

Induced neurotoxicity by α -synuclein (α SN), a protein type known to accumulate in common neurodegenerative disease such as AD and PD, could be diminished by TQ in cultured hippocampal and hiPSC stem cells. TQ marked an increase in the level of synapsin 1 and synaptophysin levels in hippocampal and hiPSC stem cells, respectively. Synaptic and spontaneous firing activities were maintained in both cells (Alhebshi et al., 2013).

Besides the CNS, a study by Üstün and team (2018) demonstrated positive effects of TQ on damages in the PNS. Peripheral nerve injury (PNI) is a pathological condition linked to motor, sensory and autonomic functions. The task in repairing these nerves is substantially carried out by Schwann cells (SC) surrounding the axons. Treatment of 50 and 75 nM TQ in

a PNI dorsal root ganglion primary culture model elevated SC proliferation and migration, fibroblast proliferation and the survival rate of damaged neurons.

Table 2.2: In vivo studies on the protective effects of TQ against neurotoxicity

Toxicant	TQ dosage	Animal model	Neuroprotective effects	Reference
Acrylamide	2.5, 5 and 10	Wistar rats	Dose-dependent improvement in severe gait abnormalities	Tabeshpour
(ACR)	mg/kg		↑ GSH levels in sciatic nerve	et al., 2019;
			↑ P-ERK ratio, MBP content	Mehri et al.,
			↓ P-JNK/JNK, P-P38/P38, BAX/BCL2, caspase3 and caspase9	2014
			↓ MDA levels in sciatic nerve and in cerebral cortex	
Alcohol	10, 20 and 30 mg/kg	Mice	↓ locomotor activity in 30 mg/kg TQ group	Khan et al., 2015
Arsenic (As)	2.5 and 5	Wistar rats	↑ CAT, SOD, GPX, and GR antioxidants	Firdaus et
()	mg/kg		↑ NE, DHA, 5-HT, Na+-K+-ATPase levels	al., 2018;
	8 8		↑ mitochondrial membrane potential	Kassab &
	10 mg/kg		ROS, MDA, TNF-α, BAX and caspase3 mRNA	El-
				Hennamy, 2017
D-galactose (D-	20 mg/kg	Male Sprague	↓ escape latency time in MWM test	Abulfadl et
gal) and		Dawley rats	↑ time spent in target quadrant in MWM test	al., 2018
aluminium			↑ ACh immunoreactivity, BDNF, BCL2, SOD and TAC	
chloride (AlCl ₃)			↓ MDA, NO, AChE activity and TNF-α immunoreactivity	
Glutamate	2.5 and 10	Male albino rats	↑ SAB% in Y-maze test	Fouad et
	mg/kg		↓ MEL in MWM test	al., 2018
			↓cyto-C, caspase3, LDH and Aβ-42 levels	
Lead	20 mg/kg	Male Sprague Dawley rats	↓ incidence of pathological lesions in brain	Radad et al., 2014

Table 2.2, continued

Toxicant	TQ dosage	Animal model	Neuroprotective effects	Reference
Imidacloprid	10 mg/kg	Male and female	↑ CAT levels	Ince et al.,
(IMI)		Swiss albino mice	↓ MDA level	2013
Morphine	10 mg/kg	Male Swiss- Webster mice	Inhibited tolerance development towards morphine analgesia ↑ brain neuronal NO synthase mRNA expression ↓ brain intracellular GSH, GPX, MDA and serum nitrite levels ↓ development of withdrawal manifestations	Abdel- Zaher et al., 2013, 2017
Spinal cord ischemia- reperfusion (I/R) injury	10 mg/kg	Male Wistar albino rats	Better angles in inclined-plane (IP) test ↑ SOD, GPX, CAT levels in spinal cord tissue ↓ severity of hindlimb motor dysfunction ↓ MDA, NO, caspase3, TNFα and IL-1 levels ↓ pathological scores of spinal cord samples	Gökce et al., 2016
Toluene	50 mg/kg	Male Wistar albino rats	 ↓ intensity of neuronal changes ↓ immunoreactivity of degenerating neurons ↓ severity of nucleic and cytoplasmic degeneration 	Kanter 2008a
Traumatic brain injury (TBI)	5 mg/kg	Female Wistar albino rats	Absence of darkly stained nucleus Reduced shrunken nerve cells ↑ neuron densities in contralateral hippocampal regions ↓ levels of oxidative DNA damage	Gülşen et al., 2016
6-hydroxy dopamine (6- OHDA)	5 and 10 mg/kg	Adult male Wistar rats	Prevented loss of substantia nigra pars compacta (SNC) neurons ↓ rotations in apomorphine-induced rotations ↓ MDA level in brain	Sedaghat et al., 2014

Table 2.3: In vitro studies on the protective effects of TQ against neurotoxicity

Toxicant	Dosage	Cell line	Neuroprotective effects	Reference
Amyloid beta-protein 1-42 $(A\beta_{1-42})$	100nM	hiPSC-derived cholinergic neurons	Restored cell viability and caspase 3/7 activities ↑ GSH level ↓ H ₂ O ₂ concentration ↓ uptake of FM1-43	Alhibshi et al., 2019
Arsenic (As)	10μM and 20μM	SH-SY5Y human neuroblastoma cells	Restored BAX and BCL2 protein level markers ↓ intracellular LDH activity and ROS ↓ cleaved PARP1 and degree of DNA fragmentation	Firdaus et al., 2019
α-synuclein (αSN)	100nM	Cultured hippocampal and human induced pluripotent stem cells (hiPSC)	Maintained synaptic activities in hippocampal neurons Maintained spontaneous firing activity in both cells ↑ synapsin 1 levels in hippocampal neurons ↑ synaptophysin levels ↓ synapse damage in hiPSC neurons	Alhebshi et al., 2013
β-amyloid	0.1 and 1 μM	Primary cultured cerebellar granule neurons	Preserved intact cell bodies and neurite network Maintained cell viability LDH activity and production of free radicals condensed chromatin caspase3 activity	Ismail et al., 2013

Table 2.3, continued

Toxicant	Dosage	Cell line	Neuroprotective effects	Reference
Ethanol	10, 15, 25 and 35 μM	Prenatal rat cortical neurons	Maintain physiological mitochondial transmembrane potential ↑ expression of BCL2 ↓ expression of BAX ↓ release of cytochrome-c into cytosol ↓ cleaved PARP-1 level and caspase-3 activation ↓ elevation of cytosolic free calcium	Ullah et al., 2012
LPS/IFNγ or H ₂ O ₂	Range of 0- 40 μM	BV-2 murine microglial cells	↑ GSH and SOD levels in both cells ↑PRDX1, SXRN1 genes ↓ superoxide levels in both TQ treated cells ↓ NO in TQ treated LPS/IFNγ cells ↓ H ₂ O ₂ in TQ treated H ₂ O ₂ cells ↓ lipid hydroperoxides and catalase in both cells ↓ C-C, CCL5, NOS2, PTGS and TXNIP genes	Cobourne- Duval et al., 2016
Peripheral nerve injury (PNI) model	50, 75, 100, 250, 500 nM	Dorsal root ganglion (DRG) primary culture	↑ survival rate of damaged neurons in 50 and 75nM TQ ↑ schwann cells (SC) proliferation and migration ↑ fibroblast proliferation	Üstün et al., 2018

CHAPTER 3: MATERIALS AND METHOD

3.1 Experimental design

The study consisted of three main experiments that comprised two preliminary experiments, in which results from the two were used in the final experiment. Based on the specific objectives mentioned in Chapter 1, Experiment 1 and 2 were carried out to separately examine effects of toluene or NS treatments involving NS seeds (NSS), NS oil (NSO), and its bioactive constituent, thymoquinone (TQ) on mouse brain histology and recognition memory by NOR test, respectively. Experiment 3 demonstrated effects of NSS, NSO, and TQ against toluene on the recognition memory performance, brain morphology, and morphometric properties of the hippocampal CA1 pyramidal neurons of the experimental animals. The general overview of methodology used in this study is as shown in Figure 3.1.

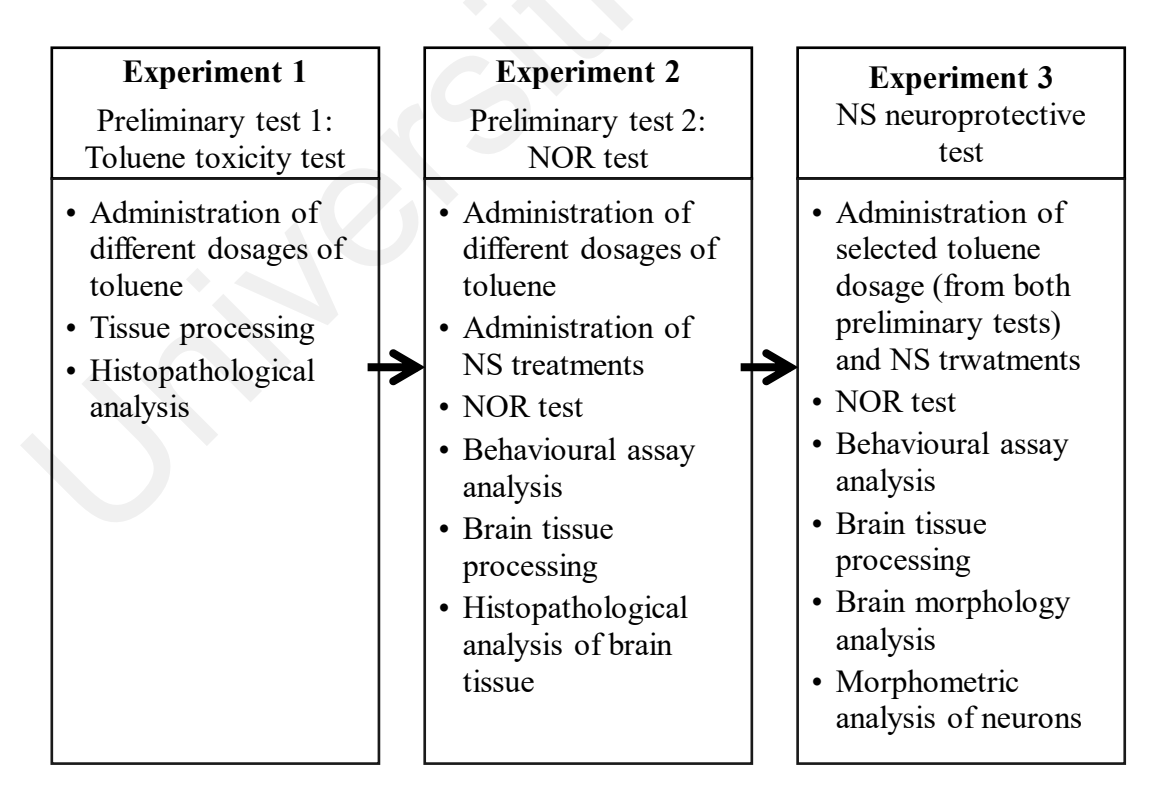


Figure 3.1: General overview of research methodology

3.1.1 Preliminary test 1: Toluene toxicity test

This toluene toxicity test was conducted to determine the lowest toluene dosage with the highest neurotoxicity effects. The direct effects of different dosages of toluene on mice were evaluated, based on histopathological effects on tissue of selected vital organs. Mice were randomly divided into 4 groups (n=3 per group) as shown in Table 3.1. Three different concentrations of toluene as established by previous studies (Seo et al., 2010; Win-Shwe & Fujimaki, 2013) were intraperitoneally (i.p.) administered to the mice daily for 7 consecutive days. The mice were sacrificed 24 hours after the final administration and the brains were dissected and processed for histological analysis.

Table 3.1: Grouping, type of treatments and dosage

Group	Treatment	Dosage
1	Corn oil (toluene carrier)	1 ml/100 g b.w.
2	Toluene	100 mg/kg b.w.
3	Toluene	300 mg/kg b.w.
4	Toluene	500 mg/kg b.w.

[•] b.w. = body weight

3.1.2 Preliminary test 2: Novel Object Recognition test

NOR test was conducted to investigate the memory performance of mice treated with toluene and/or NS treatments. Toluene dosages were similar as used in Experiment 1. As for NS treatments, the dosages used were based on (Baghcheghi et al., 2018; Al-Nailey, 2010; Cheema et al., 2018). Mice were randomly divided into groups (n=3 per group) as shown in Table 3.2. Treatments were administered daily for 7 consecutive days followed by NOR test for 4 days. The mice were sacrificed 24 hours after NOR test and the brains were dissected

and processed for histological analysis. Brain tissue sections were examined to evaluate whether the 4-days gap of NOR test had any different effects on the tissue histology, as compared to the tissue sections in Experiment 1.

Table 3.2: Grouping, type of treatment, dosage, and route of administration

Group		Treatment	Dosage	Route of administration	
Toluene treatment groups	1	Corn oil (control)	1 ml/100 g b.w.	Intraperitoneal	
	2	Toluene	100 mg/kg b.w.		
	3	Toluene 300 mg/kg b.w. inje		injection	
	4	Toluene	500 mg/kg b.w.		
	1	Corn oil (control)	1 ml/100 g b.w.		
NS treatment groups	2	NSS	10 mg/kg b.w.	Oral gavage/	
	3	NSO	0.1 ml/kg b.w.	Force-feeding	
	4	TQ	10 mg/kg b.w.		

3.1.3 Test 3: Nigella sativa (NS) neuroprotective test

This test was conducted to investigate the neuroprotective effects of NS treatments against neurotoxicant toluene from the aspects of: (i) behavioural performance, (ii) brain morphology, and (iii) cellular morphometry. Mice were randomly divided into 5 groups (n=6 per group) as shown in Table 3.3. NS supplementation was carried out for 14 consecutive days. On day 8 until 14, toluene was administered to the NS-supplemented mice. The dosage of toluene administered was 500 mg/kg, based on the results obtained from the preliminary tests.

Table 3.3: Grouping and type of treatment

Group	Treatment		
1	CO : Corn oil (10 ml/kg b.w.)		
2	TOL	: Toluene (500 mg/kg b.w.)	
3	TOL-NSS	: NSS (10 mg/kg b.w.) + Toluene (500 mg/kg b.w.)	
4	TOL-NSO	: NSO (0.1 ml/kg b.w.) + Toluene (500 mg/kg b.w.)	
5	TOL-TQ	: TQ (10 mg/kg b.w.) + Toluene (500 mg/kg b.w.)	

3.2 Animal care and maintenance

Adult male ICR mice (8 weeks old) with average weight of 20-40 g were used in the current study. Animals were procured from Takrif Bistari Enterprise, a local supplier in Serdang. Upon arrival, mice were quarantined at the Laboratory Animal Centre (LAC) for 14 days. Mice were housed in polypropylene cages, with 3-6 mice per cage, maintained at room temperature and exposed to 12 hours light/dark per day. Each cage was labeled for treatment and record purposes (Figure 3.2). Markings were made on the tail of each mouse using different colours of marker pens. This was important to be able to distinguish individuals within a cage. Autoclavable mice pellet (Altromin) and filtered tap water were provided *ad libitum* daily.

Corn cob was used as the cage bedding. Usage of corn cob as rodent bedding was preferable as it produced no dust, reduced the spread of allergens, absorbed better, and minimized the production level of ammonia. Thus, the cages remained clean and dry for a longer time. Cage bedding was only changed every 2 weeks. Shredded paper were put inside each cage as environment enrichment. Animal handling was carried out for 3 to 5 days prior to treatment to familiarize animals with the experimenter. All experiments were carried out in accordance with the ethics and regulation approved by the Institutional Animal Care and

Use Committee University Malaya, with an ethics clearance number of S/03122018/01082018-01/R (Appendix A).



Figure 3.2: Animals in labeled cages

3.3 Body weight monitoring

Body weight of animals were measured and recorded daily before administration of treatments to ensure the correct dosage of administration (Figure 3.3).



Figure 3.3: Animals were weighed daily before treatment administration

3.4 Treatment administration

3.4.1 Oral gavage/ Force feeding

Mouse was picked up from the cage by its tail and placed on the wire cage top. While holding the tail near the base, the loose skin along the neck was gripped with the opposite hand using a cloth. The head should be slightly pulled back to allow a straightened esophagus and neck axis. Its tail was placed between fingers to secure it. Once secured, the blunt-end tip of the 22G gavage needle was placed into the right lateral slide of the animal's mouth, slid down at the back of the mouth into the esophagus, before slowly administering the treatments (Figure 3.4).



Figure 3.4: Oral administration using a feeding needle

3.4.2 Intraperitoneal injection

Mouse was restrained using similar method as described for oral administration. Once secured, mouse was tilted with its head downwards. Area of injection was swiped with an

alcohol swab. A needle was inserted at the lower left or right quadrant of abdomen at a 30° angle and treatment was administered slowly (Figure 3.5).



Figure 3.5: Intraperitoneal administration

3.5 Treatment solution preparation

Corn oil, toluene, NSS suspension (Elshama et al., 2013), NS oil, and TQ were prepared prior to experiment (Figure 3.6). Each prepared solution was labeled and kept in different bottles to avoid contamination. All treatment solutions were kept in a cool and dry place at room temperature.

3.5.1 Corn oil

Corn oil served as a blank control for toluene and NS treatment groups. Corn oil (Vecorn, Malaysia) was administered directly without further dilution. Dosage given to the mice was 1 ml/100 g body weight of mice.

3.5.2 Toluene

Toluene (99.9% purity, EMSURE ® ACS, ISO, Reagent Ph Eur, Sigma Aldrich) was diluted with corn oil. Toluene dosages of 100, 300 and 500 mg/kg body weight of mice, to a final concentration of 1 ml/100 g body weight of mice were prepared. For 100 mg/kg, 0.001 ml toluene was diluted with 0.099 ml corn oil. For 300 mg/kg, 0.003 ml toluene was diluted with 0.097 ml corn oil. For 500 mg/kg, 0.006 ml toluene was diluted with 0.094 ml corn oil (Appendix B).

3.5.3 Nigella sativa seeds (NSS)

A final concentration of 1.0 ml of diluted NSS suspension per 100 g body weight of mice was prepared. To prepare the stock solution of crude suspension, 1 g of NSS were cleaned, dried, and powdered before being mixed with 100 ml of corn oil (Essawy et al., 2012). Finally, 0.01 ml of the stock solution was then diluted with 0.09 ml corn oil (Figure 3.6a) (Appendix C).

3.5.4 *Nigella sativa* oil (NSO)

Pure NSO (Dogaci, Turkey) was used. To obtain a final concentration of 1.0 ml of diluted NSO per 100 g body weight of mice; 0.01 ml NSO was diluted with 0.99 ml corn oil (Figure 3.6b) (Appendix D).

3.5.5 Thymoquinone (TQ)

A dosage of 10 mg/kg body weight of TQ was given to the mice. To prepare the stock solution, 100 mg of TQ powder (Sigma Aldrich, United States (US)) was dissolved in 10 ml of corn oil. Then, 0.01 ml of the stock solution was diluted with 0.09 ml corn oil to obtain a

final concentration of 1.0 ml of diluted TQ solution per 100 g body weight of mice (Figure 3.6c) (Appendix E).

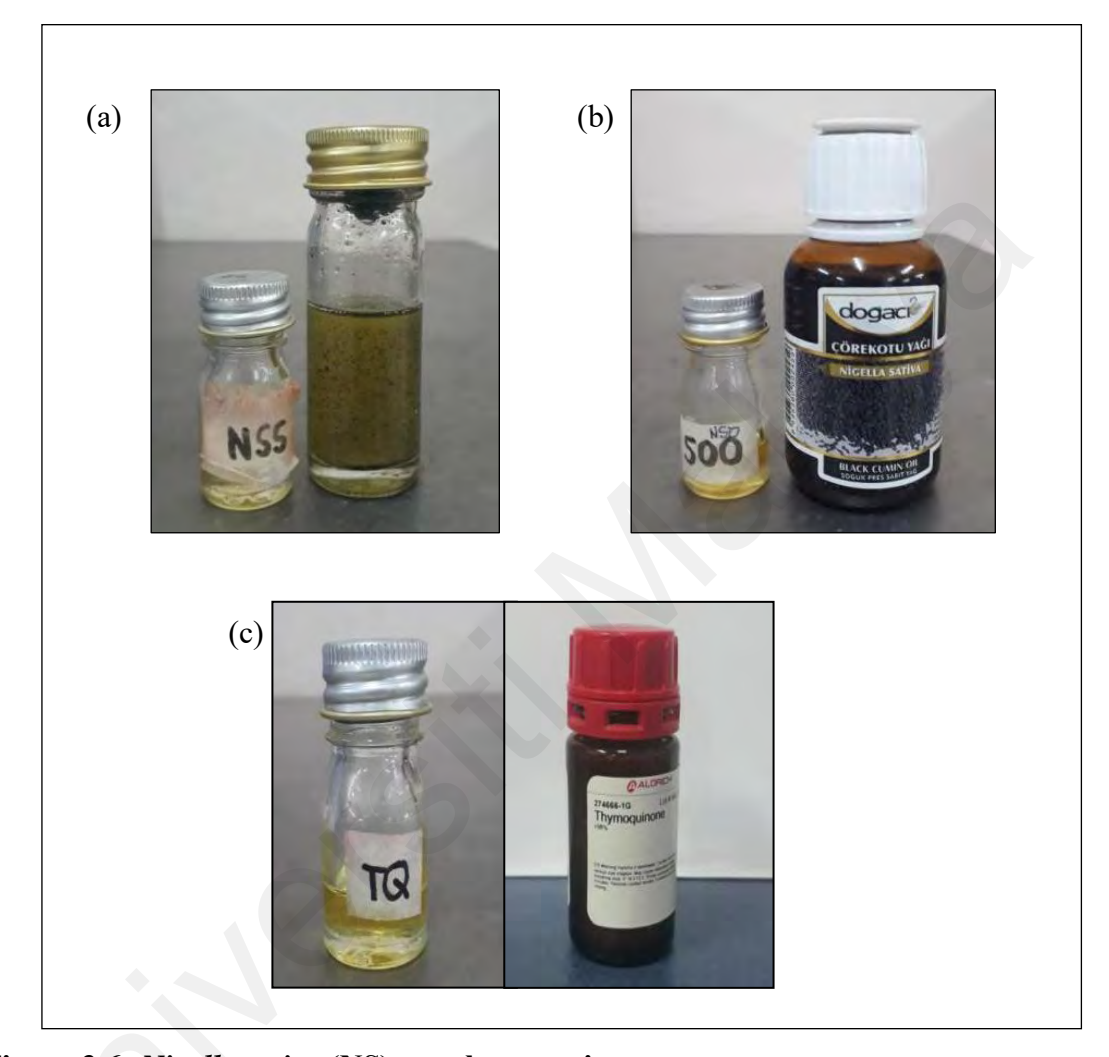


Figure 3.6: Nigella sativa (NS) supplementations

- (a) Nigella sativa seeds (NSS) suspension (Left: diluted solution, right: stock solution)
- (b) Nigella sativa oil (NSO) (Left: diluted solution, right: pure oil)
- (c) Thymoquinone (TQ) (Left: diluted solution, right: pure compound)

3.6 Novel Object Recognition (NOR) test

Novel Object Recognition (NOR) test is a widely used test to examine the recognition memory performance of animals. The test in this study was conducted according to previously described protocol by Huang and Hsueh (2014).

3.6.1 Task protocol

NOR test consisted of three (3) phases, which were habituation phase (Phase 1), familiarization phase (Phase 2), and test phase (Phase 3) (Figure 3.7). NOR test was conducted for 4 days, 24 hours after the final treatment. Animal behaviour was video recorded during Phase 3. Every test was conducted between 8.30 a.m. to 12 p.m. to ensure a standardized environment and to avoid unnecessary light, noise or other stressful events that could have influenced the animal behaviour.

On the first two days of the test, mouse was subjected to the habituation phase (Phase 1). Every day before the test was conducted, the arena was thoroughly wiped with 70% ethanol solution. During habituation phase, mouse was placed in the middle of the arena and allowed to explore the empty arena for 10 minutes each day. The purpose of this phase was to enable the mouse to become familiar with the environment inside the arena; hence, increasing the probability of its interest to explore objects presented during the next two phases of NOR test. The duration of exploration was monitored using a stopwatch with its alarm sound muted. It was important to keep the environment quiet during this time to avoid any noise that would cause disturbance to the mouse. In between animals, the arena was wiped with 70% ethanol solution to remove any olfactory cues.

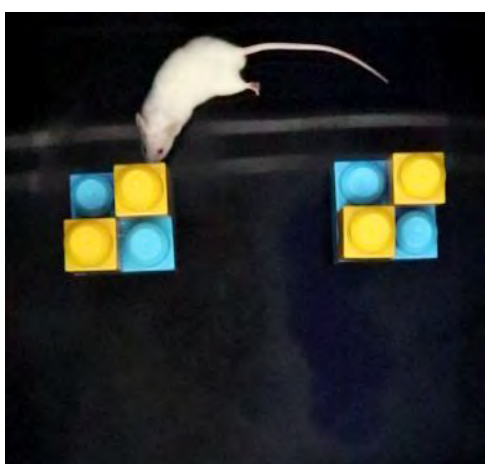
During both familiarization and test phases, objects were placed inside the arena at the far end away from the end where the mice were placed. On the third day, mouse was subjected to familiarization phase. During this phase, two identical objects (A+A) or (B+B) were put inside the arena, each towards the left or the right side. Half of the mice were familiarized with objects A while the other half were familiarized with objects B. Mouse was gently placed at the opposite end of the arena, far from the objects and facing the wall, to prevent coercion. Mouse was allowed to explore the two similar objects for 10 minutes. The duration was again monitored using a stopwatch with its alarm sound muted. Both objects and the arena were wiped with 70% ethanol solution in between animals to remove any olfactory cues.

On the last day, mouse was subjected to test phase. During this phase, one of the objects used in the familiarization phase was replaced by a novel object (A+B). Use of each object (A and B) were counterbalanced to ensure that the objects were used equally as a novel object. The position of the novel object was also counterbalanced between left and right to ensure no location preference that might affect the results. Similar to the familiarization phase, mouse was placed at the opposite end of the arena, facing the wall to prevent coercion. Mouse was allowed to explore the objects for 5 minutes. To minimize olfactory cues, both arena and objects were thoroughly wiped with 70% ethanol solution in between tests and animals.



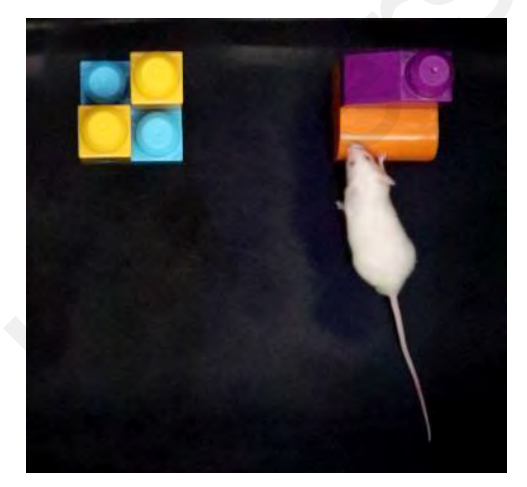
DAY 1 AND 2 Phase 1: Habituation phase

Mouse was allowed to explore the empty arena for 10 minutes each day for two days



DAY 3 Phase 2: Familiarization phase

Mouse was allowed to explore two identical structural objects that were placed at a specified distance from each other in the arena for 10 minutes



DAY 4
Phase 3: Test phase

Mouse was allowed to explore one familiar structural object and one novel structural object placed at a specified distance from each other in the arena for 10 minutes

Figure 3.7: Novel Object Recognition (NOR) test

3.6.2 Apparatus

The main reference guideline for the build-up of the NOR test arena in the present study was as described by Denninger et al. (2019). The apparatus used in this test was a square arena ($40 \times 40 \times 40$ cm), made of acrylic sheets that were strongly glued together. The base of the arena was painted black to reduce the reflection property of the acrylic sheet. The arena was placed at a fixed position at the far-right corner of the Laboratory Animal Centre (LAC) on each day of the test to minimize external noise and to ensure consistency throughout the experiment. During the test, the structural objects were placed at the back-left and back-right corner of the arena, at a specified distance of 9 cm from the adjacent walls and 9.6 cm from each other (Figure 3.8). The objects were fastened to the arena floor with a cellophane tape to avoid them from being moved by the mouse. A video camera was placed directly overhead of the arena to provide a good top-down view of the animal exploration in the arena (Figure 3.9).

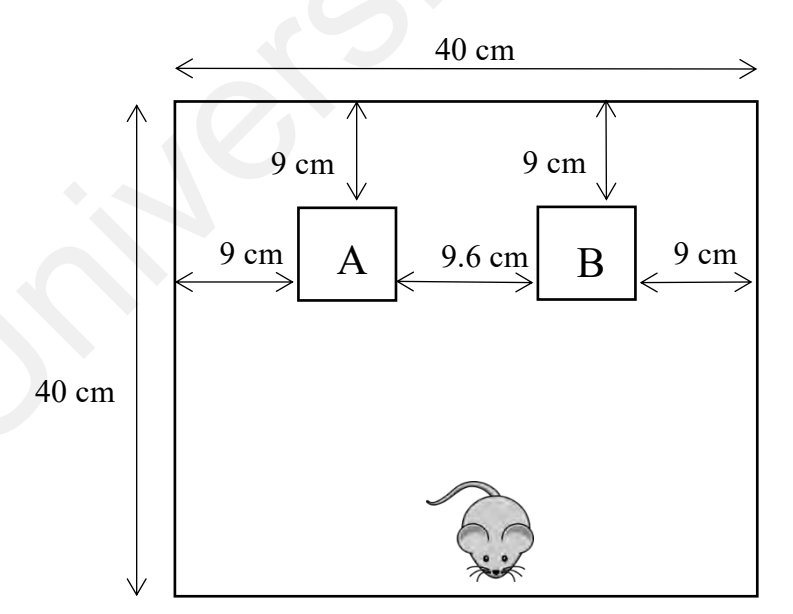


Figure 3.8: Schematic diagram of the apparatus. As shown in the image, structural objects were placed at the back-left and back-right corner of the arena.





Figure 3.9: Video camera set up for recording during the Phase 3 (test phase) of NOR test. (a) Front view (b) Top view.

3.6.3 Structural objects

Structural objects used in this test were made up of plastic play blocks of different colours and shapes, but with similar height and texture. The height of the structural objects used was 11.5 cm with a base of 6.2 cm length and 6.2 cm width (Figure 3.10), comprised of specific blocks. Two identical copies of objects were used to reduce olfactory cues. Objects were wiped with 70% ethanol solution in between tests and animals, to further prevent bias due to any olfactory cues.

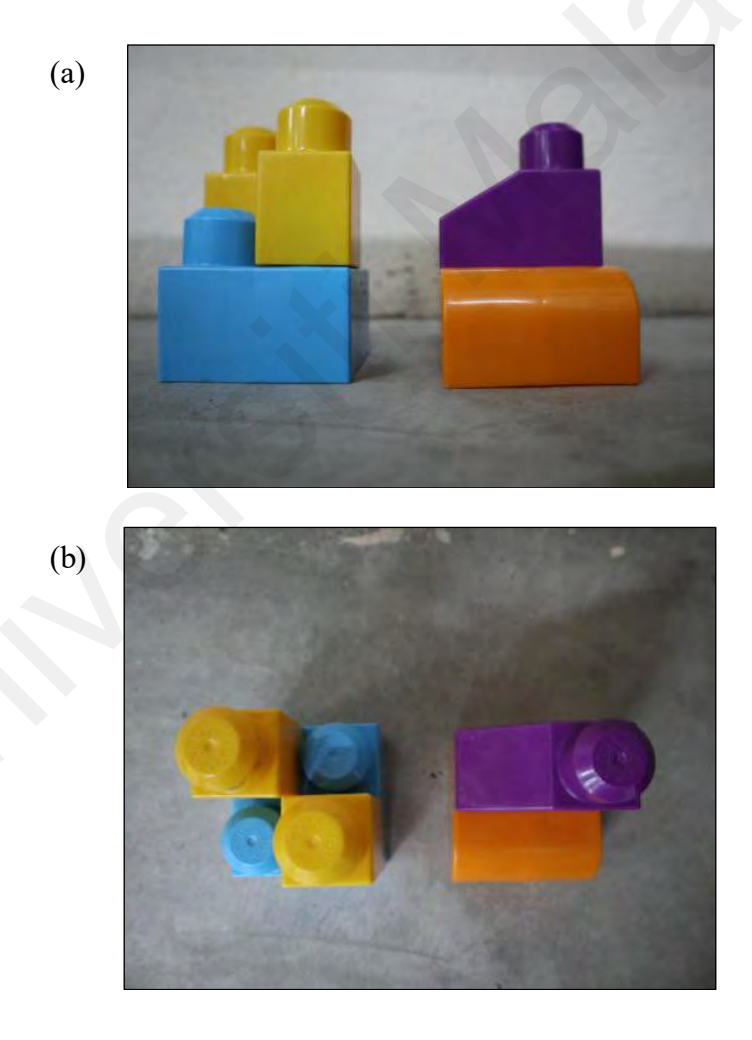


Figure 3.10: Structural objects made up of blocks that were used in the Novel Object Recognition (NOR) test. (a) Front view of structural objects (b) Top view of structural objects.

3.6.4 Behavioural analysis

Animal behaviour was recorded throughout the tests. The videos were named according to the date and time they were taken. Researcher was blinded to the treatment groups when the NOR videos were analysed. Object exploration time and locomotor activity were measured using a semiautomatic behavioural tracking software, OptiMouse (Ben-Shaul, 2017). Object exploration time was defined as the length of time of mouse directing its nose at a distance of 2 cm or less from the object, with active vibrissae sniffing or pawing the object. Just sitting or standing on the object without any active vibrissae was not included as object exploration behaviour. Results that were automatically generated by the software include: (i) distance travelled, (ii) mouse nose locations, (iii) nose zone preference, and (iv) zone visit statistics (Figure 3.11 and Figure 3.12). For the assessment of the object recognition memory performance, the percentage of object preference and discrimination index during the test phase were calculated as according to the following formulas:

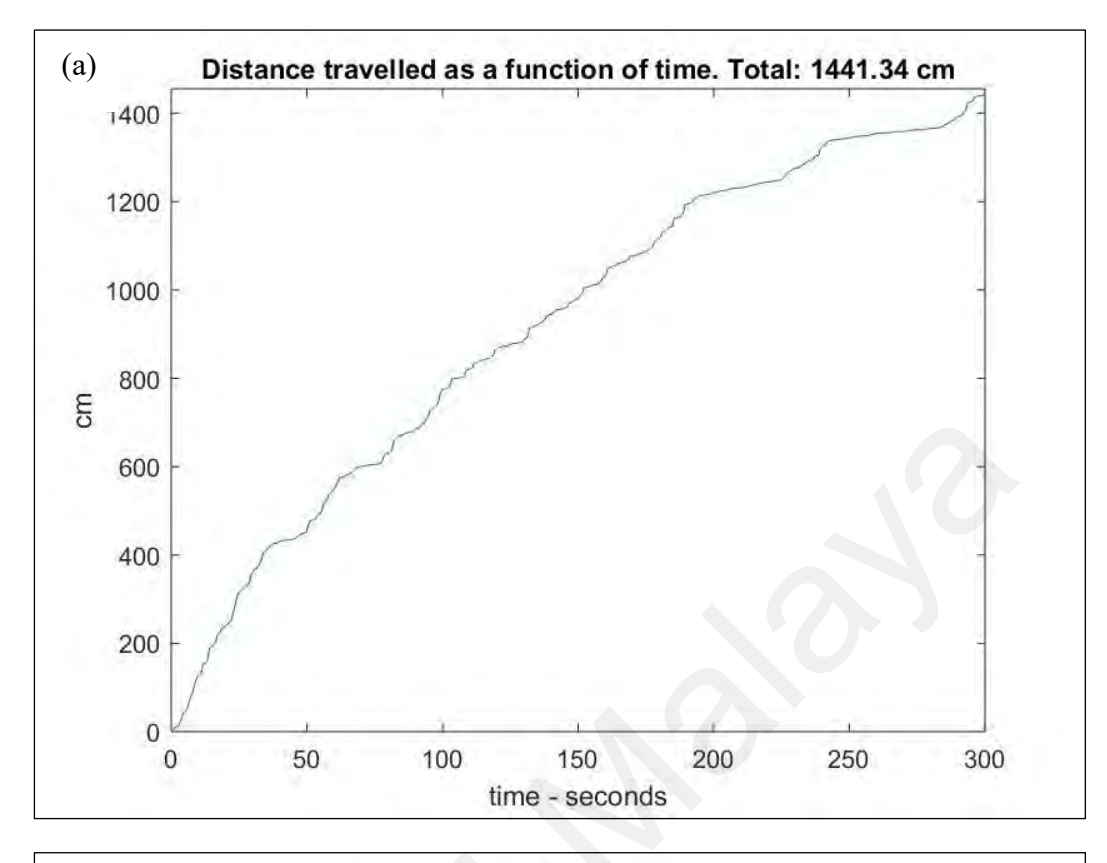
Percentage of object preference (%) =
$$\frac{\text{N or F}}{(\text{N + F})} \times 100\%$$

Discrimination index (DI)
$$= \frac{(N-F)}{(N+F)}$$

Where, N: cumulative time spent exploring novel object

F: cumulative time spent exploring familiar object

For the discrimination index, a positive value indicated more time exploring the novel object. A discrimination index of zero indicated equal time spent with both objects, while a negative value indicated more time investigating the familiar object (Denninger et al., 2018).



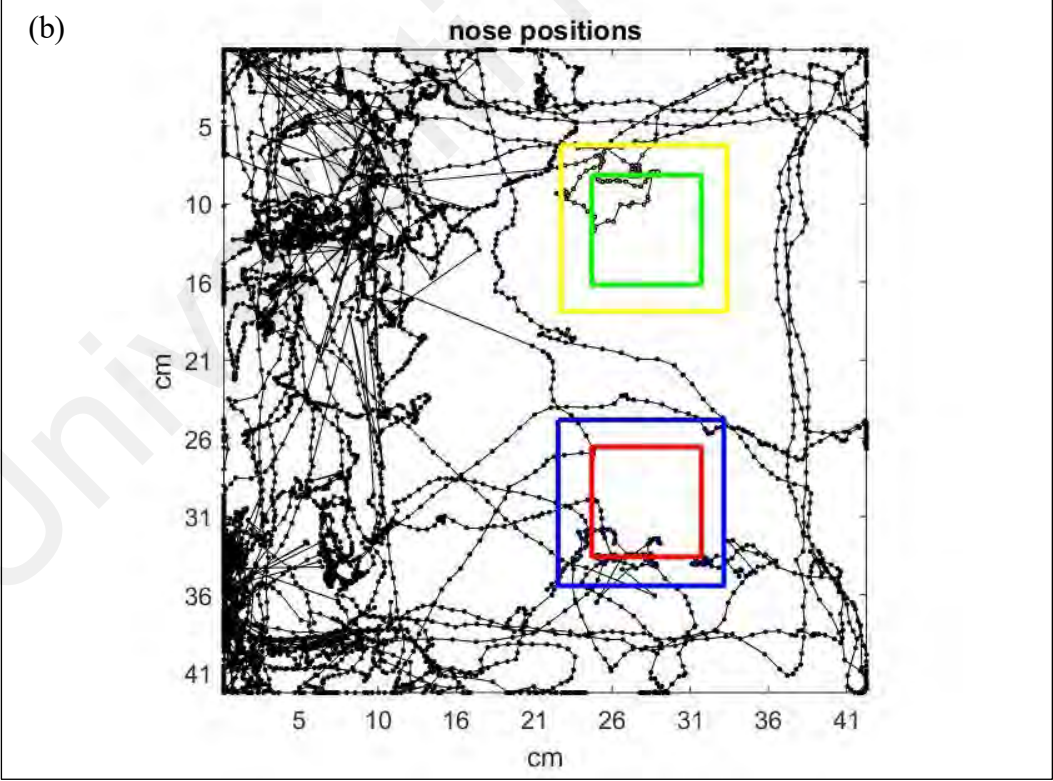
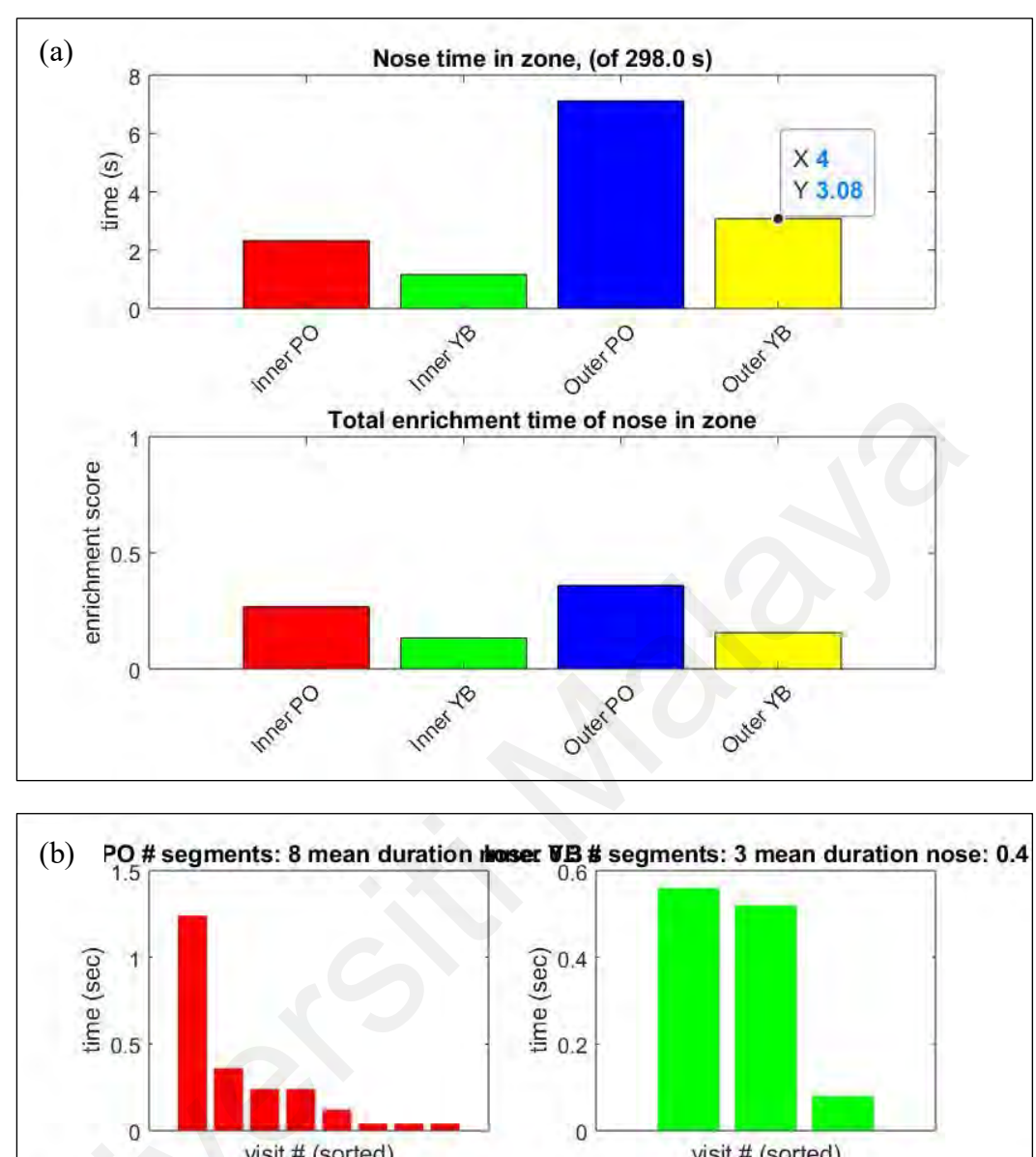


Figure 3.11: Examples of results generated by the OptiMouse semiautomatic analysis behavioural tracking software. (a) Distance travelled by mouse during test phase. (b) Positions of mouse nose in the arena during test phase.



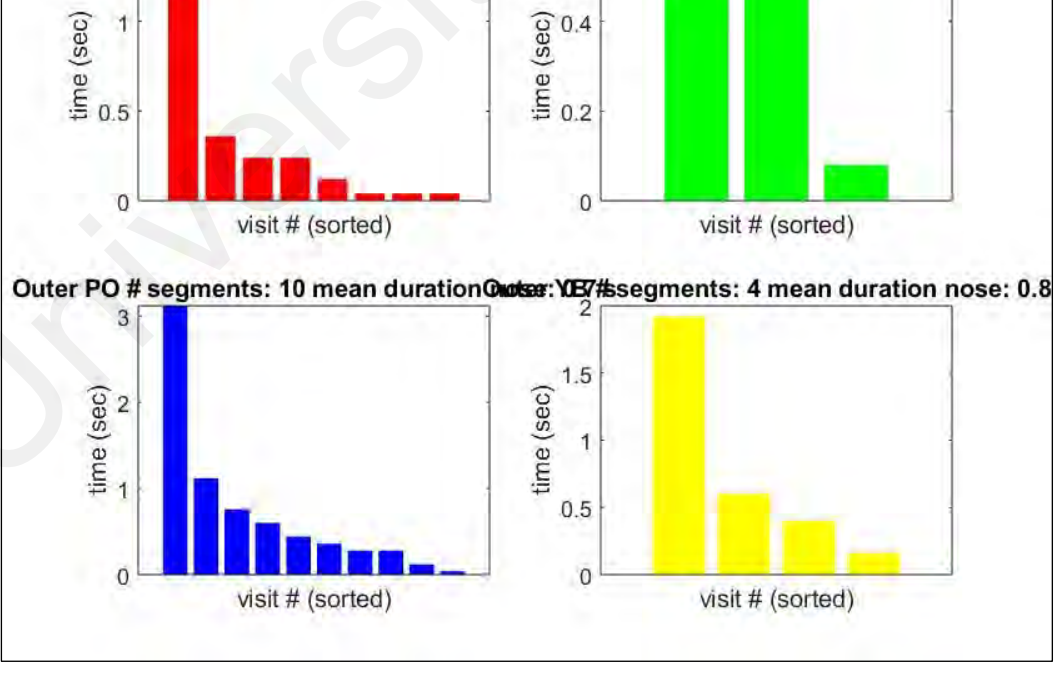


Figure 3.12: Examples of results generated as histograms from data by OptiMouse semiautomatic analysis. (a) Nose zone preference during test phase. (b) Number of visits of mouse nose in each zone during test phase.

3.7 Histological processing of brain and other vital organs

After completion of treatment administration and/or NOR test, the brain, heart, kidney, and liver were dissected for further histological analysis. Histological processing of the tissues involved several steps: fixation, dehydration, clearing, infiltration, embedding, tissue sectioning, mounting of tissue sections onto slides, staining and cover slip mounting (Figure 3.20).

3.7.1 Intracardiac perfusion

Fixation was a procedure conducted to preserve the tissue in a life-like state. Intracardiac perfusion used in this study utilized the natural vascular network of the organism to achieve a more rapid and thorough fixation. This method directly introduced the fixative solution via the circulatory system, either through the heart or the abdominal aorta after flushing of the blood within the system. This enabled the fixative solution to reach each brain region and other tissues at the same rate.

Prior to starting the perfusion fixation procedure, the animal concerned was anesthetized with a ketamine/xylazine cocktail. The ketamine/xylazine cocktail was purchased from the Animal Experimental Unit (AEU) in Faculty of Medicine, Universiti Malaya. The dosage of anesthetics was 80 mg/kg of ketamine and 8 mg/kg xylazine, administered via intraperitoneal route. Once the mouse reached a surgical plane of anesthesia, it was placed on the dissecting tray. The setup of apparatus and equipment for intracardiac perfusion is shown in Figure 3.13. Tape or needles were used to hold its appendages to ensure that the mouse was securely fixed onto the tray. The depth of anesthesia was determined by toe pinch-response method. The mouse must be unresponsive before the procedure was continued. Before surgery was conducted, the mouse's abdomen surface was sanitized with 70% alcohol solution.

A lateral incision was made at the abdomen to expose the abdominal cavity. Then, the cut was continued in the rostral direction until beneath the rib cage. By holding on to the sternum, a small incision was made in the diaphragm and along the rib cage, opening access to the thoracic cavity. The sternum was lifted to allow a clearer view of the heart and vessels and any connective tissue enveloping the heart was cut out. The heart was observed to be still beating.

While holding the heart steady with forceps, a cut was made at the atrium with sharp scissors. Then, a 27-gauge needle that was connected to a perfusion pump, was inserted directly into the protrusion of the left ventricle. The perfusion pump was switched on, allowing saline solution to flow into the heart. This would flush out blood from the circulatory system. Once the blood flowing out of the cut at the atrium had become clear, the outlet tube of the peristaltic pump was changed from saline to 10% formalin solution. No air bubbles were allowed to be introduced. At times, spontaneous movement of the mouse's limbs could be seen indicating muscles being fixed. Lightened colour of livers indicated that the perfusion process was almost complete and once the mouse stiffened, the perfusion process was terminated.



Figure 3.13: Setup of apparatus for intracardiac perfusion

3.7.2 Dissection and sample abstraction

The head of the perfused mouse was removed using scissors. A midline incision was made from the back of the head towards the nose, and skull was exposed. Any remaining muscles attached to the skull was trimmed off. A small cut was made at the back edge of the skull using sharp scissors. Next, the tips of forceps were inserted slowly into the cranial cavity slightly beneath the skull, and pushed upwards, to peel off the skull. This step was repeated cautiously without causing any damage to the brain, until the skull was completely cleared away. Using a small spatula, the olfactory bulbs, and nervous connections along the ventral surface of the brain were severed. The brain was gently lifted and placed in a vial containing 10% formalin solution. The brain was kept in the fixative solution for 48 hours.

Other vital organs including heart, liver, and kidney, were cut into smaller sections. For the heart, a longitudinal cut was made at the midline separating it into halves. For the kidney, a transverse cut was made, dividing it into three parts, and only the middle part was taken. Meanwhile, the liver was cut into 3-5 mm thick. All organ parts were also placed in separate vials containing 10% formalin solution for 24 hours (Figure 3.14).



Figure 3.14: Brain and other vital organs kept in 10% formalin

3.7.3 Measurement of brain gross morphology

The weight, length and width of the whole brain structure were measured before subsequent steps of processing the neural tissue (Figure 3.15).

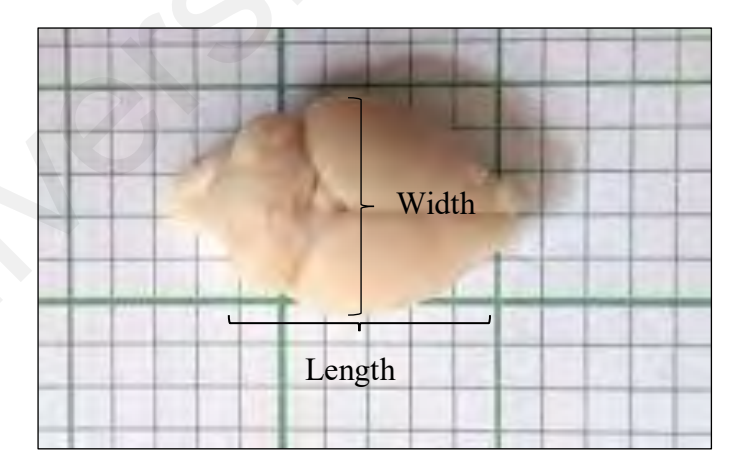


Figure 3.15: Gross morphology measurements of whole brain structure

3.7.4 Dehydration

Dehydration was a process of removing water from the tissue. After fixation, tissue samples were transferred into 70% alcohol solution for 24 hours. Next, the tissue samples were passed through progressively higher concentrations of alcohol solutions. During the first step, they were transferred into 85% alcohol solution. This was followed by two steps of 95% alcohol solution (I and II) and two steps of 100% alcohol solution (I and II), with 60 minutes of immersion in each solution. During this dehydration process, water was totally removed from the tissue and replaced with alcohol.

3.7.5 Clearing

Clearing was a process of clearing out alcohol solution in the tissue samples. Terpineol, which was the clearing agent used in this study, could mix with both alcohol solution and the embedding medium used. After the dehydration process, tissue samples were transferred to terpineol solution twice (I and II), with 60 minutes for each immersion.

3.7.6 Paraffin infiltration

Infiltration was a process of replacing the clearing agent with the embedding medium paraffin. After the clearing step, tissues were transferred into a mixture of terpineol and melted paraffin (1:1) for 60 minutes in the oven at 60°C. Tissues were then transferred into melted paraffin I and later into melted paraffin II, with 60 minutes for each immersion. Transition from terpineol-paraffin mixture to melted paraffin immersions removed any remnants of clearing agent progressively and rendered a rigid consistency to the tissues before being finally embedded.

3.7.7 Embedding

Embedding was a process of which tissues were surrounded by paraffin medium, to provide sufficient support to the tissue making it firm enough to facilitate sectioning. Embedding kept all parts of tissue intact and enabled thin sections to be cut.

Paper boxes were prepared as embedding molds. The infiltrated tissues were transferred from melted paraffin II using a pair of forceps into the molds containing paraffin. The tissues were placed into melted paraffin which was in fluid form before the paraffin solidified. This step enabled it to thoroughly infiltrate the tissues without causing any damage. Tissues were placed properly in a manner that ensured the paraffin fully covered the tissues with no air bubbles. Orientation of tissues in the melted paraffin was noted and labels were marked at the block face. This was done to secure a correct direction for sectioning later (Figure 3.16).



Figure 3.16: Embedded tissues in solidified paraffin

3.7.8 Sectioning

The hardened paraffin blocks were cut into very thin sections using a rotary microtome (American Optical Microtome 820) (Figure 3.17). Prior to sectioning, the hardened paraffin blocks were removed from the paper molds and trimmed to appropriate sizes, depending on the types of sections to be made. The paraffin blocks were trimmed into a truncated pyramid with a trapezoidal upper surface. This was done to indicate the direction of the tissue, where the smaller edge was the top part where sectioning began, and the larger edge was the bottom part adhered to the block stage. The surface of the block must be parallel to ensure a long and straight ribbon to be obtained.

Extra paraffin chips from the trimmed blocks were put on a heated spatula and placed near the top surface of the wooden block stage. As the paraffin chips melted onto the block stage, the base of the trimmed paraffin blocks was quickly placed on the heated spatula. Melting of the base of the paraffin block and paraffin chips allowed a firm adherence of the block to the block stage. The block stage was then clamped tightly at the microtome holder, with the trapezoidal block surface facing the microtome blade. Trimming was done using the microtome blade before it reached the embedded tissue. Once the first section of tissue appeared, the blocks were carefully sectioned at a thickness of 10 µm each, until a ribbon of tissue sections was obtained. The ribbon of tissue sections was manipulated using a brush and arranged systematically and chronologically on a tray.



Figure 3.17: Tissue sectioning using a rotary microtome

3.7.9 Mounting of sections onto microscope slides

Before mounting, glass slides were treated, and warm water bath was prepared. Glass slides were labeled and numbered accordingly. A drop of albumin was dropped and spread onto the slides. Albumin acted as an adhesive coat that attached tissues onto the slide; thus, prevented them from sliding off during staining process. Water bath was heated at a temperature of 40°C. It was ensured that the hot water bath was not overheated because it not only could cause paraffin to melt but also might induce changes in tissue morphology. Due to the hydrophobic property of paraffin, tissue sections floated when placed on the surface of the water. Tissues that were compressed and crinkled from sectioning flattened out when placed on the warm water. The treated glass slides were then used to pick up the floating tissues. Extra caution was taken to ensure that no air bubbles were trapped between the tissue sections and the glass side. Air bubbles could cause tissues to be distorted and even float off during staining.

Excess water from the slides were removed using a paper towel. Tissue sections were carefully positioned to the center of the slide before placed on the slide warmer at a temperature of 40°C to 45°C. This allowed the sections to remain attached on the slide once the water had evaporated. The slides were then dried thoroughly in an oven at a temperature of 40°C overnight.

3.7.10 Staining

Staining was a process where specific dyes were used to colour the various components of tissue sections to be visualized for further histological examination. Two staining techniques were employed: Hematoxylin and Eosin (H&E) and Nissl stainings.

3.7.10 (a) Hematoxylin & Eosin (H&E) staining

Hematoxylin and eosin dyes were used to stain the nuclei and cytoplasm. Tissue samples from Experiment 1 and 2 were stained using this staining technique for basic histological analysis. Hematoxylin stained the nuclei blue while eosin stained the cytoplasm and extracellular fluid pink.

Prior to staining, the mounted sections were deparaffinized with xylene twice 3 minutes for each immersion. Next, tissue sections were hydrated in decreasing concentration of alcohols (95% and 70% alcohol solutions) and distilled water. Following dehydration, tissue sections were stained in hematoxylin for 10 seconds and rinsed in running tap water for 3 minutes. The sections were rinsed again in distilled water for another 3 minutes. After that, sections were stained in 1% eosin Y for 1-2 minutes. Sections were then quickly rinsed in 95% alcohol solution before dehydrated in 100% alcohol solution twice, 3 minutes for each

immersion. Lastly, the tissue sections were cleared in xylene twice for 3 minutes in each immersion (Figure 3.18).



Figure 3.18: Hematoxylin and eosin (H&E) staining solution step

3.7.10 (b) Nissl staining

Cresyl violet dye was used to identify neurons. Neuronal nuclei and Nissl bodies e.g. rough endoplasmic reticulum were stained bluish purple. Brain tissues from Experiment 3 were stained using this dye. Prior to staining, tissue sections were deparaffinized in xylene twice, 3 minutes for each immersion. Tissues were hydrated in descending alcohol solutions (95%, and 70% alcohol solutions). Hydration in 95% alcohol solution was done twice with 3 minutes in each immersion, followed by 70% alcohol solution for 3 minutes. The tissue sections were rinsed in distilled water twice before stained in cresyl violet solution for 20 minutes at room temperature. After staining, the sections were quickly rinsed in 70% alcohol solution for differentiation. The tissue sections were dehydrated in tertiary butyl alcohol solution twice, 2 to 3 minutes for each immersion. Lastly, they were cleared in xylene twice for 3 minutes in each immersion (Figure 3.19).



Figure 3.19: Nissl staining solution step

3.7.11 Mounting of coverslip onto tissue sections

Coverslip mounting was a process where a thin cover glass slip was placed onto tissue sections to support and preserve the sections for microscopy examination. Slides were taken out from xylene and placed on a paper towel. Dibutylphthalate polystyrene xylene (DPX) mounting medium was applied to the surface of the cover slip. The cover slip was held at a 45° angle to the surface of the slide and slowly tipped onto the glass slide to avoid formation of air bubbles. Excess mounting medium was carefully removed with a tissue paper. The cover slipped slides were then dried in the oven for 48 hours at a temperature of 40°C.

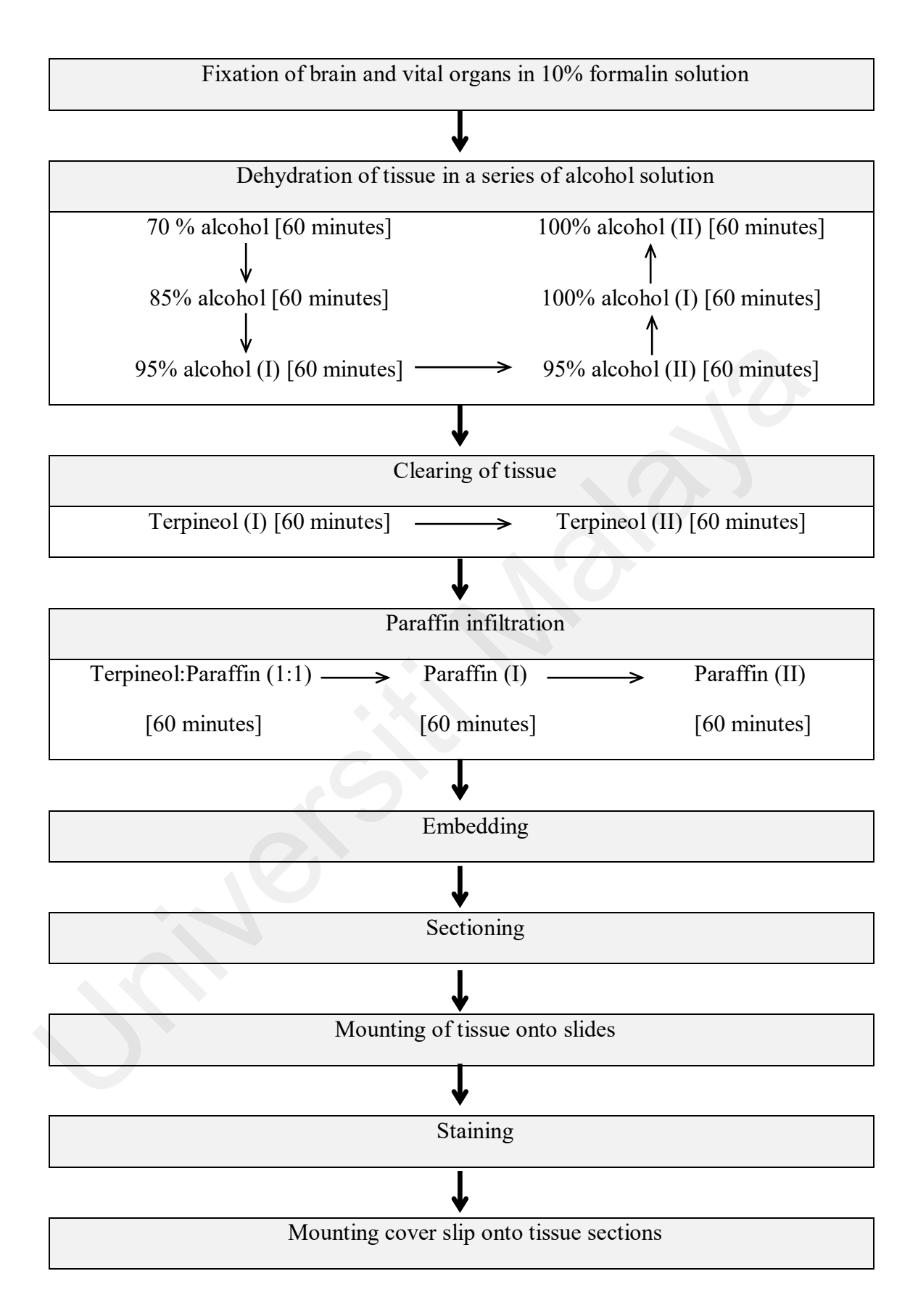


Figure 3.20: Overview of steps and solutions in histological processing

3.8 Morphometric analysis of neuronal soma

3.8.1 Image acquisition

For every group, six (6) consecutive best-stained slides were selected. Each slide has 6-8 brain tissue samples, with a 10 μ m thickness section per each sample. From every slide, only the two (2) best samples were selected, and the difference between the selected samples were ensured to be 30 μ m. This was done to minimize the possibilities of analyzing the same cells. After the selection process was finished, images were captured using inverted microscope equipped with Leica Application Suite (LAS) Version 4.0 microscope imaging software (Leica Microsystems (Switzerland) Limited) with the following parameters: Camera exposure = 20.4 ms, Camera image type = colour, Image size = 2560 \times 1920 pixel, and real size image = 435 \times 326 μ m. Each image was observed under a 20 \times lens and saved in Tag Image File Format (TIFF) format.

Only images of the hippocampal CA1 region from the right hemisphere of the brain were acquired in this study. Position of camera during image acquisition were maintained for every group to ensure that comparisons of similar hippocampal CA1 regions were conducted (Figure 3.21).

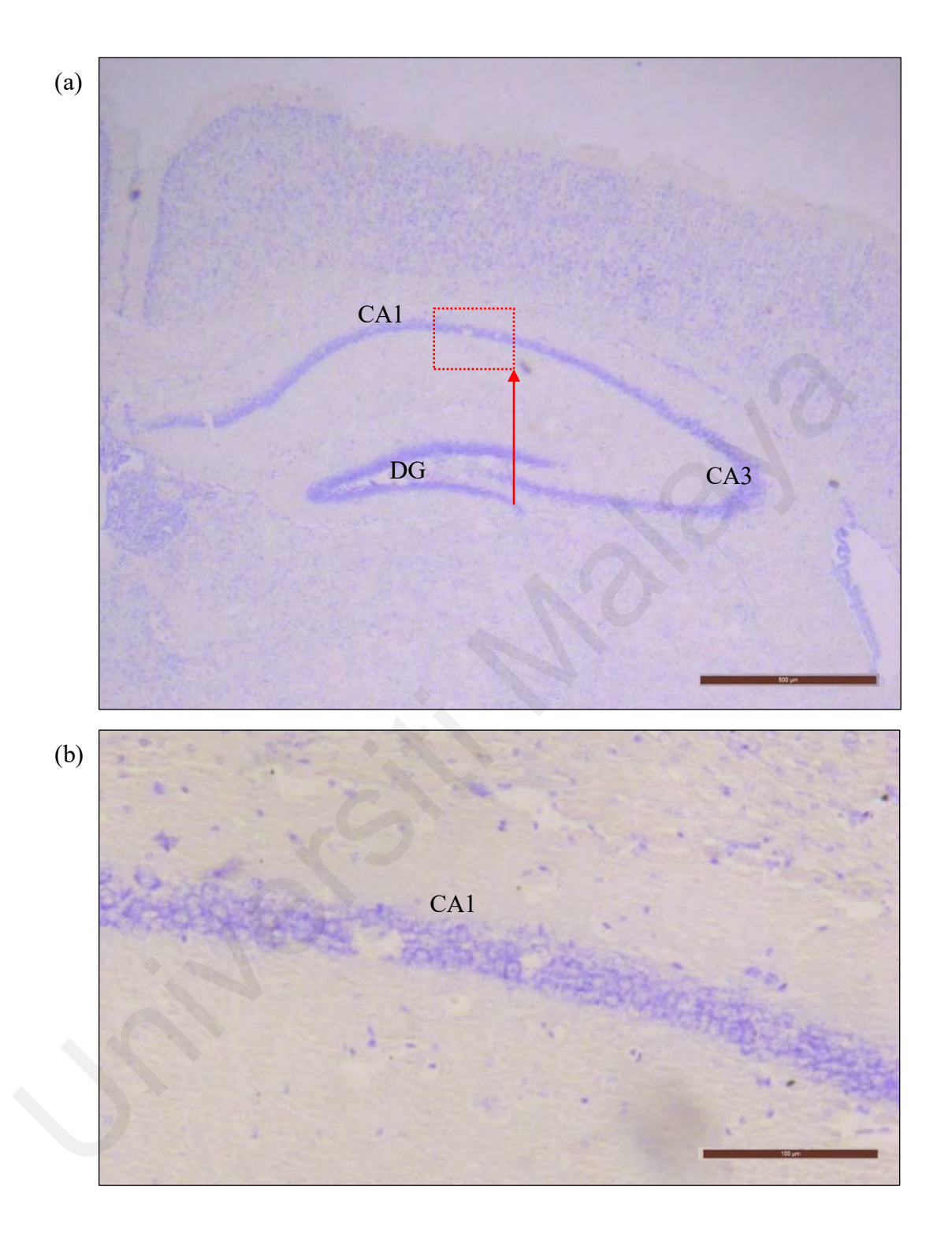


Figure 3.21: Image acquisition of hippocampal CA1 region of brain tissue sample. (a) Photomicrograph of right hemisphere of brain tissue sample at a $40\times$ magnification and 500 μ m calibration. Red arrow shows camera movement from the dentate gyrus region to the region of interest (ROI). Red dotted box shows ROI in hippocampal CA1 layer. (b) Photomicrograph of hippocampal CA1 region at a $200\times$ magnification and $100~\mu$ m calibration.

3.8.2 Image processing

Measurements of somatic area, somatic perimeter, somatic circularity, somatic aspect ratio, and somatic roundness were conducted using ImageJ analysis software. For each of the image acquired, 20 neuronal somas with clear nucleus and nucleolus were traced. Neurons were distinguished from glia by the visible presence of a nucleolus, a well-defined nuclear envelope, and nongranular cytoplasm (Meitzen et al., 2011). Selected morphological variables were in accordance with the quantitative criteria outlined by Tsiola et al. (2003). After the parameters were measured, data were further processed for statistical analysis.

3.9 Statistical analysis

Data obtained were analysed using Statistical Package for the Social Sciences (SPSS) statistical software (SPSS for Windows, version 23.0). All numerical values were presented as mean \pm standard error mean (SEM). Data were analyzed using one-way analysis of variance (ANOVA), followed by Tukey's *post hoc* test. Differences were considered significant when probability was equal or less than 0.05 (p \leq 0.05).

CHAPTER 4: RESULTS

The chapter covers the three tests done involving toluene toxicity test, Novel Object Recognition (NOR) test, and NS neuroprotective test.

4.1 Preliminary test 1: Toluene toxicity test

Different dosages of toluene treatments resulted in different effects on the selected vital organs. Since toluene has high affinity towards lipids, it easily diffused into lipid-rich organs including brain, kidney, and liver. A study by Yasar et al. (2016) has reported morphological changes in the liver, kidney, central nervous system (CNS), and heart of mice after toluene exposure. Generally, histological changes were seen in higher doses of toluene; 300 mg/kg and 500 mg/kg.

4.1.1 Brain hippocampal histopathology

Figure 4.1 shows the hippocampal sections of mice brain at a low magnification of 100×. All sections from the various treatments allowed visualization of the cornu ammonis 1 (CA1) or the hippocampus proper and the dentate gyrus (DG) structures which resemble the two interlocking, U-shaped laminae, one attaching into the other. Figure 4.2 shows a higher magnification at 400× of the CA1 region. No obvious morphological differences and atypical neuronal structures were observed between all the experimental groups. Later, a more specific Nissl-stained hippocampal sections were studied and further morphometric measurements of the CA1 neurons were conducted for more detailed analysis.

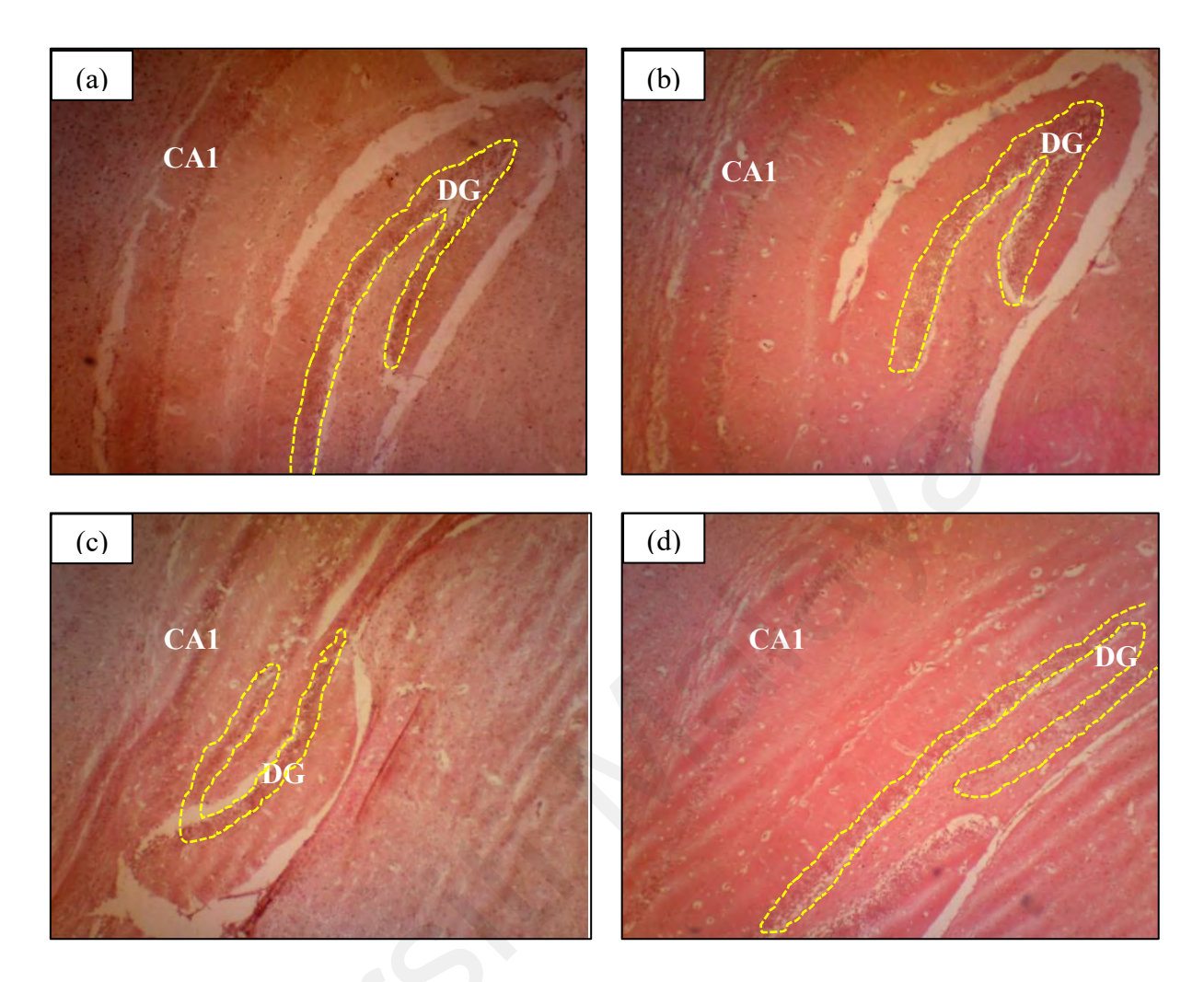


Figure 4.1: Photomicrographs of hippocampus sections stained with H&E at $100\times$ magnification for (a) control, (b) 100 mg/kg toluene, (c) 300 mg/kg toluene, and (d) 500 mg/kg toluene experimental groups, respectively.

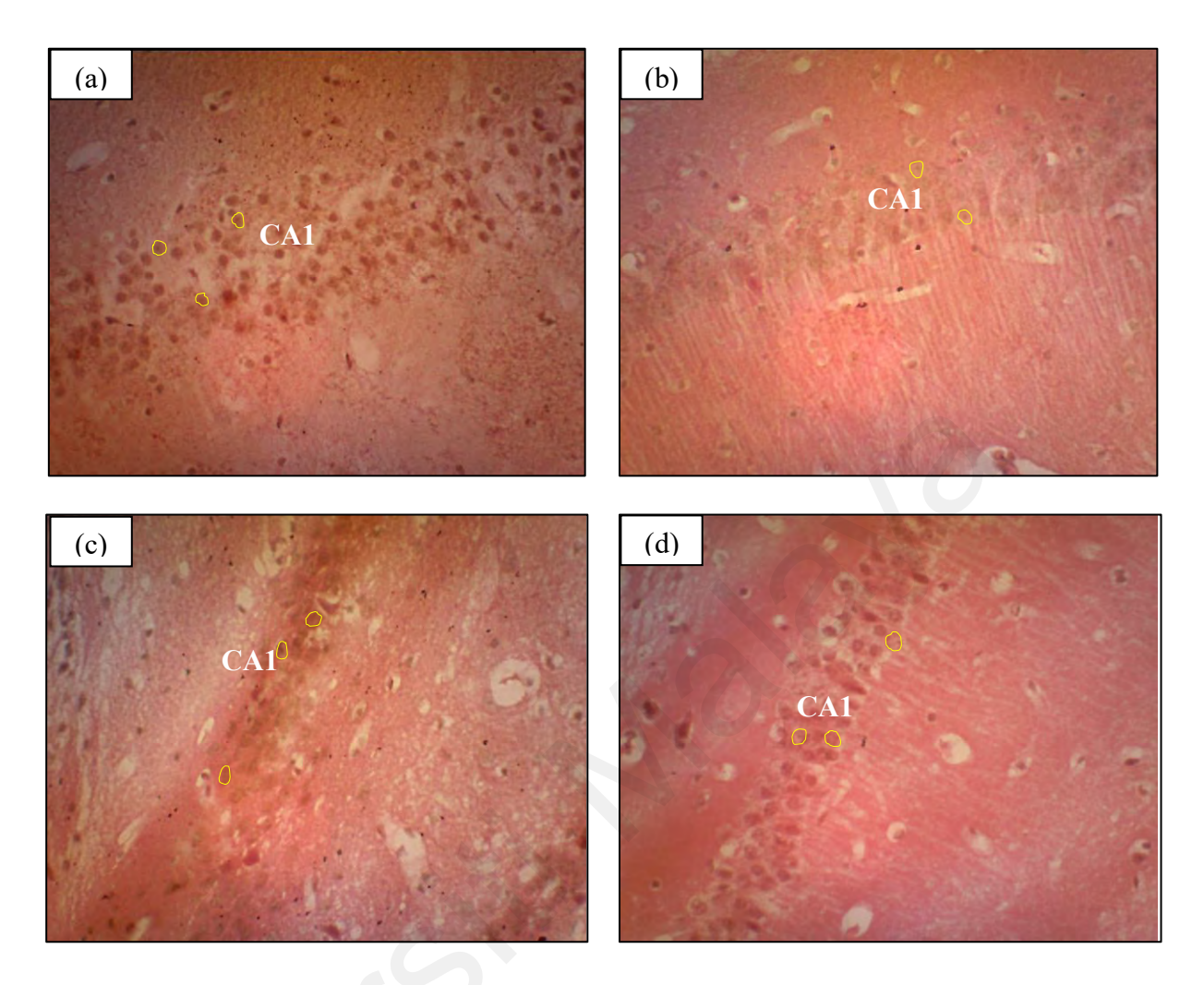


Figure 4.2: Photomicrographs of hippocampus sections stained with H&E at $400\times$ magnification for (a) control, (b) 100 mg/kg toluene, (c) 300 mg/kg toluene, and (d) 500 mg/kg toluene experimental groups, respectively

4.1.2 Liver histopathology

Figure 4.3 shows the liver architecture and components of basic liver lobules, with portal tract and central venule at a low magnification, while Figure 4.4 shows more detail condition of the liver sections at a higher magnification. At a magnification of 100×, liver sections in Figure 4.3 (a), (b) and (c) exhibited normal histology. The liver structure was organized into lobules with portal triads (T) at the vertices and a central vein (CV) in the middle. At a higher magnification of 400× in Figure 4.4 (a) (b) and (c), within each lobule, hepatocytes were observed to appear normal with round, centrally-placed nuclei and granular cytoplasm, arranged into hepatic cords running radially from the central vein and separated by adjacent sinusoids (green-coloured areas). In Figure 4.4 (c), a binucleate hepatocyte was observed (in blue-coloured circle). In Figure 4.4 (d), the sections exhibited sinusoid dilation (as shown by the red dashed lines). The hepatocytes also showed vacuolization of the cytoplasm with their nuclei displaced into the periphery (as shown in the blue-coloured circles). This condition was not observed in the control group and the groups that were treated with lower dosage of toluene.

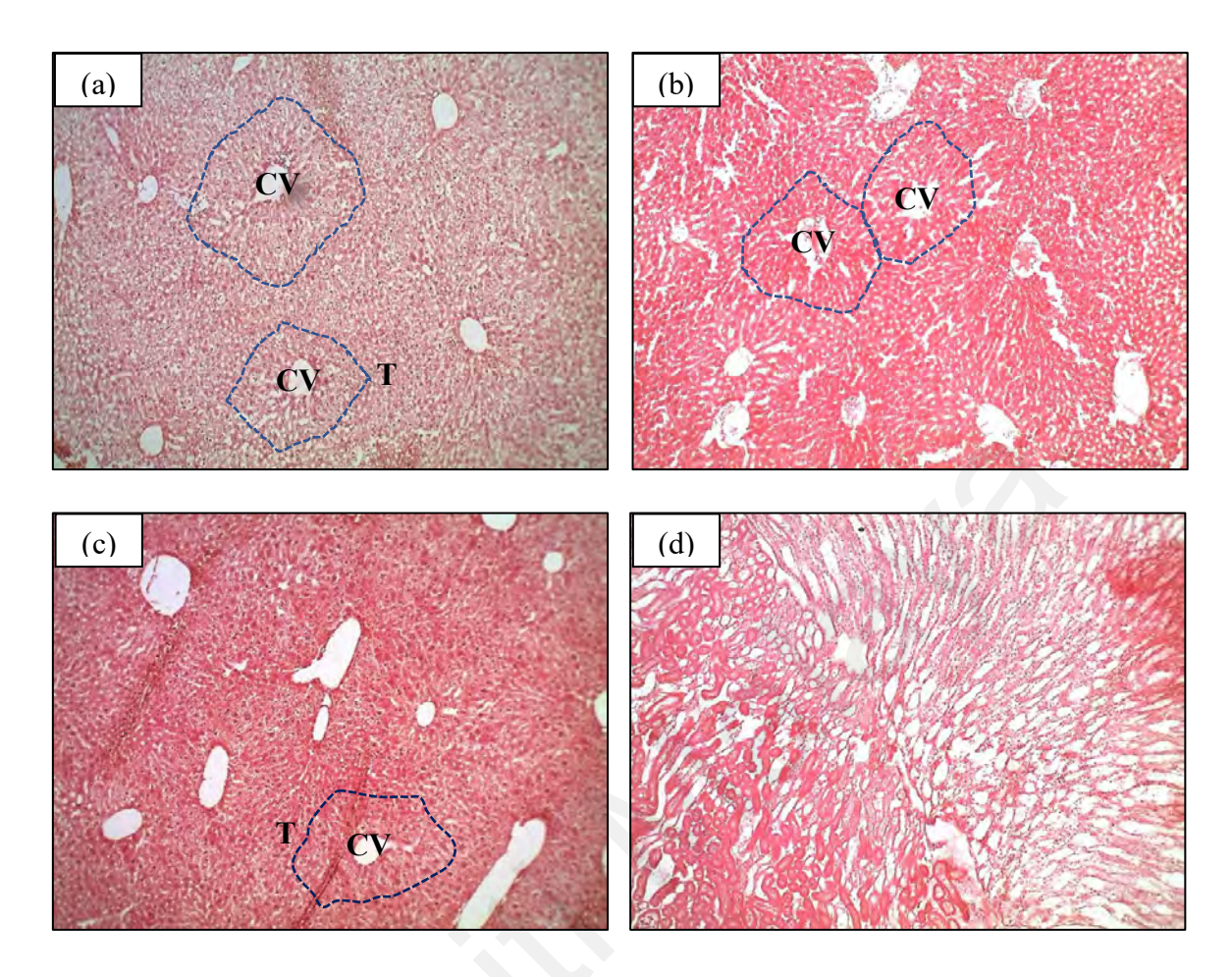


Figure 4.3: Photomicrographs of liver sections stained with H&E at $100 \times$ magnification for (a) control, (b) 100 mg/kg toluene, (c) 300 mg/kg toluene, and (d) 500 mg/kg toluene experimental groups. (CV: central vein, T: portal tract).

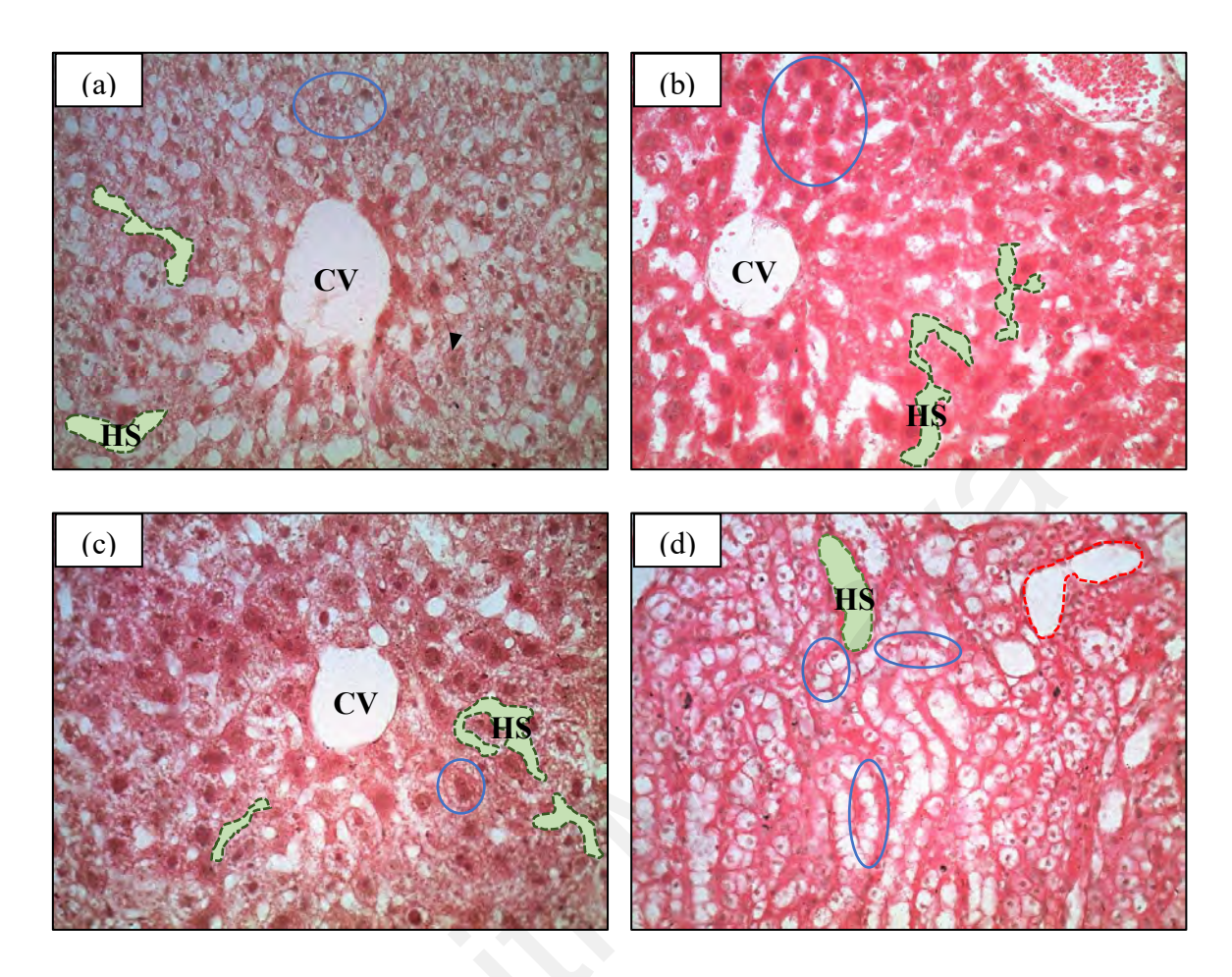


Figure 4.4: Photomicrographs of liver sections stained with H&E at 400× magnification for (a) control, (b) 100 mg/kg toluene, (c) 300 mg/kg toluene, and (d) 500 mg/kg toluene experimental groups. (CV: central vein, HS: hepatic sinusoid, blue circle: hepatocyte).

4.1.3 Kidney histopathology

Figure 4.5 shows the kidney architecture and components at a low magnification, while Figure 4.6 shows more detail condition of the kidney sections at a higher magnification. At 100× magnification, Figure 4.5 (a), (b), (c) and (d) showed distinguished characteristics of of renal corpuscle, each of which consists of a glomerulus where it is surrounded by a fluidfilled space, Bowman's space, with an outer envelope of Bowman's capsule. Distal and proximal tubular structures were also observed. Distal convoluted tubules have nuclei spaced farther apart and its luminal surface does not have a brush border, so its lumen appeared wider and clearer. Proximal convoluted tubule were observed to stain more intensely eosinophilic than distal tubules, due to the abundance of dark-staining organelles including the vesicles and mitochondria. Proximal tubules has microvilli that make up the brush border that fills the lumen, thus the lumen appeared to have a characteristic "fuzzy" appearance. At a higher magnification of 400×, kidney sections in Figure 4.6 (a), (b), and (c) showed normal structures while structural changes of the glomerulus, proximal convoluted tubules, and distal convoluted tubules were observed in Figure 4.6 (d). The glomeruli appeared diminished and distorted while the distal and proximal tubular structures were dilated. Histopathological changes in atrophic proximal tubular structures were apparent with loss of brush border of the proximal tubules.

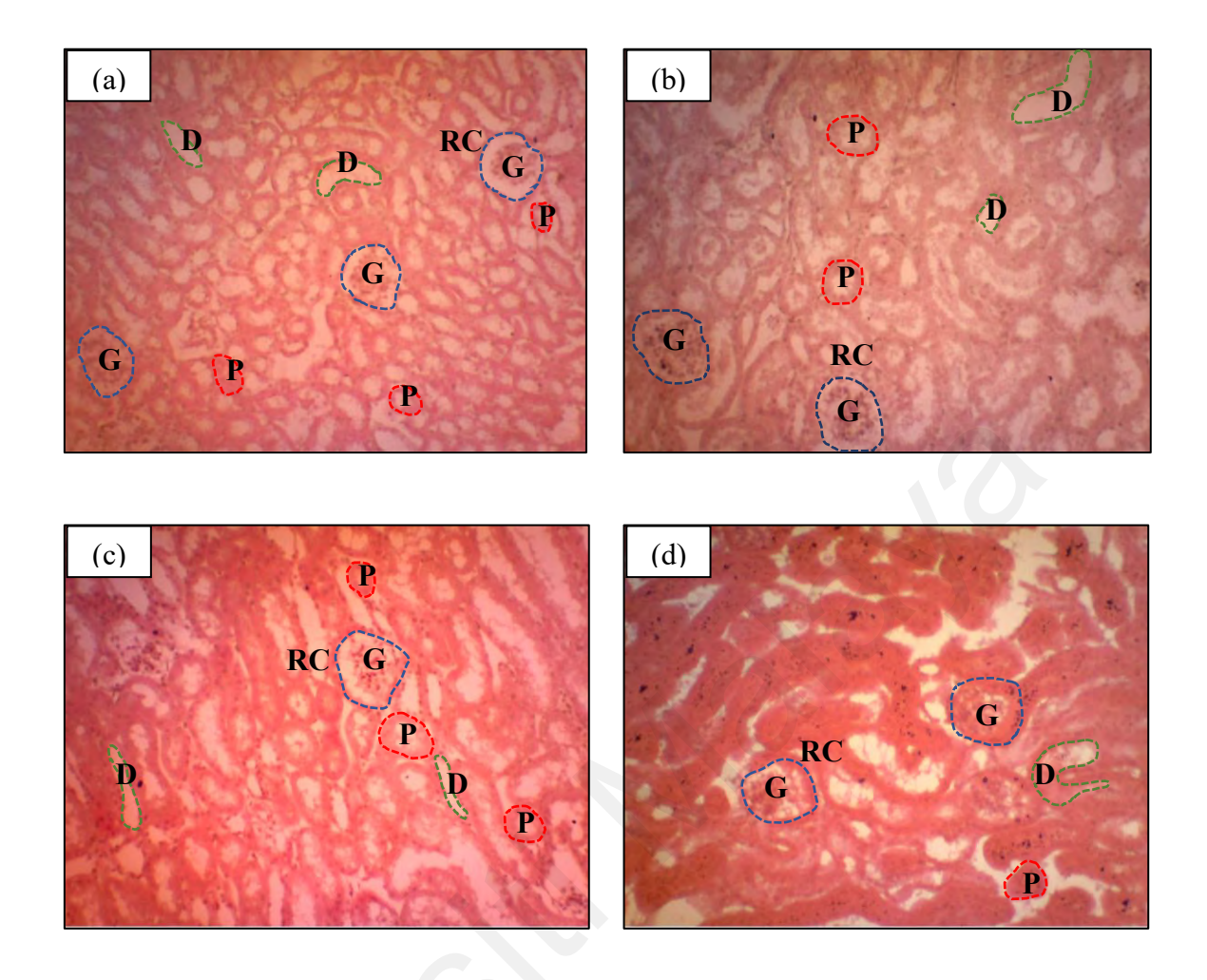


Figure 4.5: Photomicrographs of kidney sections stained with H&E at $100 \times \text{magnification}$ for (a) control, (b) 100 mg/kg toluene, (c) 300 mg/kg toluene, and (d) 500 mg/kg toluene experimental groups. (G: glomerulus, RC: renal corpuscle (blue dashed line), D: distal convoluted tubule (green dashed line), P: proximal convoluted tubule (red dashed line)).

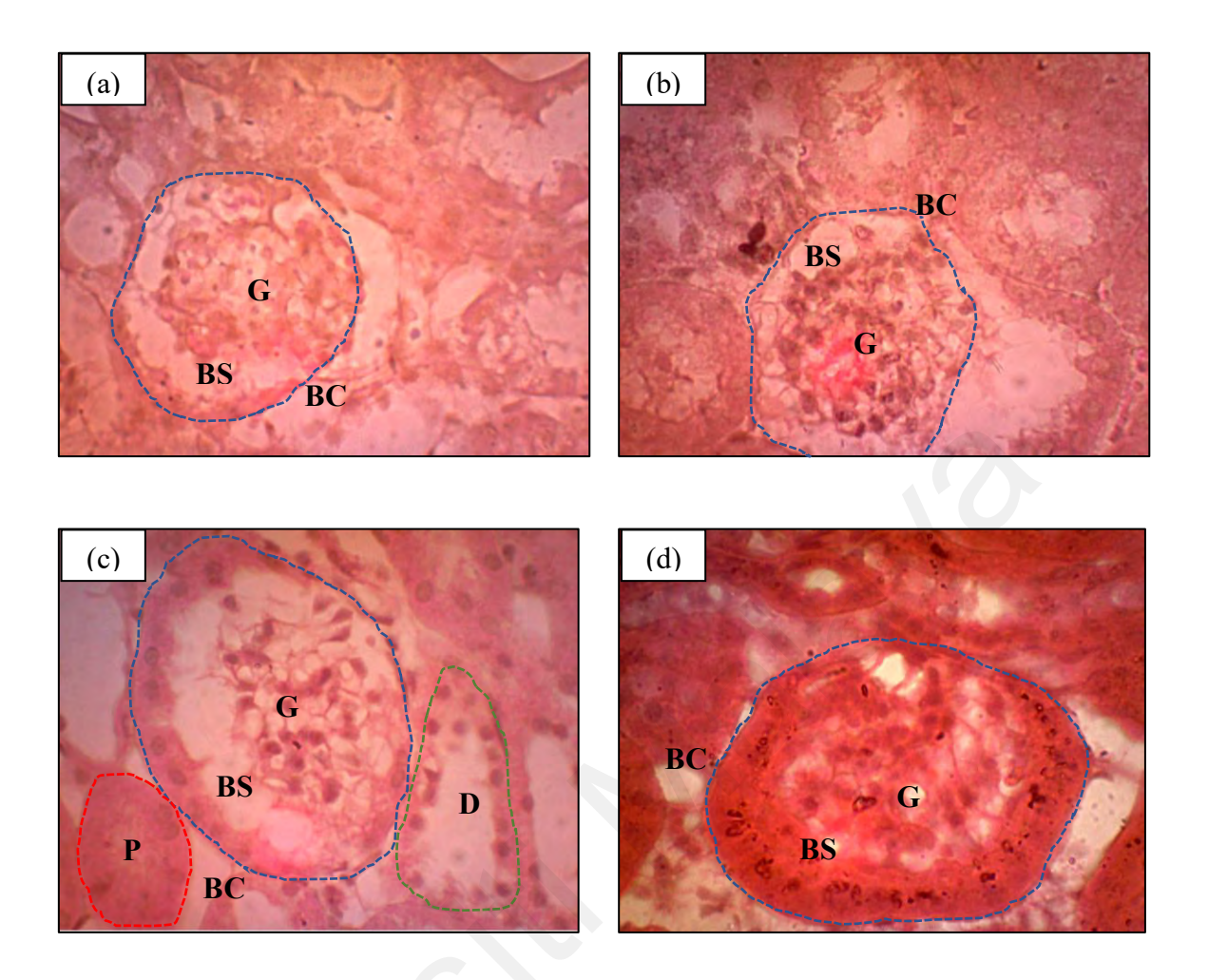


Figure 4.6: Photomicrographs of kidney sections stained with H&E at 400× magnification for (a) control, (b) 100 mg/kg toluene, (c) 300 mg/kg toluene, and (d) 500 mg/kg toluene experimental groups. (BC: Bowman's capsule, BS: Bowman's space, G: glomerulus, RC: renal cortex (dashed lines), D: distal convoluted tubule, P: proximal convoluted tubule)

4.1.4 Heart histopathology

Figure 4.7 shows the longitudinal sections of heart architecture at a low magnification, while Figure 4.8 shows more detail condition of the heart sections at a higher magnification. At 100× magnification, not much details were showed. Figure 4.7 (a), (b), (c), and (d) showed the myocardium layer of the heart. In Figure 4.7 (a), the mesothelium which comprises the layer of simple squamous epithelium cells is observed. At a higher magnification of 400×, the heart sections of mice in Group 1, 2 and 3 shown in Figure 4.8 (a), (b) and (c) exhibited single, oval, and centrally located nuclei of cardiomyocytes with regularly arranged cardiac myofibers. Tissue sections of Group 4 in Figure 4.8 (d) showed deformation in size and shape in the nuclei of cardiomyocytes in tissue sections. Cardiac myofibers were also observed to be in a disarrayed pattern.

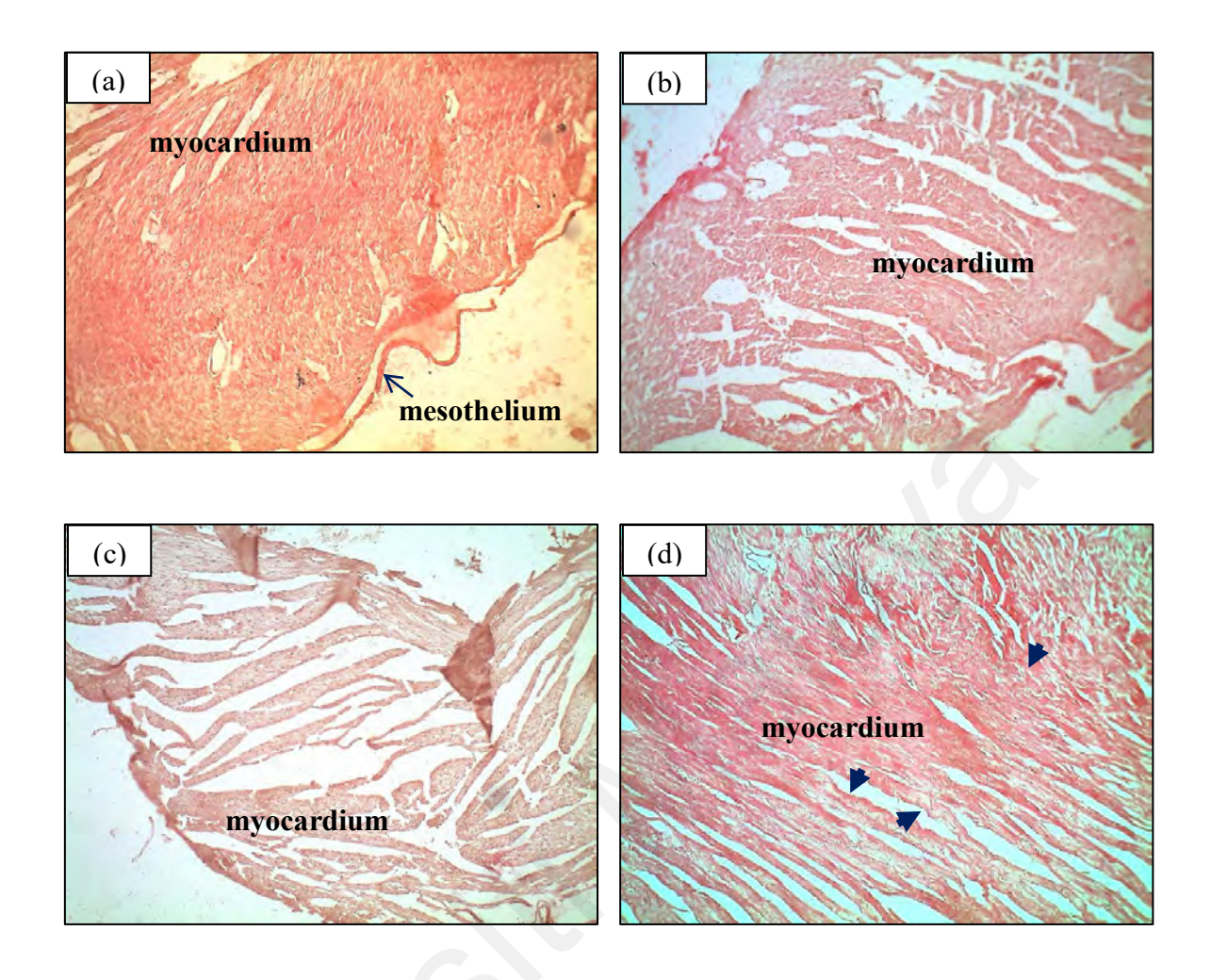


Figure 4.7: Photomicrographs of heart sections stained with H&E at 100×100 magnification for (a) control, (b) 100 mg/kg toluene, (c) 300 mg/kg toluene, and (d) 500 mg/kg toluene experimental groups. Cardiac myofibres were found to be in a disarrayed pattern (arrowhead).

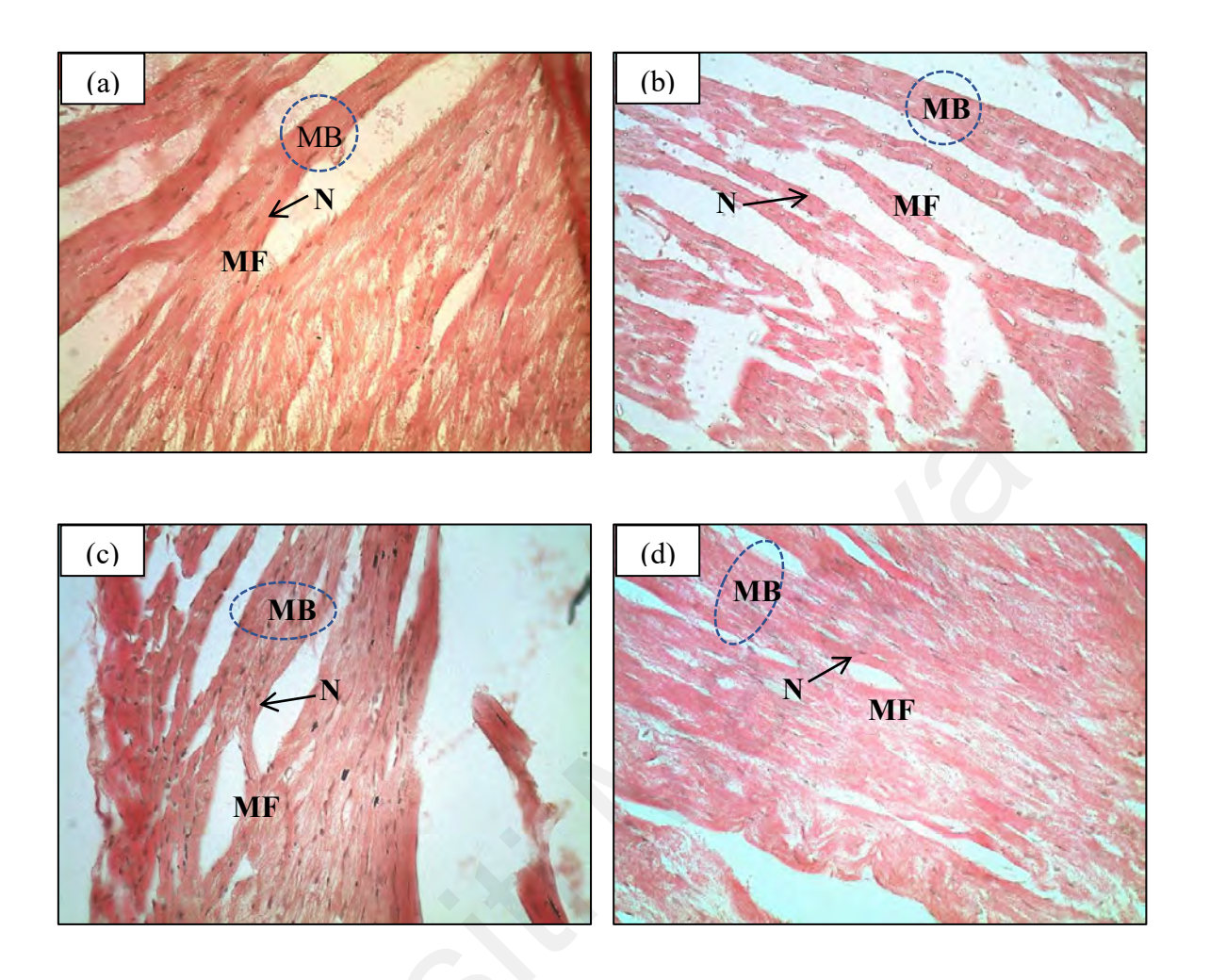


Figure 4.8: Photomicrographs of heart sections stained with H&E at $400\times$ magnification for (a) control, (b) 100 mg/kg toluene, (c) 300 mg/kg toluene, and (d) 500 mg/kg toluene experimental groups. (N: nuclei, MF: muscle fiber, MB: muscle bundle (blue dashed line)).

4.2 Preliminary test 2: Novel object recognition (NOR) test

Based on memory performance in NOR, data from various dosages of toluene and NS supplementations (NSS, NSO, and TQ) were analysed. Histopathological analysis was also carried out on the slides of hippocampal sections.

4.2.1 Memory performance in NOR test

One-way analysis of variance (ANOVA) showed that there was no statistically significant difference in discrimination index (DI) and object preference between toluene (TOL) and corn oil (CO) treatment groups ($p \ge 0.05$) (Table 4.1 and 4.2, Figure 4.9). Results showed that when compared to mice in the control group and Group 1 (0.117 \pm 4.44), mice administered with 500 mg/kg toluene (Group 4) had the lowest DI (-0.125 \pm 1.65) followed by mice administered with 300 mg/kg toluene (Group 3) (-0.094 \pm 5.65) and 100 mg/kg toluene (Group 2) (0.055 \pm 2.81) (Figure 4.10). Therefore, the preliminary findings indicated that 500 mg/kg toluene administration impaired recognition memory performance most drastically in mice.

Table 4.1: Mean squares from ANOVA for novel object preference of mice treated with CO and TOL treatment groups

Source of Variation	SS	df	MS	F	P-value	F crit
Between Groups	304.26	3	101.42	2.055429	0.184702	4.066181
Within Groups	394.74	8	49.3425			
Total	699	11				

Table 4.2: Mean squares from ANOVA for discrimination index of mice treated with CO and TOL treatment groups

Source of Variation	SS	df	MS	F	P-value	F crit
Between Groups	0.121611	3	0.040537	2.162166	0.17048	4.066181
Within Groups	0.149987	8	0.018748			
Total	0.271598	11				

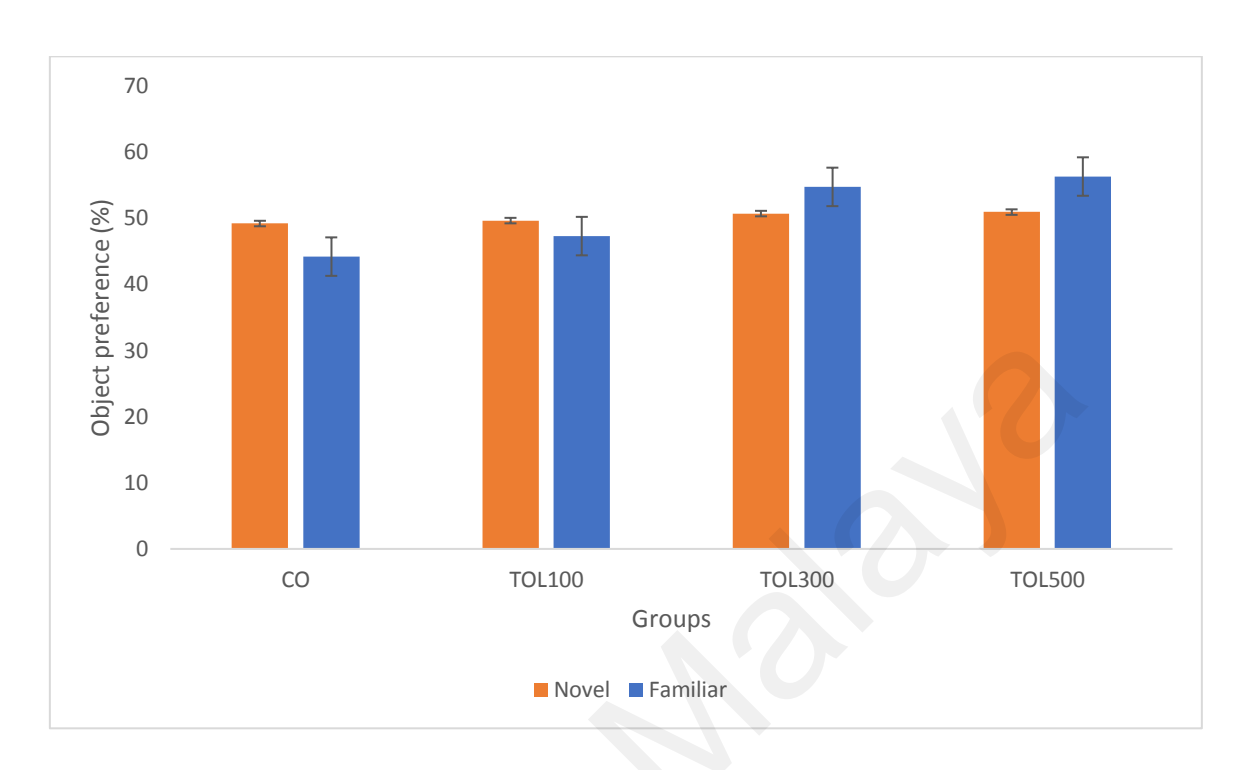


Figure 4.9: Percentage of novel and familiar object preference during test session

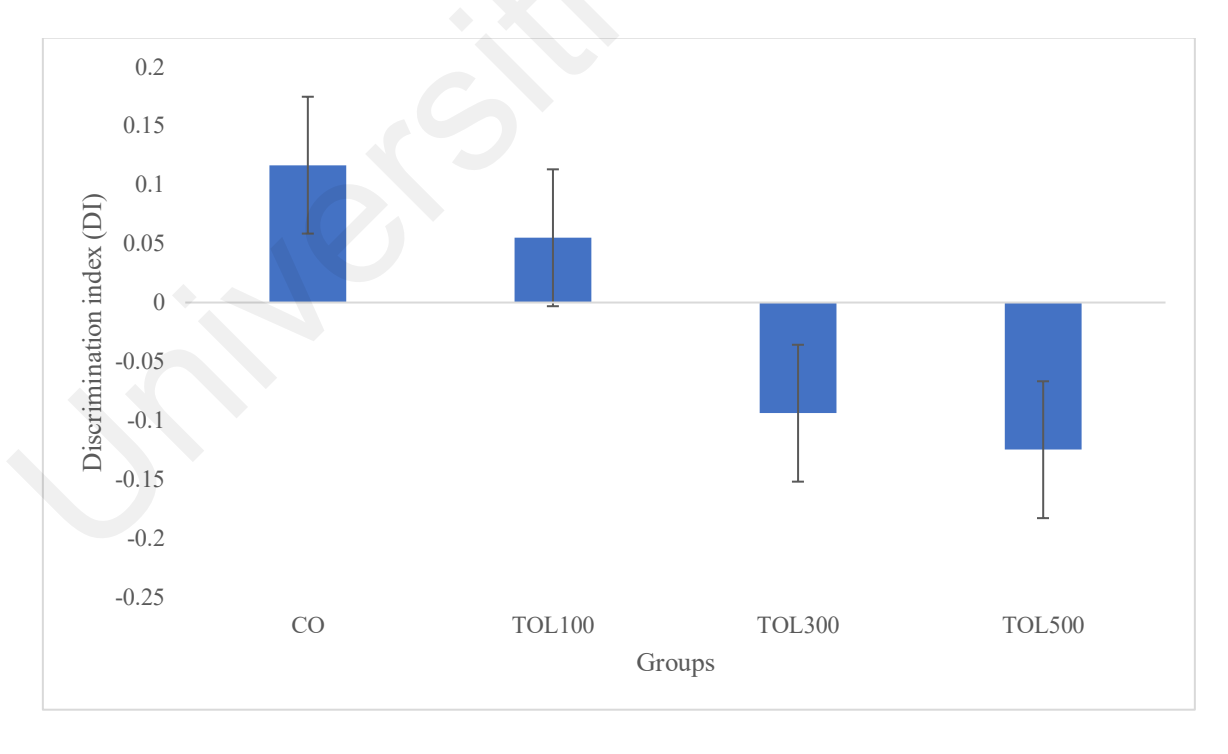


Figure 4.10: Discrimination index (DI) during test session

One-way analysis of variance (ANOVA) showed that there was no statistically significant difference in object preference between corn oil (CO) and the three NS treatment groups $(p\geq0.05)$ (Table 4.3). In all groups, mice showed higher preference towards the novel object than the familiar object (Figure 4.11).

Table 4.3: Mean squares from ANOVA for novel object preference of mice treated with CO, NSS, NSO and TQ treatment groups

Source of Variation	SS	df	MS	F	P-value	F crit
Between Groups	237.93	3	79.31	4.224234	0.045813	4.066181
Within Groups	150.2	8	18.775			
Total	388.13	11				

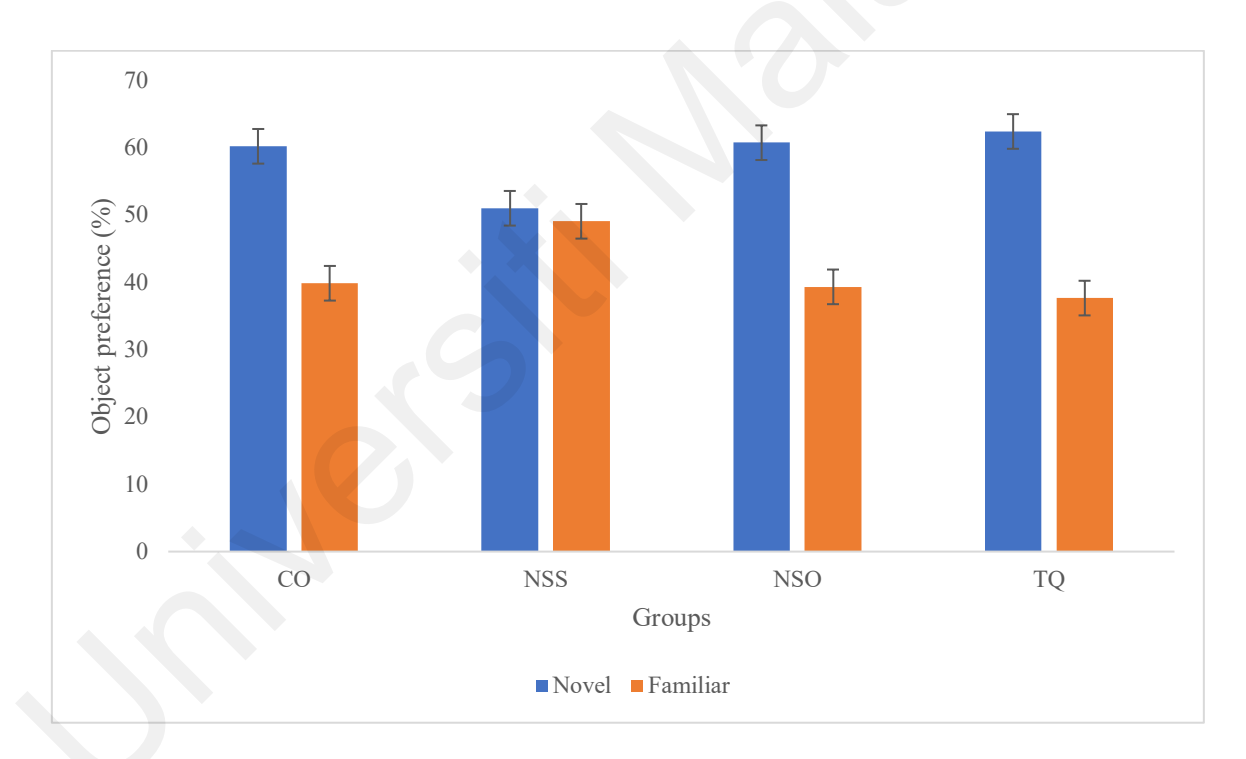


Figure 4.11: Percentage of novel and familiar object preference during test session

One-way ANOVA showed statistically significant difference in DI between the NS-treated groups (p \leq 0.05) (Table 4.4). *Post hoc* Tukey's test revealed that there were significant differences in NSO and NSS groups, when compared to the TQ group. Results showed that when compared to mice in the control group or CO, Group 1 (0.203 \pm 0.06), mice administered with TQ (Group 4) had the highest DI (0.247 \pm 0.05) followed by mice administered with NSO (Group 3) (0.213 \pm 0.04) and NSS (Group 2) (0.020 \pm 0.05) (Figure 4.12). Therefore, the preliminary findings indicated that TQ administration caused the highest enhancement in recognition memory performance in mice.

Table 4.4: Mean squares from ANOVA for discrimination index of mice treated with CO, NSS, NSO and TQ treatment groups

Source of Variation	SS	df	MS	F	P-value	F crit
Between Groups	0.094092	3	0.031364	4.154157	0.047613	4.066181
Within Groups	0.0604	8	0.00755			
Total	0.154492	11				

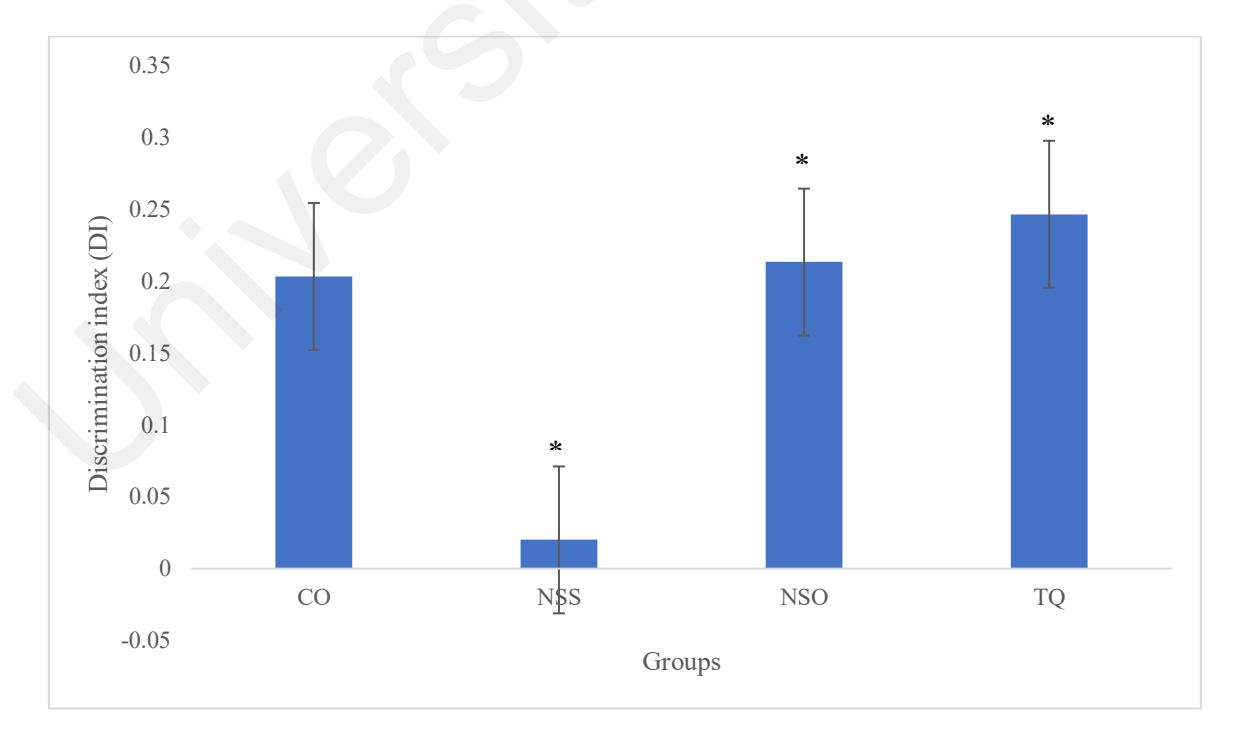


Figure 4.12: Discrimination index (DI) during test session

4.2.2 Brain CA1 hippocampal histopathology

No obvious morphological differences and atypical structures of the hippocampal CA1 pyramidal neurons were observed in the mouse brain sections between the experimental groups (Figure 4.13 and 4.14). All sections from the various treatments of toluene and NS supplementations (NSS, NSO, and TQ) focused on the visualization of the cornu ammonis 1 (CA1) structure. Slight reduction in cell size of hippocampal neurons was observed in Group 3 (300 mg/kg) and 4 (500 mg/kg) of the toluene treatments. Further morphometric measurements were conducted for more detailed analysis and presented later.

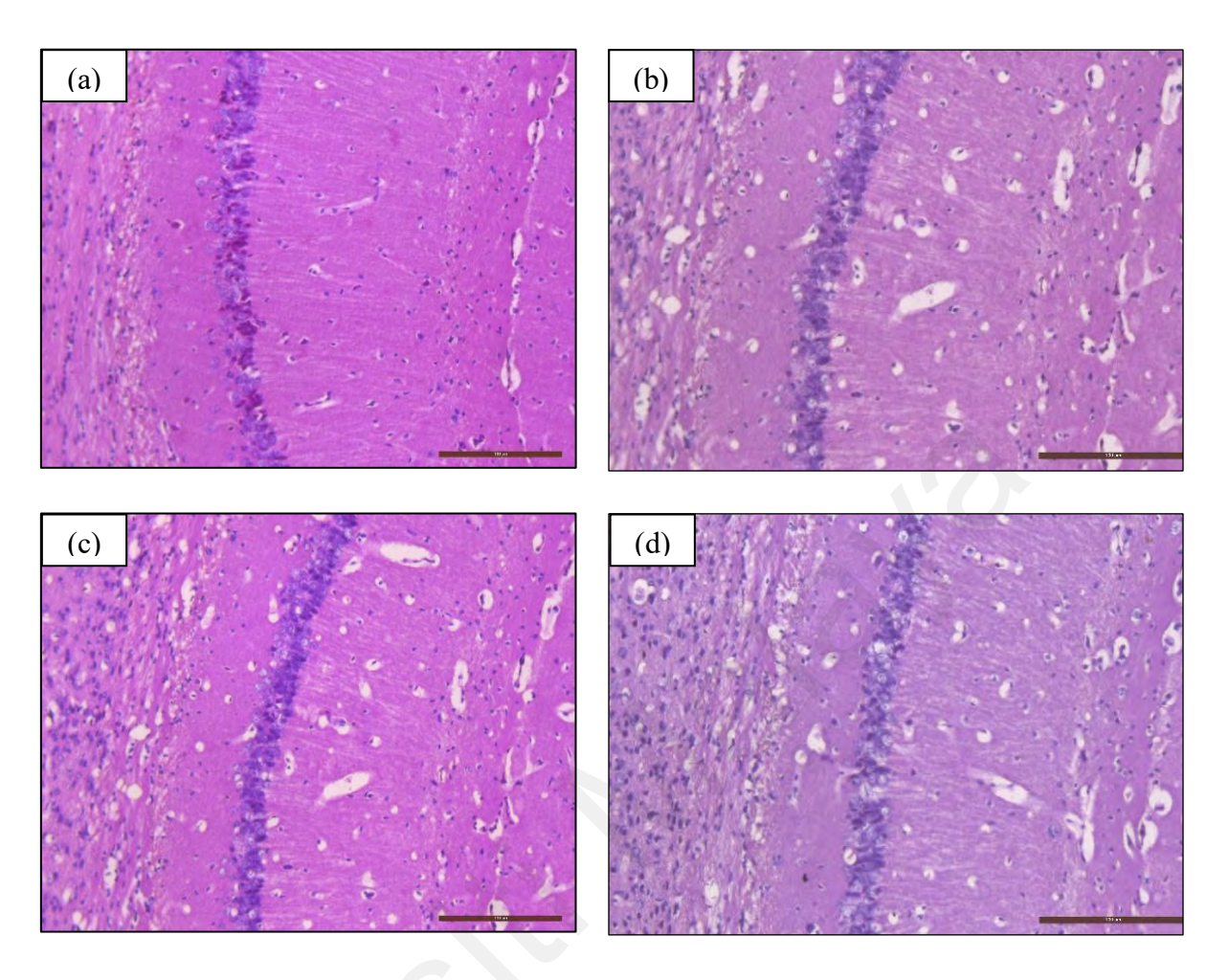


Figure 4.13: Photomicrographs of hippocampal CA1 pyramidal neurons stained with H&E at $200\times$ magnification for (a) control (CO), (b) 100 mg/kg toluene, (c) 300 mg/kg toluene, and (d) 500 mg/kg toluene experimental groups.

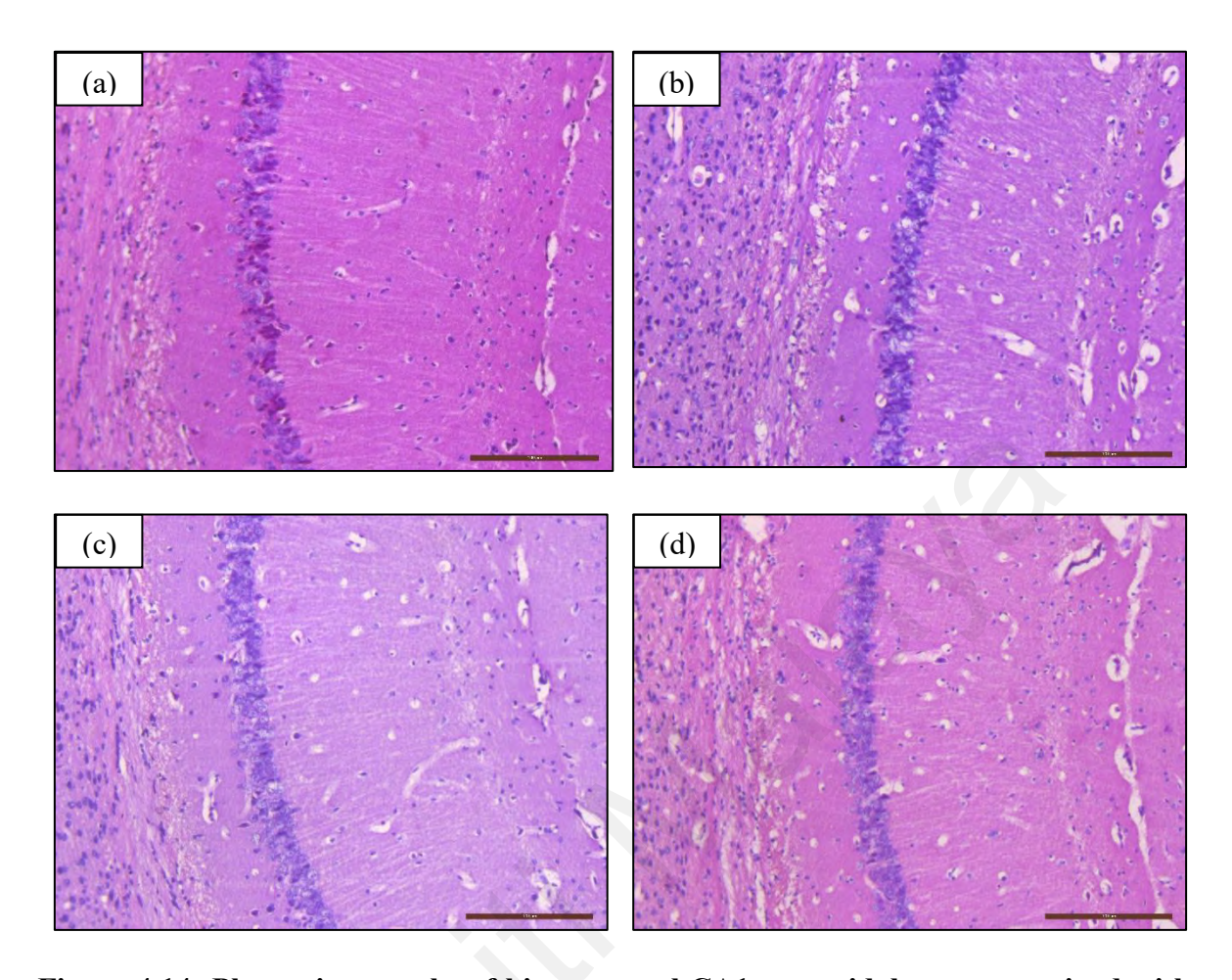


Figure 4.14: Photomicrographs of hippocampal CA1 pyramidal neurons stained with H&E at $200\times$ magnification for (a) control (CO), (b) NSS, (c) NSO, and (d) TQ experimental groups.

4.3 Nigella sativa (NS) neuroprotective test

The potential of NS playing a neuroprotective role was demonstrated by effects of NS supplementations against negative effects of toluene 500 mg/kg. Parameters used were performance of NOR test, histopathology of hippocampal sections, and morphometric of hippocampal CA1 pyramidal neurons.

4.3.1 Novel object recognition (NOR) test

Performance of novel object discrimination was determined by comparing the mean object preference of mice (Figure 4.15). Further analysis of the novel object recognition performance was determined by the discrimination index (DI) (Figure 4.16). One-way ANOVA showed that there was no statistically significant difference between the groups (Table 4.5 and 4.6). However, mice were observed to spend more time exploring the novel object over the familiar object in the control group and all NS treatment groups. Mice in the toluene treated group showed higher preference towards the familiar object rather than the novel object. Mice in group TOL-TQ demonstrated the highest DI (0.33 \pm 0.20) followed by TOL-NSO (0.12 \pm 0.12), TOL-NSS (0.05 \pm 0.23), CO (0.04 \pm 0.14), and the lowest DI observed in group TOL (0.02 \pm 0.13). Figure 4.17 shows the nose position track of mouse from each group during test session, generated by the semiautomatic analysis software, OptiMouse.

Table 4.5: Mean squares from ANOVA for novel object preference of mice treated with CO, TOL and NS treatment groups

Source of Variation	SS	df	MS	F	P-value	F crit
Between Groups	1730.302	4	432.5755	1.033495	0.409554	2.75871
Within Groups	10463.9	25	418.556			
Total	12194.2	29				

Table 4.6: Mean squares from ANOVA for familiar object preference of mice treated with CO, TOL and NS treatment groups

Source of				\ 1//		
Variation	SS	df	MS	F	P-value	F crit
Between Groups	1730.111	4	432.5276	1.033376	0.409611	2.75871
Within Groups	10463.94	25	418.5577			
Total	12194.05	29				

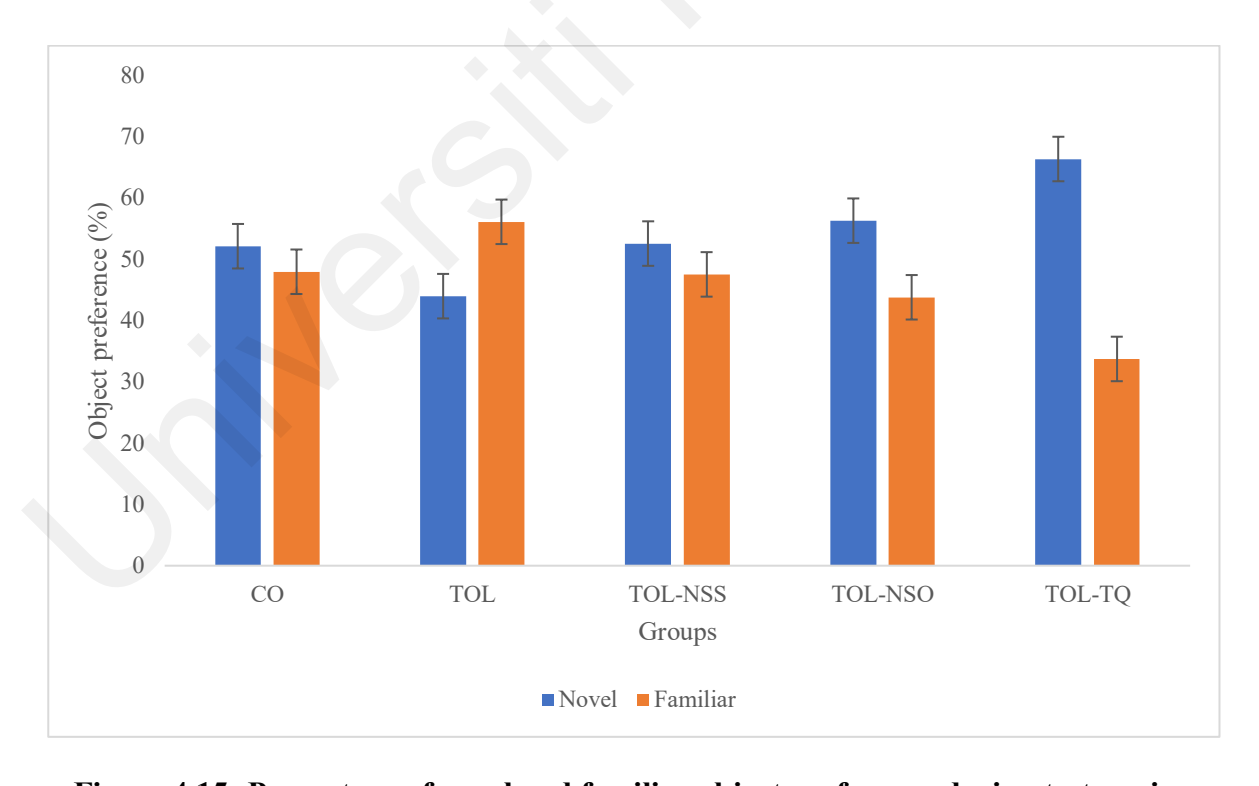


Figure 4.15: Percentage of novel and familiar object preference during test session

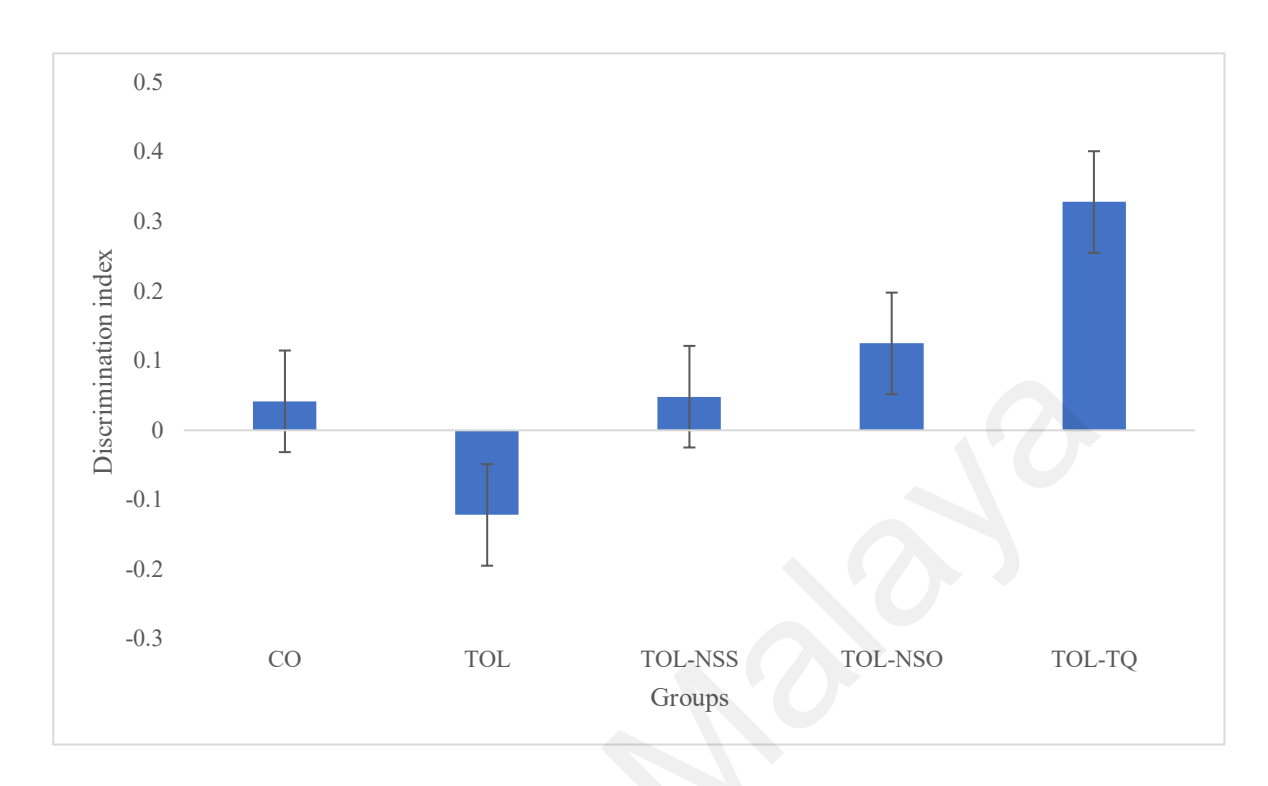


Figure 4.16: Discrimination index (DI) during test session

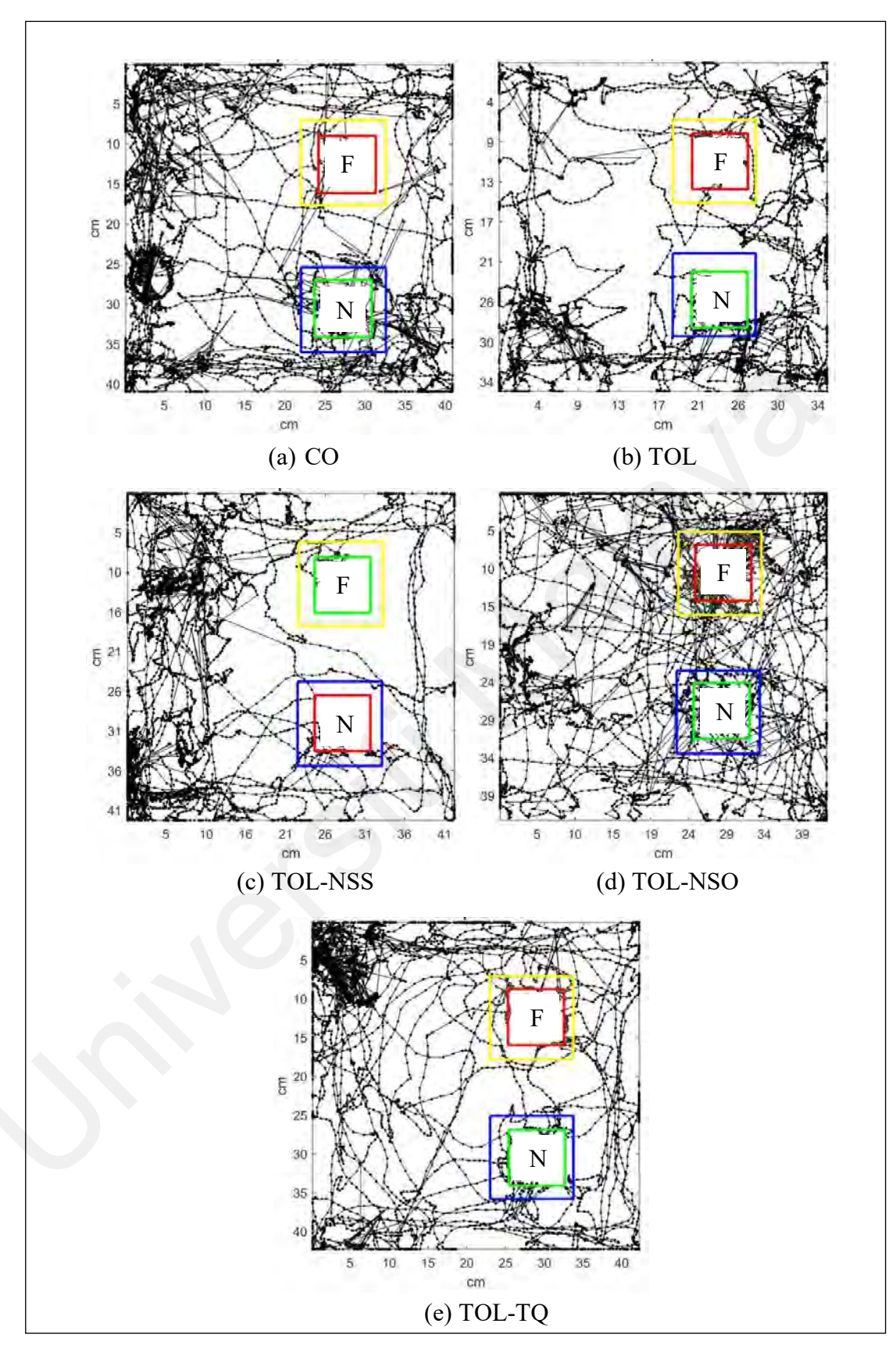


Figure 4.17: Nose position track of mouse from each group during test session. F-familiar structural object, N- novel structural object

4.3.2 Gross morphology measurements of brain

Figure 4.20 shows the gross anatomical structures of the mouse brain after formalin fixation, in which the weight, length and width of the mouse brain were measured. One-way ANOVA demonstrated non-significant effect of treatment on brain weight (g) between all groups: CO (0.50 ± 0.016) , TOL (0.36 ± 0.032) , NSS-TOL (0.37 ± 0.030) , NSO-TOL (0.39 ± 0.039) and TQ-TOL (0.38 ± 0.043) (Table 4.7; Figure 4.18). However, all treated groups had tendency to have lesser brain weight. They all had received toluene.

Table 4.7: Mean squares from ANOVA for weight of mice brain treated with CO, TOL and NS treatment groups

Source of Variation	SS	df	MS	F	P-value	F crit
Between Groups	0.071822	4	0.017956	2.701421	0.053528	2.75871
Within Groups	0.166168	25	0.006647			
Total	0.23799	29				

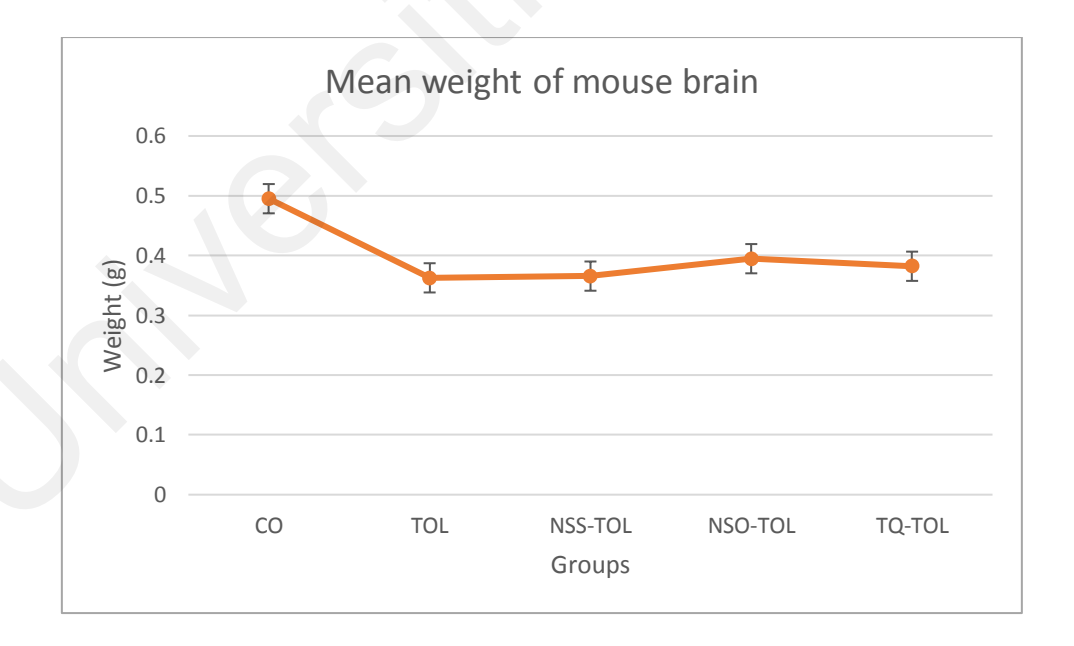


Figure 4.18: Mean weight of mouse brain

Toluene and NS treatments also had no significant effects on the length and width of mice brain as compared to the control group (one-way ANOVA, $p \ge 0.05$; Table 4.8 and 4.9; Figure 4.19). However, all treated with toluene had decreased length and weight of brains compared to control.

Table 4.8: Mean squares from ANOVA for length of mice brain treated with CO, TOL and NS treatment groups

Source of Variation	SS	df	MS	F	P-value	F crit
Between Groups	0.065333	4	0.016333	2.247706	0.092542	2.75871
Within Groups	0.181667	25	0.007267			
Total	0.247	29				

Table 4.9: Mean squares from ANOVA for width of mice brain treated with CO, TOL and NS treatment groups

Source of Variation	SS	df	MS	F	P-value	F crit
Between Groups	0.018667	4	0.004667	0.328638	0.85606	2.75871
Within Groups	0.355	25	0.0142			
Total	0.373667	29				

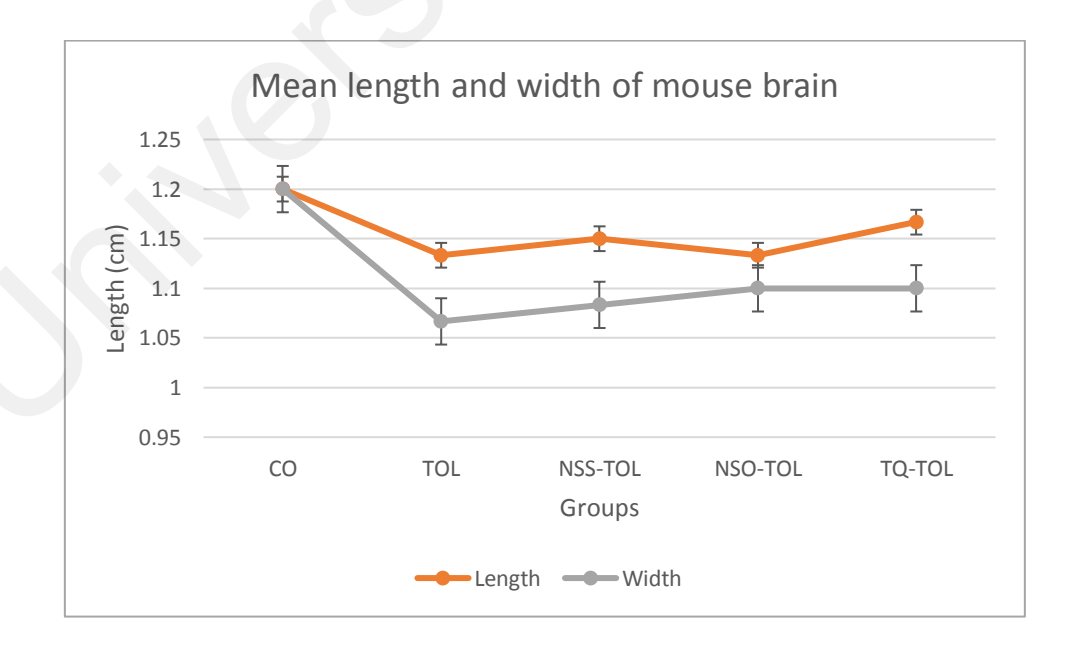


Figure 4.19: Mean length and width of mouse brain

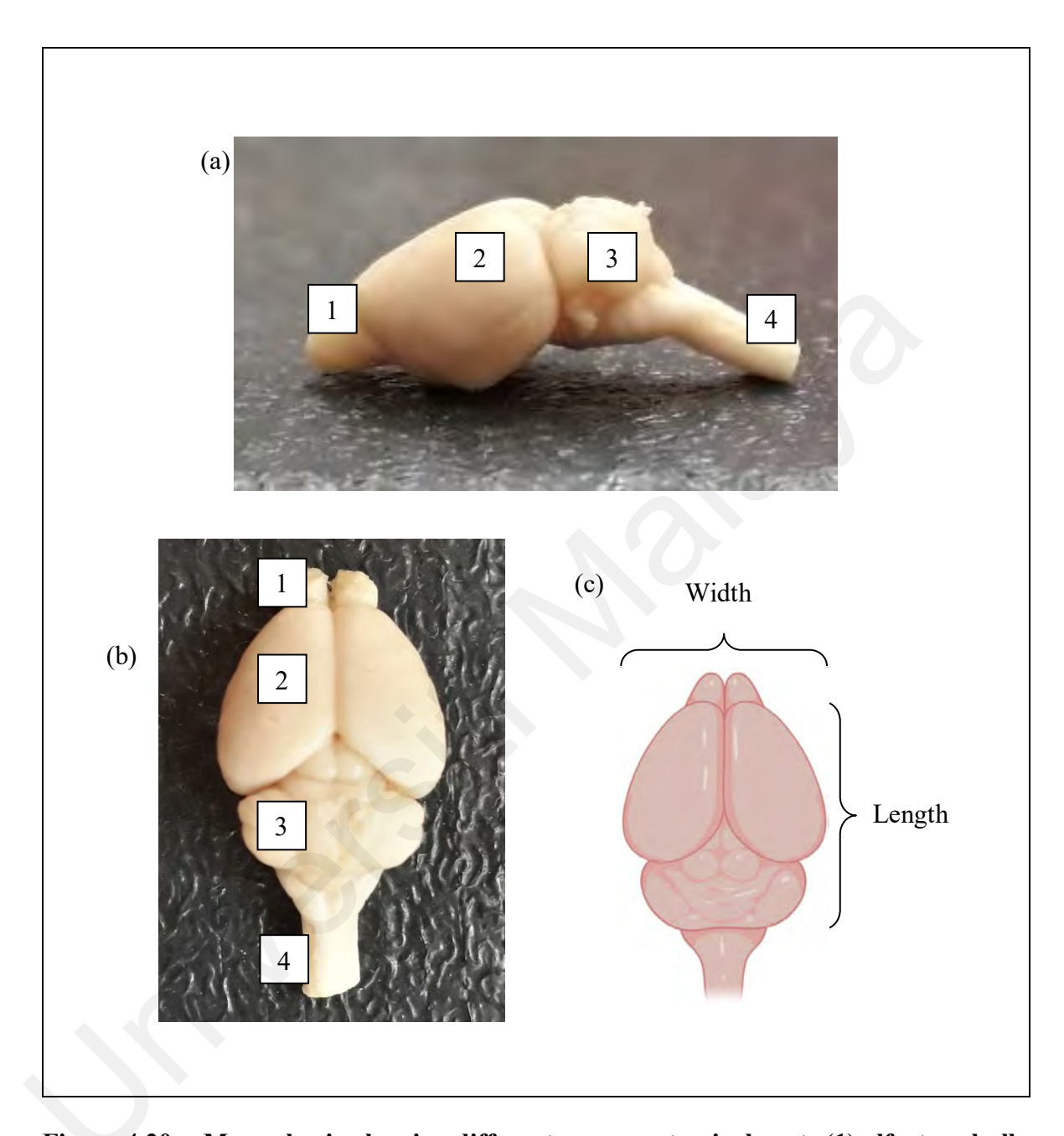


Figure 4.20: Mouse brain showing different gross anatomical parts (1) olfactory bulb, (2) telencephalon, (3) cerebellum, and (4) medulla oblongata. (a) Lateral view of mouse brain. (b) Dorsal view of mouse brain. (c) Schematic diagram of mouse brain showing measurements parameters.

4.3.3 Morphometric analysis of hippocampal CA1 pyramidal neurons

Evaluations were conducted on the hippocampal CA1 pyramidal neurons in the right brain hemisphere of mice. Figures 4.21 shows the intact morphology of the hippocampus, where the CA1, CA3 and DG regions were observed. Cells were densely stained making up the specific CA1, CA3, and DG layers. Figure 4.22 shows the CA1 region of the hippocampus. The pyramidal neurons of CA1 region demonstrated a normal profile with pale nucleus and prominent nissl granules in the cytoplasm.

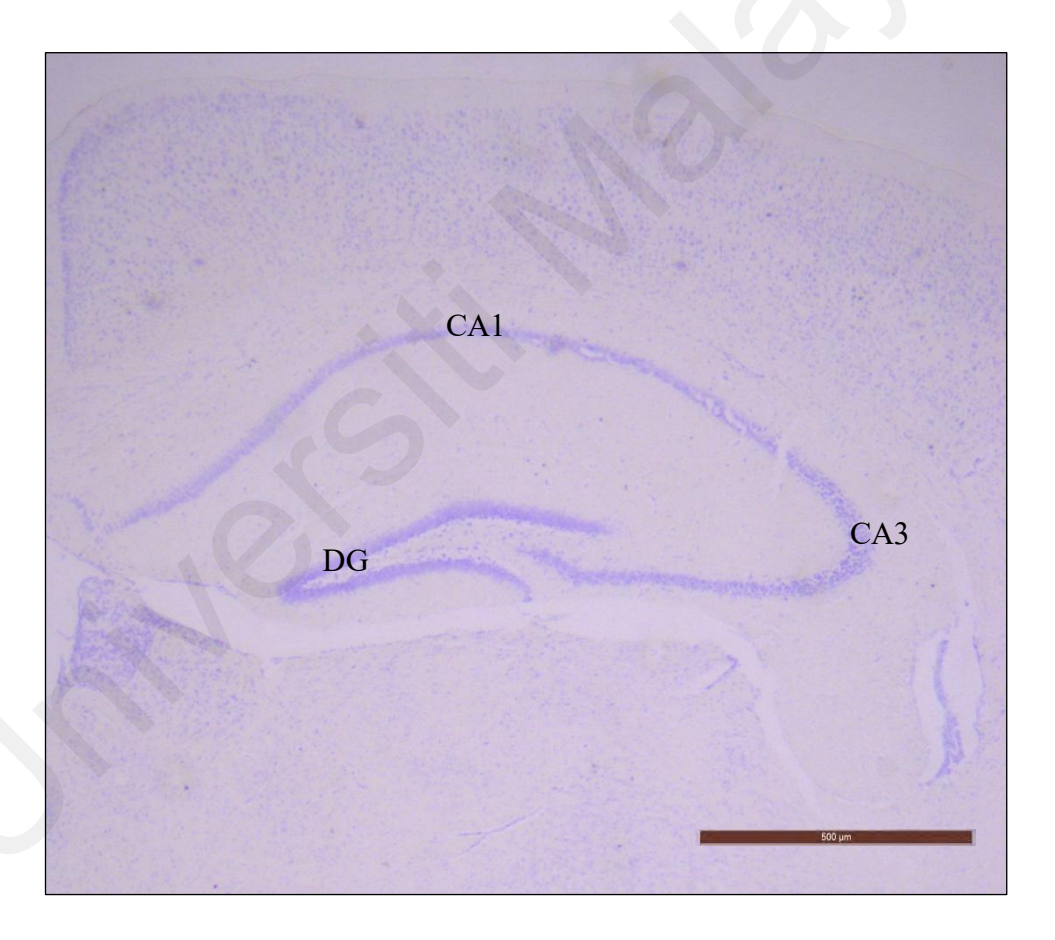


Figure 4.21: Photomicrograph of hippocampus of right brain hemisphere analysed in this study. ($40 \times$ magnification, 500 μ m calibration).

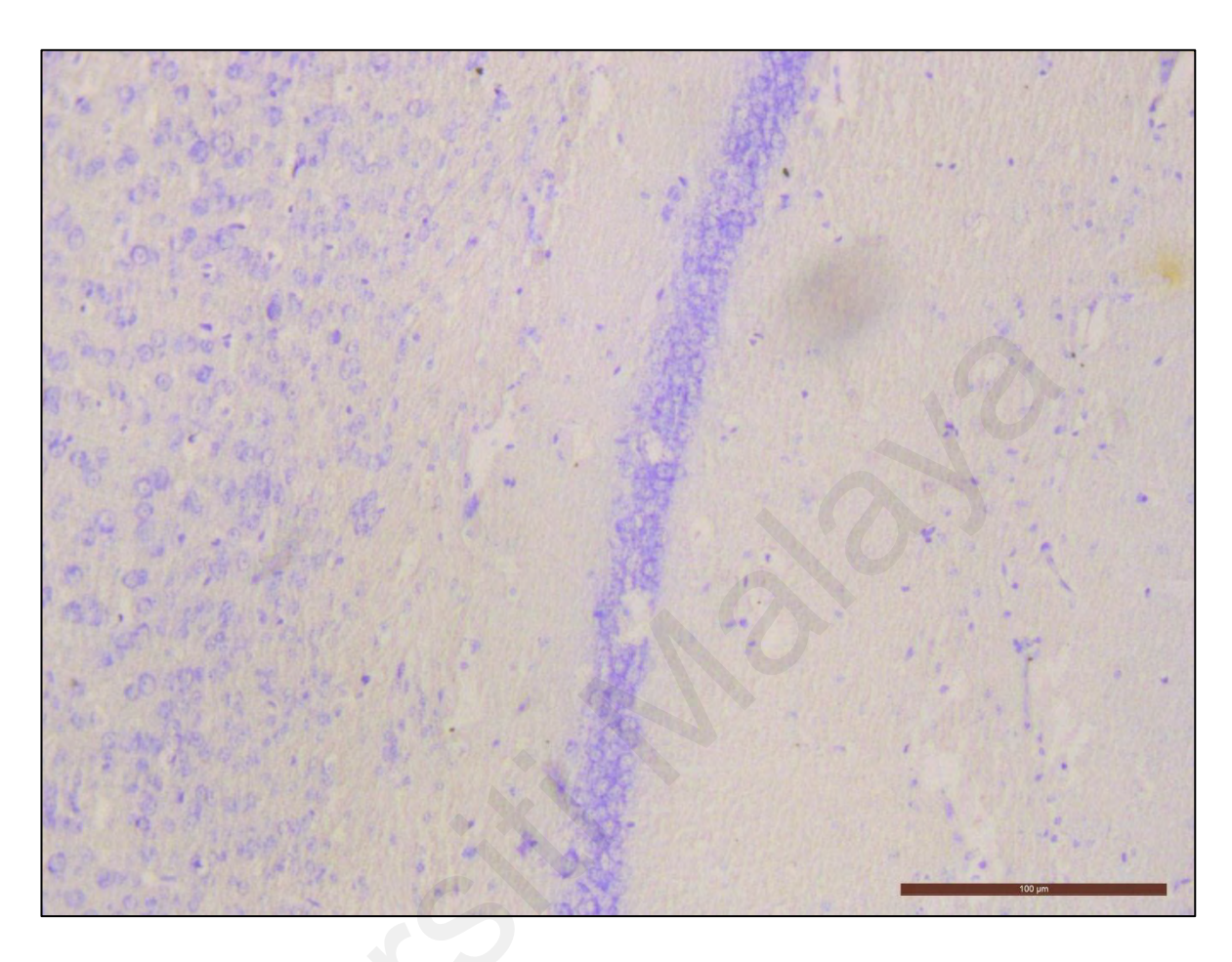


Figure 4.22: Photomicrograph of hippocampal CA1 pyramidal cell layer analysed in this study. (200× magnification, 100 μ m calibration)

4.3.3.1 Effects of TOL, NSS, NSO and TQ treatments on CA1 pyramidal neurons

Effects of TOL and NS supplementations were investigated using a few selected parameters, namely, somatic area, somatic perimeter, somatic circularity, somatic aspect ratio, and somatic roundness.

4.3.3.1 (a) Somatic area

Figure 4.23 shows developmental changes in the somatic area of hippocampal CA1 pyramidal neurons. One-way ANOVA demonstrated non-significant effect of treatments on somatic area of CA1 pyramidal neurons between all groups ($p \ge 0.05$) (Table 4.10). As seen from the figure, group TOL-NSO showed the largest somatic area of 25.75 μ m².

Table 4.10: Mean squares from ANOVA for somatic area of CA1 pyramidal neurons of mice treated with CO, TOL and NS treatment groups

Source of Variation	SS	df	MS	F	P-value	F crit
Between Groups	148.3961	4	37.09904	0.960861	0.446133	2.75871
Within Groups	965.2547	25	38.61019			
Total	1113.651	29				

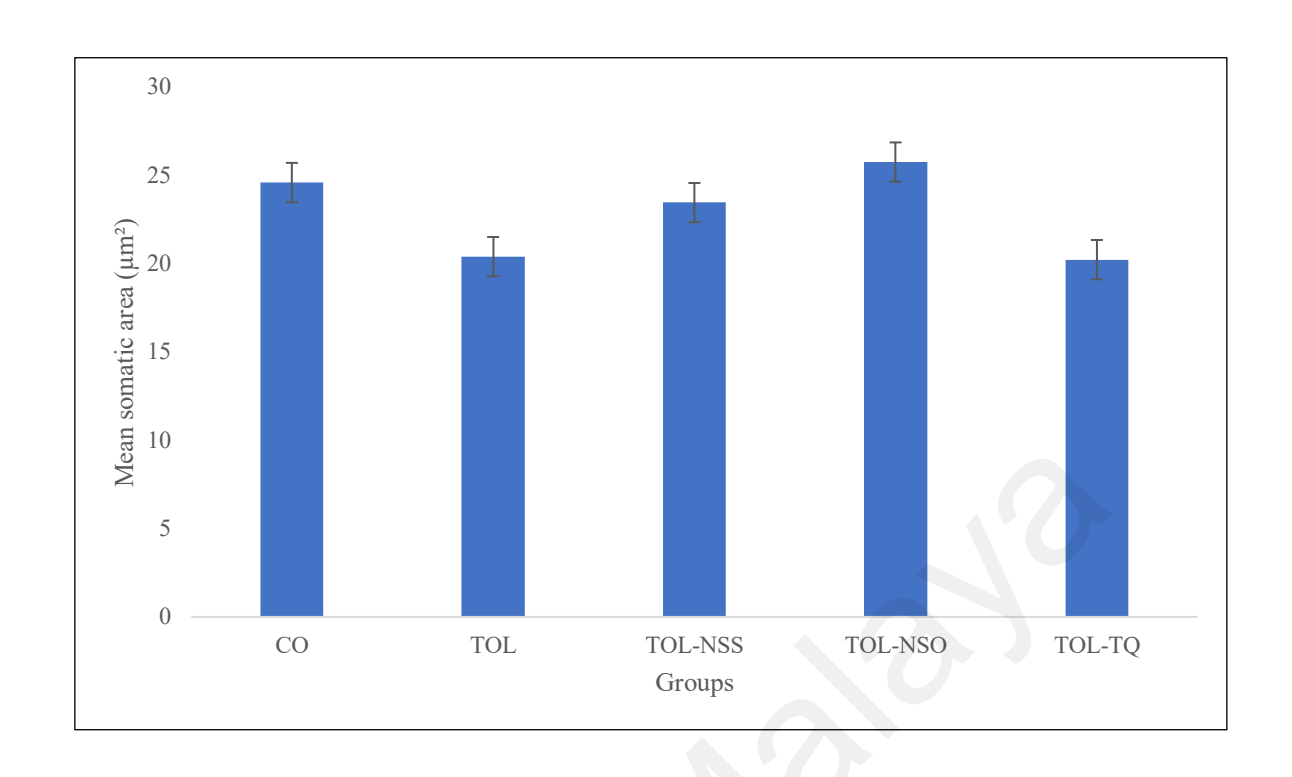


Figure 4.23: Mean somatic area of CA1 pyramidal neurons

4.3.3.1 (b) Somatic perimeter

One-way ANOVA yielded non-significant effect of treatments on somatic perimeter of CA1 pyramidal neurons between all groups (p \geq 0.05) (Table 4.11). TOL-NSO showed the largest somatic perimeter of 18.50 μ m, while group TOL showed the smallest somatic perimeter of 16.45 μ m (Figure 4.24).

Table 4.11: Mean squares from ANOVA for somatic perimeter of CA1 pyramidal neurons of mice treated with CO, TOL and NS treatment groups

Source of Variation	SS	df	MS	F	P-value	F crit
Between Groups	21.1793	4	5.294825	0.911326	0.472608	2.75871
Within Groups	145.2507	25	5.810026			
Total	166.43	29				

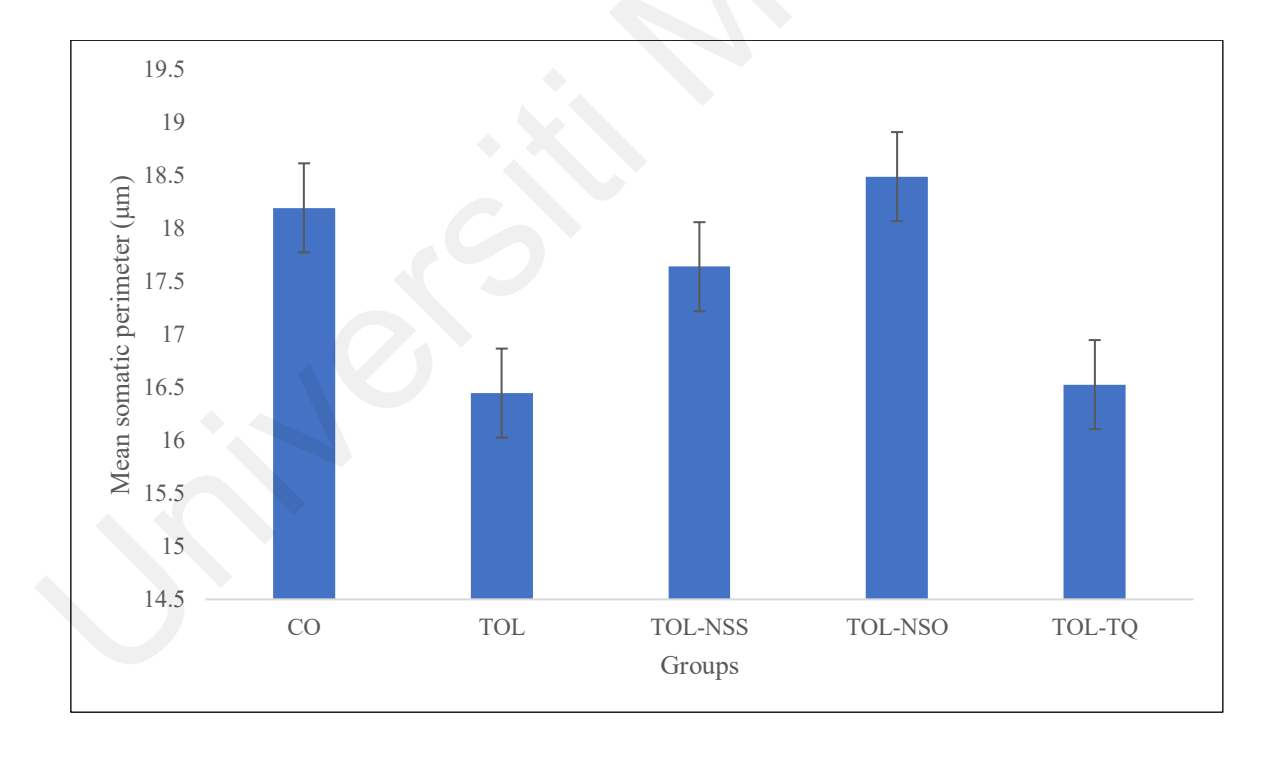


Figure 4.24: Mean somatic perimeter of CA1 pyramidal neurons

4.3.3.1 (c) Somatic circularity

One-way ANOVA indicated non-significant effect of treatments on somatic circularity of CA1 pyramidal neurons between all groups (p \geq 0.05) (Table 4.12). The mean somatic circularity of CA1 pyramidal neurons was greater than 0.900 μ m. Group TOL-NSO showed the largest somatic circularity of 0.922 μ m, while group TOL-NSS showed the smallest somatic circularity of 0.901 μ m (Figure 4.25).

Table 4.12: Mean squares from ANOVA for somatic circularity of CA1 pyramidal neurons of mice treated with CO, TOL and NS treatment groups

Source of Variation	SS	df	MS	F	P-value	F crit
Between Groups	0.002114	4	0.000529	2.155898	0.103529	2.75871
Within Groups	0.00613	25	0.000245			
Total	0.008244	29				

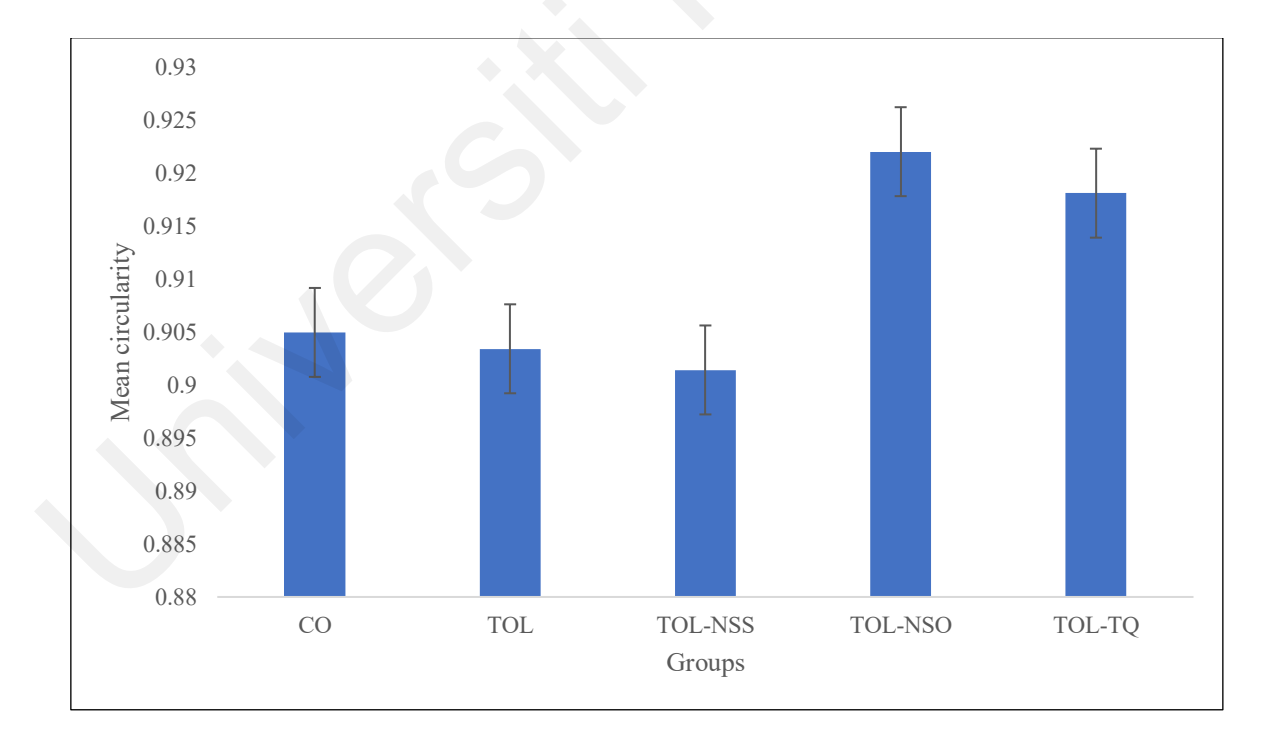


Figure 4.25: Mean somatic circularity of CA1 pyramidal neurons

4.3.3.1 (d) Somatic aspect ratio

One-way ANOVA demonstrated non-significant effect of treatments on somatic aspect ratio of CA1 pyramidal neurons between all groups (p \geq 0.05) (Table 4.13). The mean somatic aspect ratio of CA1 pyramidal neurons was greater than 1.25. Group TOL-NSS showed the largest somatic circularity of 1.33, while group TOL-NSO showed the smallest somatic circularity of 1.28 μ m (Figure 4.26).

Table 4.13: Mean squares from ANOVA for somatic aspect ratio of CA1 pyramidal neurons of mice treated with CO, TOL and NS treatment groups

Source of Variation	SS	df	MS	F	P-value	F crit
Between Groups	0.00965	4	0.002412	0.635668	0.641821	2.75871
Within Groups	0.09488	25	0.003795			
Total	0.10453	29				

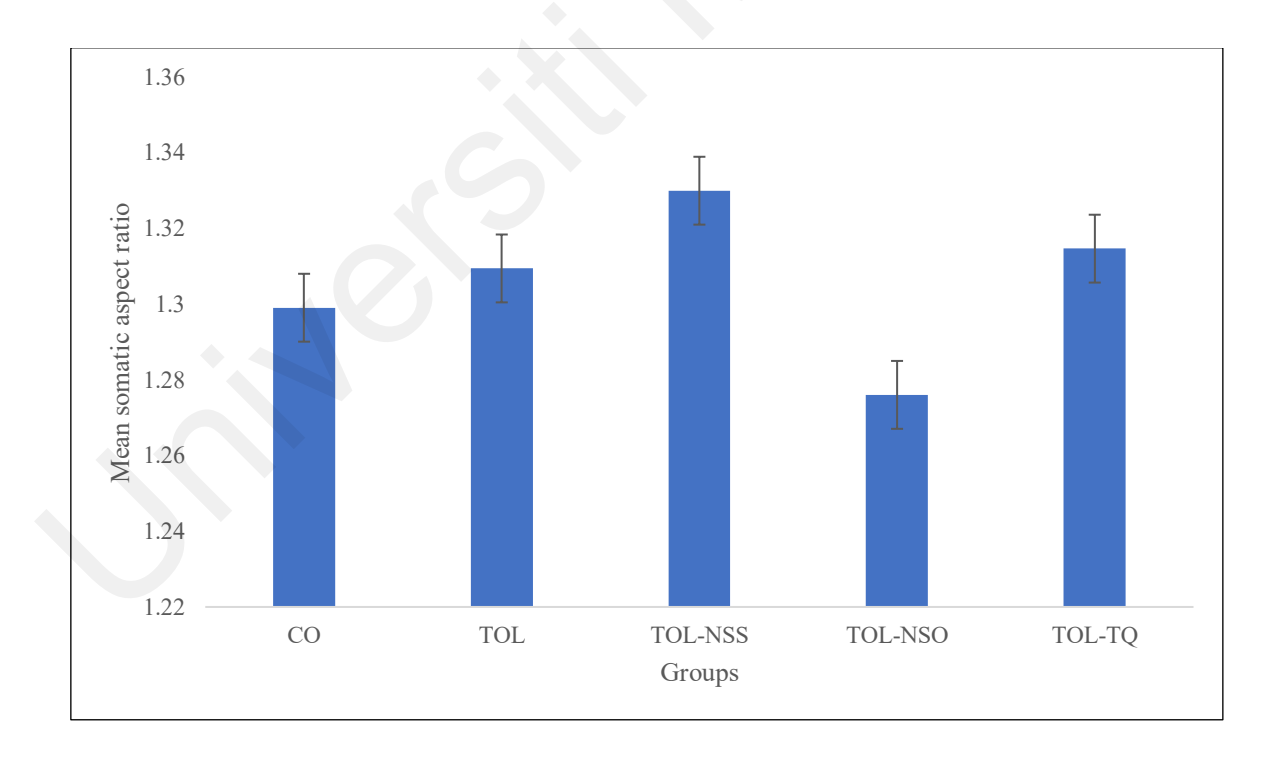


Figure 4.26: Mean somatic aspect ratio of CA1 pyramidal neurons

4.3.3.1 (e) Somatic roundness

One-way ANOVA demonstrated non-significant effect of treatments on somatic roundness of CA1 pyramidal neurons between all groups (p \geq 0.05) (Table 4.14). The mean somatic roundness of CA1 pyramidal neurons was greater than 0.700 μ m. Group TOL-NSO showed the largest somatic roundness of 0.797 μ m, while group TOL-NSS showed the smallest somatic roundness of 0.770 μ m (Figure 4.27).

Table 4.14: Mean squares from ANOVA for somatic roundness of CA1 pyramidal neurons of mice treated with CO, TOL and NS treatment groups

Source of Variation	SS	df	MS	F	P-value	F crit
Between Groups	0.002134	4	0.000533	0.547485	0.7025	2.75871
Within Groups	0.024356	25	0.000974			
Total	0.026489	29				

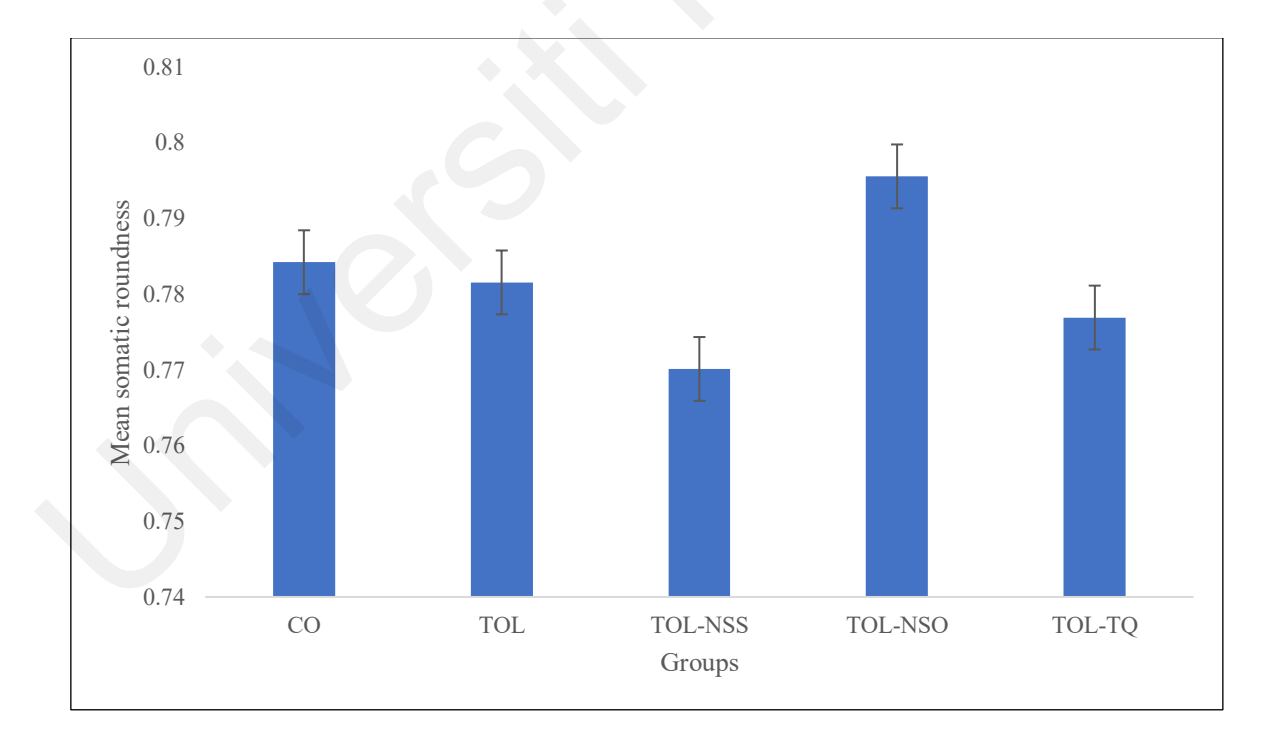


Figure 4.27: Mean somatic roundness of CA1 pyramidal neurons

CHAPTER 5: DISCUSSION

5.1 Effects of TOL, NSS, NSO and TQ treatments on memory

The present study aimed to evaluate the changes in recognition memory performance in mice after treated with TOL and NS supplementations of NSS, NSO and TQ. The results of this study did not show a significant difference in recognition memory performance between the treatment groups. However, the findings demonstrated that mice treated with TOL only had the lowest discrimination index (DI) as compared to the control and other treatment groups. Similar results were shown in the percentage of object preference. The mice in TOL group demonstrated higher interest towards the familiar object over the novel object.

5.1.1 Effects of TOL treatment

Past studies showed that toluene exposure leads to memory damage. The present study showed a reduction in mice recognition memory performance between the toluene and control group. This is similar to a study conducted by Win-Shwe and Fujimaki (2012), where they found that although not statistically significant, mice treated with acute toluene exposure of 300 mg/kg body weight showed poor discrimination between novel and familiar object. The mice had higher preference towards the familiar object, as compared to its control group. Similarly, in another study conducted by Montes et al. (2017) on acute toluene exposure (single dose of 1000-6000 ppm toluene), mice exposed to 1000 ppm toluene showed reduction in the recognition index, though reduction was only significant in the groups of mice exposed to 2000-6000 ppm toluene.

Armenta-Reséndiz et al. (2019) observed a concentration-dependent effect of toluene on memory performance through the PAT. The latency to step through the dark phase

significantly lessened from a concentration of 4000 ppm to 8000 ppm, hence indicated a reduction in the rats' memory retention. Prolonged exposure of mice to solid air freshener, known to majorly contain VOC, which also includes toluene, demonstrated memory impairment in Y-maze and NOR tests. High doses of the air freshener caused significant memory dysfunction, while no changes were observed in lower doses (Umukoro et al., 2021).

Data from this present study suggested that a marked reduction in recognition memory performance of adult mice would be unlikely with low toluene exposure. This is supported by a study conducted by Kantachai et al. (2020) on ICR mice and healthy employees of a car painting industry exposed to low concentrations of toluene for a continuous period. There was no significant difference in recognition index of NOR test in mice exposed to 50, 100 and 150 ppm toluene. However, reduction in dopamine levels was noted. Memory performance of the employees that were exposed to 50 ppm toluene also showed no difference when compared to its control group. No abnormal conditions of the staffs were reported.

Malondialdehyde (MDA) is an intermediate product of lipid peroxidation that may cause tissue or organ damage. High concentrations of MDA has been proven to induce memory and learning disabilities and impair CA1 hippocampal neurons (Jianguang & Dazhong, 2011). Interestingly, in a cross-sectional study conducted on workers of a printing industry in Surabaya, no significant relationship was concluded between toluene exposure (mean concentration of 1.23 ppm) and MDA levels. However, workers reported health complaints concerning coughing, mild headaches, and shortness of breath (Ayu et al., 2020).

Meanwhile, in another study involving 1000, 2000, 4000 and 6000 ppm toluene exposure, rats exposed to both acute (a single 30-min exposure) and chronic (30-min exposure, twice a

day, for 10 days) concentration of toluene were found to exhibit significant impairment in memory acquisition (Huerta-Rivas et al., 2012). As opposed to the present study conducted on adult mice (8 weeks old), their study was conducted on adolescent (postnatal day (PN) 35) and young adult (PN 56) rats; thus, might explain the significance of the toluene impact. In addition, the rats in their study underwent the NOR test 30 minutes after exposed to toluene, which differs from the present study where mice were subjected to NOR test 24 hours after the last toluene treatment. There was also a study that showed 250, 500 and 750 mg/kg body weight toluene administration in mice 30 minutes before the NOR test caused significant reduction in the recognition index (Chan et al., 2012). The different results might be due to the time factor of toluene administration.

Studies using higher concentration of toluene have shown evidence of significant recognition memory impairments after toluene exposure (Hsieh et al., 2020; Lin et al., 2010; Wu et al., 2018). Repeated exposure of 8000 ppm toluene, twice a day, for 10 days, manifested significant memory impairments in rats, depicted in a significant decrease of DI in NOR and a reduction in the latency to step through in PAT (Cruz et al., 2020). Another study that utilized the MWM test to study cognitive memory reported significant memory deficits in rats exposed to 12,000 ppm toluene (Callan et al., 2017).

Decreased and tendency for decreased memory performance in toluene treated subjects might be due to the effects of toluene on neurotransmitters involved in memory, such as the dopaminergic and GABAergic neuronal systems. Stimulation of dopamine neurotransmitter is known to be part of a hippocampal-striatal-prefrontal loop that coordinates new memories; thus, makes it vital in memory encoding and consolidation processes (Clos et al., 2018). *In vitro* assays manifested that toluene caused an increase of dopamine release in several regions of the brain, via stimulation of the dopaminergic neurons in the tegmental ventral area (Soares

et al., 2020b). Previous findings by Win-Shwe and Fujimaki (2012) showed that a single toluene exposure prominently reduced the expression level of NR1 and NR2 messenger ribonucleic acid (mRNA), resulting in changes in the synaptic function and impairments in the long-term memory. This was supported by a study where rats treated with MK801, a noncompetitive NMDA receptor antagonist, showed a destructive effect on short and long-term memory performance in the object recognition test (De Lima et al., 2005). NMDA receptor is a subtype of glutamate receptor that converts certain neuronal activities into structural and functional changes of the synapse which are essential for higher cognitive functions (Jinping Liu et al., 2019). These findings suggest that NMDA receptor activation plays an important role in memory functions.

5.1.2 Effects of NS supplementations

Present results showed an increase, although not significant, in the DI and novel object preference in TOL-NSS, TOL-NSO, and TOL-TQ groups as compared to TOL and CO groups. Among the three NS supplementations, TQ seems to alleviate the TOL-induced memory impairment effects better than NSS and NSO. It was previously reported that there was a significant increase in memory in hyperthyroid juvenile rats supplemented with TQ, indicated by a marked reduction in time latency to reach the platform in MWM test and an increase in time latency to enter the dark phase in PAT (Baghcheghi et al., 2018). TQ has been reported as the main pharmacologically active substituent of NS seeds and oil. Chronic oral administration of TQ (25mg/kg) per day for 12 weeks in adult rats showed a notable improvement in the PAT, associated with the increment of BDNF. Stimulation of cAMP-response element-binding protein (CREB) phosphorylation was also stimulated (Hashimoto et al., 2021). This finding suggests that BNDF is involved in the memory enhancement effects of TQ.

Other previous studies also showed the protective effect of TQ on memory. For example, rats suffering from induced AD after long-term administration of D-galactose (D-Gal)/aluminum chloride (AlCl₃) combination showed marked decrease in the step-through PAT, but when treated with 20 mg/kg TQ, the step-through latency increased significantly (Abulfadl et al., 2018a, 2018b). Improved cognitive performance in the rats were associated with increased SOD and TAC levels, decreased MDA and NO levels, and reduced acetylcholinesterase (AChE) activities. The performance of AD-induced rats supplemented with 10 mg/kg TQ for 4 weeks in Y-maze spontaneous alteration test was also significantly better than the non-supplemented rats, indicated by a higher spontaneous alteration performance. Besides that, decreased MDA and increased acetylcholine (Ach) levels were observed (Fanoudi et al., 2019; Fiasal Zaher et al., 2019). The group suggested that TQ meliorates cognitive strength through the enhancement of cholinergic function and attenuation of oxidative stress.

Similar to results from the present study, a low dose of 10 mg/kg TQ significantly hampered the memory deficits of global cerebral ischemia-reperfusion injured rats, demonstrated by an increase of DI in the NOR test (Hussien et al., 2020). Correspondingly, significantly increased SOD and GSH-Px levels, and significantly decreased MDA levels were observed.

In agreement with the present study, 0.5ml/kg of NSO administered orally for 10 days improved spatial memory of rats in the MWM test, displayed by a significant reduction in the escape latency time (Asrar et al., 2020). Male Wistar rats co-administered orally for 2 weeks with pentylenetetrazole (PTZ), probiotics and 400 mg/kg ethanolic extract of NS seeds showed inhibitory effects on kindling-induced learning and memory impairments. NS extract highly improved the learning of MWM tasks, proven through a nearly similar behavioural

function to the control group, in both the acquisition and probe trial tests (Tahmasebi et al., 2020). The group suggested that the ameliorating effects of NS against PTZ toxicity might be due to its antioxidant properties and its protection against AChE activity. In a study conducted by Toktam et al. (2011), pre-treatment of 200 and 400 mg/kg hydro-alcoholic extract of NS for 3 weeks in rats treated with scopolamine showed longer time latency in entering the dark compartment in the PAT. The prevention of scopolamine-induced memory impairment by NS is suggested due to the lower AChE activity, increased total thiol activity, and lower cortical MDA concentrations.

Previous data from human and animal studies strongly support the importance of the central cholinergic system as part of the neural circuitry in learning and memory. In the brain, Ach inhibits neuroinflammation and stimulates synaptic plasticity, an activity associated with the mechanisms responsible for memory formation (Bali et al., 2019). AChE hydrolyses Ach into inactive choline and acetate (Figure 5.1), thus modulates the brain Ach level which then causes disruption in the normal memory functions (Taqui et al., 2022). High levels of Ach is required for well-preserved memory performance (Maurer and Williams, 2017). A study on different grades of NSO containing different amount of TQ content demonstrated notable capabilities of AChE inhibition (Kannan et al., 2019). NSO with higher TQ content demonstrated higher AChE inhibition activity. This finding suggests that AChE inhibition imparts a huge role in the neuroprotective effect of NSO and TQ on memory.

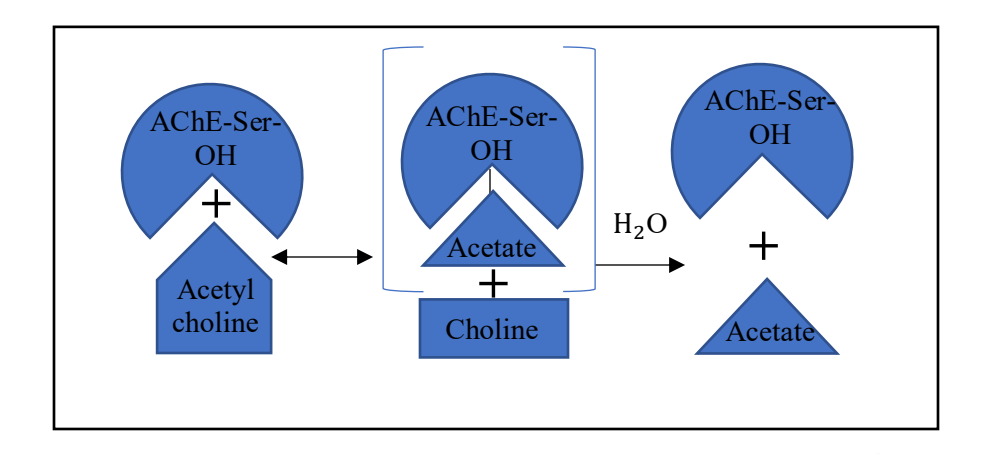


Figure 5.1: Hydrolysis of acetylcholine (ACh) to choline and acetate via acetylcholinesterase (AChE) activity. Adapted from Taqui et al. (2022).

Hydroalcoholic extract of NS and its bioactive constituent TQ administered orally in cerebral hypoperfusion-induced rats for 10 days showed significant ameliorating effects as evidenced by decreased time latency to reach platform, decreased swimming time, and increased time spent in the target quadrant in the probe trial in the MWM task. Improved memory performance in the rats might be influenced by the alleviated changes of hippocampal lipid peroxidation and enhanced SOD and AChE activities (Fanoudi et al., 2019). In another study, memory performance in MWM test improved and AChE along with NO and ROS activities were found to decrease in rats administered with 1 ml/kg of NSO for 14 consecutive days (Aminu et al., 2019). The reduced AChE activity in NS-treated groups supports the findings that it plays an essential role in memory mechanisms.

In a separate study involving NS-treated albino mice, it was reported that though not significant, the latency to locate platform in MWM test decreased; thus, indicating improved memory in mice (Imam et al., 2017). Similarly, it has been reported that NSO could exert enhancing effects in memory performance of rats after chronically treated with nicotine, through a significant improvement in the radial arm maze (RAM) test (Sahak et al., 2013). Administration of 200 mg/kg of NS extract in lipopolysaccharide (LPS)-treated rats was

found to restore the LPS-induced memory impairments in rats, through a lower time latency and traveled length to reach the platform in the MWM test, as compared to the control LPS group (Anaeigoudari et al., 2018). These findings are similar to the present study, where the DI in NOR test of NS-treated mice showed an increase, though not significant, as compared to its control group. This finding suggests that acute administration of NS still has beneficial effects on learning and memory in animals.

5.2 Effects of TOL, NSS, NSO and TQ treatments on brain morphology

In the present study, changes in brain morphology were evaluated after treatments with TOL and NS supplementations (NSS, NSO, and TQ). Mice in all treatment groups showed no significant changes in brain morphology.

5.2.1 Effects of TOL treatment

The weight, length and width of toluene-treated mice brain showed no significant differences when compared to the control group. Similar to present result, a study on rabbits showed that 1000 ppm of toluene exposure for 8 hours a day for 14 days had no significant changes in the brain weight/body weight (Abouee-Mehrizi et al., 2020). Another study on rat model of chronic intermittent toluene also showed that exposure to 3,000 ppm toluene had no significant effects on brain weight (Duncan et al., 2012). Similarly, prenatal exposure of 650 mg/kg body weight toluene to rat pups resulted in no significant changes in brain weight (Gospe & Zhou, 2000). Gospe and Zhou (2000) suggested that despite the abnormal proliferation and migration of neurons, the insignificant reduction in brain weight of the rats might be due to the increased development of glia or neuropil.

In contrast, a study by Pascual et al. (2010) discovered that there were significant changes in gross brain measurements of pre-weaning rats exposed to a solvent mixture of toluene and hexane for 10 days. The brains were drastically reduced in weight and size. Rats aged 50 days old that were exposed to 80 ppm toluene for 4 weeks (5 days/week, from 0830 to 1430 h) also showed significant reduction in brain weight (Von Euler et al., 2000). In addition, Burry et al. (2003) reported similar findings in rats administered with toluene for 7 days. Inhibition of neurons and astroglia proliferation were attributed to the reduced brain weight, as evidenced by a decrease in glial fibrillary acidic protein (GFAP) level.

Data from these studies demonstrated significant results, which differ from the present study. The different results might be due to several factors. Firstly, the age of the animals used in the studies were pre-weaning and young (P50) animals, instead of adult mice (8 weeks old) used in the current study. According to Jackson et al. (2017), age has a significant impact on the experimental outcomes. The key immunological marker B-cells have shown to have an immature phenotype until four weeks of age while T-cell responses mature around eight weeks of age. Moreover, the production of T and B-lymphocyte only starts to increase after the first 26 weeks of life. For the CNS development in rats, significant brain growth is ongoing until nine weeks of age and myelination in limbic structures completes at six weeks of age while in mice, the spinal cord, hippocampus and olfactory structures is fully develops after 11 weeks of age. Secondly, the dosage of the toluene exposure in the studies far exceed the dosage used in the current study. Thirdly, the duration of toluene exposure were longer in the studies as compared to the current experiment.

There were studies that reported that male mice in their late postnatal period exposed to 5 or 50 ppm toluene for 6 hours per day for 5 days showed no significant changes in brain weight (Win-Shwe et al., 2012). However, contradictorily, an increase in the GFAP level was

noted in mice exposed to 5 ppm toluene. This finding suggests that reduced brain weight may not directly reflect a reduction in the survival and development of brain neurons.

5.2.2 Effects of NS supplementations

NSS, NSO, and TQ administered on mice in the present study showed no significant changes in terms of brain morphology. In contradiction, Mohamadin et al. (2010) revealed that NSO significantly increased the weight of various regions of the brain in propoxurtreated rats. It was also found that socially isolated mice pre- and post-treated with 1 ml of NSO orally for 10 days had increased relative brain weight (Folarin et al., 2020). The difference in results may be due to the different dosage and duration of NS treatments administered.

5.3 Effects of TOL, NSS, NSO and TQ treatments on morphometric properties of CA1 pyramidal neurons

Gross morphology examination of brain tissue is a laboratory procedure in which pathological and medical examinations are carried out under the visibility of naked eyes, whereas microscopical examination is carried out to examine histopathological aspects under the microscope. In most aspects, results of gross morphological observations precede microscopic examination. However, for further clarification and better confirmation of the tissue conditions, microscopical examination is a more reliable and affirming approach (Alturkistani et al., 2015).

Results from present study showed no significant changes in terms of somatic size and somatic shape of hippocampal CA1 pyramidal neurons in mice treated with TOL, TOL-NSS, TOL-NSO, and TOL-TQ. To date, no studies have been conducted in terms of morphometric analysis on the somatic size and shape of CA1 hippocampal pyramidal neurons after TOL

and NS supplementations (NSS, NSO and TQ treatments). Somatic development of neurons in terms of their size was analysed based on the changes in somatic area and somatic perimeter. The results of this study showed that there was no significant difference in somatic area and somatic perimeter between the groups. However, for both parameters, neurons in the TOL group had lower somatic size than the control group.

Studies have investigated that morphological dysregulation in neurons and neuronal soma area may have substantial consequences on the brain circuit function, which may cause certain neurodevelopmental and neurological disorders (Paramo et al., 2021; Sathe et al., 2017). Previous studies have reported alterations in soma size in Costello Syndrome, Rett Syndrome, and depression. Rett syndrome is a neurodevelopmental disorder caused by a mutation in the MeCP2 gene, encoding methyl-CpG-binding protein 2. *In vitro* studies revealed that soma size of neurons in Rett syndrome mouse models carrying MeCP2 mutations were smaller when compared to controls (Marchetto et al., 2010; Rangasamy et al., 2016). The role of MeCP2 in the regulation of neuronal soma size and retrieval of morphological phenotypes, behaviour and neurological functions is recognized (Sampathkumar et al., 2016). Therefore, the results indicate that reduced neuron soma size is a reflective of disturbance in the mechanism of normal neuron regulatory system.

A polarized morphology allows neurons to initiate synaptic connections and construct functional circuits. Failure for neurons to retain their morphological and functional integrity leads to neurodevelopmental disorders (Parenti et al., 2020). Paramo et al. (2021) demonstrated the importance of neuregulin-4 (NRG4) in maintaining the somatic size of the motor cortex pyramidal neurons. Absence of NRG4 in mice resulted in a decrease in the neuron soma size and deficiencies in motor functions as assessed by motor rotarod performance. Besides NRG4, protein kinase B (PKB) or also known as Akt has been known

to play a key role in controlling neuronal soma size in neonatal hippocampus (Murase et al., 2011). Akt functions in multiple interconnected cell signaling systems involved in the metabolism, growth and division of cells. Interference with the Akt-regulated pathways may result in neurological diseases (Nitulescu et al., 2018). Low levels of Akt activation induced smaller soma size of pyramidal neurons.

Previous studies have also shown that compartmental size of neurons is dependent on the maintenance of mRNA levels in neurons. Ransdell et al. (2010) demonstrated that steady-state levels of 18S ribosomal RNA (Rrna) and mRNA for glyceraldehyde 3-phosphate dehydrogenase (GAPDH) and elongation factor 1 (EF1)-alpha are correlated with size of the soma of different neuron types. These gene products are involved in basic cellular metabolic functions and cellular somatic size regulation. A morphometric study on hippocampal neurons in chronic immobilization stress revealed that the perikaryonic area of hippocampal CA1 neurons in stressed rats significantly reduced, while their somas showed slight deformation and loss of contour sharpness (Dolzhikov et al., 2015).

Freas et al. (2013) studied on the somatic size of hippocampal neurons in food-caching birds, comparing between ten populations of black-capped chickadees and three populations of mountain chickadees along a gradient of winter climate harshness. They found that birds from the harsher environments had significantly larger hippocampal neuron soma size. Since birds in harsher winter environments must rely on previously stored food in the caches for survival, good spatial memory is needed for them to recall the location of their caches. Hence, this finding suggests that neuron soma size may be associated with cognitive capability. Larger cell bodies could accommodate larger cellular and metabolic systems required to provide a larger neuron dendritic, more synaptic connections, and higher neuronal activities that all correspond to a larger memory capacity. In addition, a huge number of mitochondria,

which originates in the soma, is essential for higher neuronal activities. Therefore, it can be hypothesized that neuron soma size is a potential mechanism involved in memory and learning ability, with larger neuron soma supporting improved memory functions.

5.3.1 Effects of TOL treatment

Present study showed that mice administered with toluene showed reduction in somatic area and somatic perimeter as compared to the control group. Salem and Kelada, (2020) reported that toluene caused complete loss of normal architecture in the cytoplasm, mitochondria, and nuclei of the cells. The cells exhibited vacuolated or shrunken cytoplasm, asymmetrical nuclei, and swollen mitochondria with loss of their cristae structure. Some cells showed degenerative changes, indicated by the vacuolation of cytoplasm, alteration of cellular construction, shrunken nuclei with condensed chromatin, and swollen mitochondria. Similarly, administration of 900 mg/kg toluene in rats caused shrunken neurons in the hippocampus and darkly stained cytoplasm with small nuclei size (Shaffie & Shabana, 2019). The distortion of cell structures caused by toluene is suggested due to oxidative stress.

Reduction in cell size manifests minor neurodegeneration characteristics. Apoptotic cells are commonly characterized morphologically by the shrinkage in cell size, distortion of plasma membrane, contraction of nucleus, retraction of neuronal processes, condensation of chromatin, and fragmentation of DNA (Ismail et al., 2013). Although the pathophysiological mechanisms underlying toluene neurotoxicity are still unknown, several mechanisms have been proposed. Firstly, due to its high lipophilicity, toluene could easily incorporate into cell membranes, causing distortion to the structure of neurons and their lipid-rich organelles, and disrupting the outgrowth and branching of dendrites (Moawad et al., 2021). Secondly, toluene may damage the cell integrity by accumulation of ROS and dysfunction of oxidative

metabolism. The condition of brain that requires large quantity of oxygen makes it prone towards cumulative oxidative stress (Sheikh & Mohamadin, 2012). Building up of ROS in cells develops deteriorating effects on its macromolecules especially membrane phospholipids, proteins, and DNA. Function of the neuronal plasma membrane enzymes and receptors may be disturbed, resulting in disintegration of the membrane phospholipids, thus leads to the impairment in fluidity and compartmentalization of the cells (Mousavi et al., 2010; Kanter, 2010). Since the hippocampal, cortical, and cerebellar tissues comprises mainly lipids, hydroxyl radicals and lipid peroxidation may easily damage the cells (Kanter et al., 2006).

Increment of oxidative stress markers has been reported in rats sub-chronically exposed to 1000 ppm toluene, showed by the increase of nicotinamide adenine dinucleotide phosphate (NADPH) quinone oxidoreductase-1 (NQO1) and reduced nicotinamide adenine dinucleotide (NADH) ubiquinone reductase (UBIQ-RD) activities (Kodavanti et al., 2015). Besides that, DNA damages were also observed in the hippocampus, cerebellum, and cortex of male mice administered with 5 or 15 mg/g toluene (Laio et al., 2019). Similar findings were demonstrated by Meydan et al. (2012) where rats injected with 0.5 ml/kg toluene exhibited higher MDA level as compared to its control group alongside with clear shrinkage of neuron soma, degeneration and vacuolization of neuropils, and detachments in the pia mater.

Reduction in the expression of enzymes that hinder oxidative stress has also been detected in animals treated with toluene (Demir et al., 2017; Kodavanti et al., 2015, 2011; Montes et al., 2017). In addition, glutamatergic NMDA may also play a vital role in structural cell maintenance and neural plasticity. NMDA activation promotes calcium intake in the

postsynaptic neuron, however, overexposure of this messenger to excitatory neurotransmitter activates a mechanism that causes excitotoxic neuronal death (Fouad et al., 2018).

5.3.2 Effects of NS supplementations

Based on present results, neurons in the TOL-NSS and TOL-NSO groups exhibited larger somatic size as compared to the neurons in TOL group. This is in line with the findings of the study by Kanter (2008) on the effects of NSO and TQ after chronic toluene exposure. Clearly reduced size of neurons appeared visible in the only toluene-treated group, whereas neuronal morphological improvements and reduced severity of cytoplasmic degenerative changes were observed in the NSO and TQ-treated groups. NSO and its essential oil component, TQ are reported to exhibit important antioxidant properties against generation of free radicals which are responsible in cellular oxidative damage.

Previous studies have showed the ability of antioxidants to counteract neurotoxic effects of toluene. Pre-treatment of TQ ameliorated the toxicity effects of arsenic in hippocampus of male rats (Firdaus et al., 2018), demonstrated by a significant increase in GSH content and SOD activity, and a significant decrease in the levels of lipid peroxidation through TBARS assay and protein carbonyl formation. Antioxidant properties of TQ was shown in female rats where damage caused by lead-induced free radicals on developing brain was ameliorated by TQ supplementation (Saleh et al., 2019). Not only did TQ caused reduction in MDA level and increment in SOD, CAT and GPx levels, but it also improved shape of the pyramidal neurons in the cortical layers. Another study by Lotfi and Satarian (2021) reported similar effects of TQ in increasing SOD and GSH levels as well as mitigating effects of nonylphenol-induced neuronal loss.

Glutathione-S-transferase (GST) and GSH are natural protective molecules that scavenge free radicals. Administration of TQ elevated the catalase, GSH and GST levels, enzymes, and correspondingly caused a reduction in lipid peroxidase levels. Besides that, TQ also enhanced the generation of NADPH that is required for the formation and function of GSH, which consequently decreased the amount of NO and MDA levels (Hamdan et al., 2019; Hamdy & Taha, 2009; Nagi & Almakki, 2009). Levels of oxidative marker, NO were also markedly reduced due to TQ activity that significantly inhibited p44/42 and p38 mitogenactivated protein kinases, enzymes that widely contribute to the transcriptional machinery of inducible NO synthase and NO production (Hamdy & Taha, 2009).

Alhebshi et al. (2013) elucidated on the potential of TQ in inducing structural changes and altering the dynamics of protein, thus preventing degeneration and most importantly, protecting the conformation of neurons. TQ was found to have the ability to change a soluble toxic A1-42 protein into larger insoluble, non-toxic, and high molecular weight assemblies, by increasing its sheet content. Khalife and Lupidi (2007) reported that a possible intracellular non-enzymatic reaction may also exist via chemical reactions between TQ and GSH, NADH and NADPH thus suggests that TQ has the capability to modulate cellular antioxidant defenses.

Younus (2018) elaborated on the mechanisms of TQ's antioxidant capability. TQ may prevent damages that occur due to the accumulation of ROS in cells which includes lesions of DNA, alterations of enzymatic activity and increment of membrane permeability. TQ is able to act as both antioxidant and/or pro-oxidant according to different concentrations. Reduction of TQ to thymohydroquinone by two-times reduction activity gives it the antioxidant capacity (Figure 5.2).

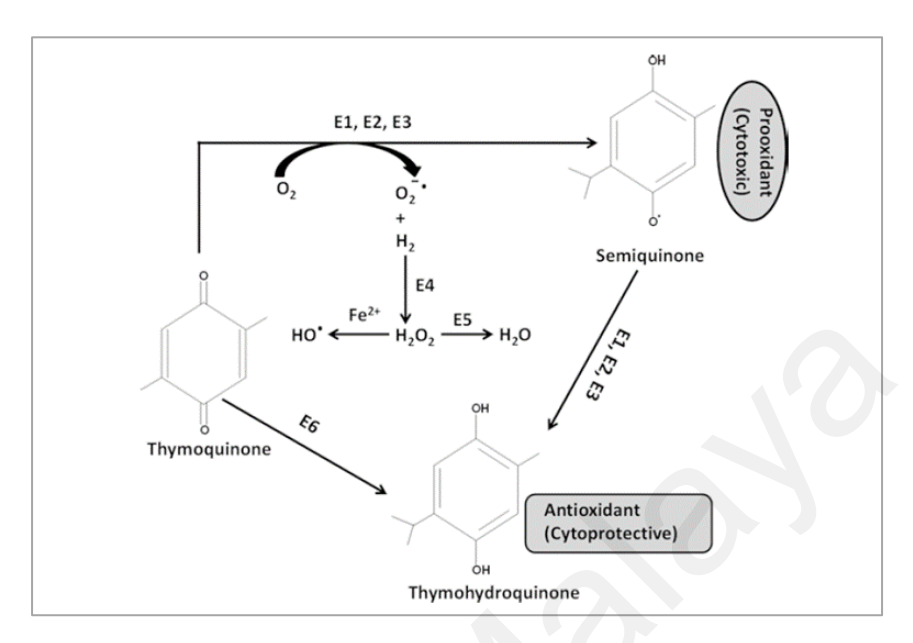


Figure 5.2: TQ redox cycle for antioxidant or pro-oxidant potential. Taken from Younus (2018).

Morphological development of the shape of cell bodies in the present study were analysed based on the somatic circularity, somatic aspect ratio, and somatic roundness. Nichols and co-workers (2018) compared the shapes of hippocampal CA1 and CA2 neurons in *Proechimys* rodents using four measures: circularity, aspect ratio, roundness, and solidity. Circularity shows how closely the shape is to a perfect circle, therefore, a high circularity value would indicate a mature, round neuronal soma. Aspect ratio and roundness reflects the elongation of a shape and solidity measures how symmetrical a shape is. Electrophysiological studies on the hippocampal neurons hypothesized that smaller soma size might stipulate a decrease in electrical resistance and a longer latency period but could not find the physiological effects of changes to the shape of neuronal somas.

The findings in this study showed that in all the soma shape parameters, no significant difference was observed. Neurons have their own unique structure that fits with their

function. Neurons in the CA1 region of hippocampus are primarily pyramidal in shape. Peinado et al. (1997) reported that there was a decrease in the neuronal soma shape as indicated by the major/minor diameter ratio in old rats. The results were suggested to be due to the consequence of neuronal degeneration due to aging. Findings from the present study suggest that TOL, TOL-NSS, TOL-NSO, and TOL-TQ exerted no noticeable changes on the shape of the CA1 pyramidal neurons, indicated by preserved pyramidal soma shape similar to the control group. This reflected the rigidity of the membrane and cytoskeleton of the soma in keeping the integrity of its shape.

5.4 Potential mechanisms of Nigella sativa effects on the CNS

Brain is the most metabolically active organ of the body, thus it is highly crucial for the brain to maintain its homeostasis by having its own method or system of removing waste proteins and neurotoxins. Previous studies has proved the interrelation between brain clearance system and CNS pathological disorders. For the past decade, studies on the clearance system have been restricted to the glymphatic system. Besides that, the blood-brain barrier (BBB), perivascular pathway and enzymatic clearance is all the brain has for clearance.

Classically, the BBB was the thought to be the fundamental of the brain's immune system. The BBB are blood vessels that anatomically vascularizes the CNS and functionally separates CNS nerve tissues from the blood, via the tight regulation and movement of ions, molecules and cells. It protects and ensures a homestatic environment in the CNS by being selectively permeable towards large hydrophilic molecules and small hydrophobic substances. Besides that, it regulates the alterations of electrolytes, hormones and metabolites (Daneman & Prat, 2022; Presta et al., 2018).

As defined by Benveniste et al. (2019), the glymphatic system is "a glial-dependent waste clearance pathway in the brain, in place of lymphatic vessels, dedicated to drain away soluble waste proteins and metabolic products". The main components of the glymphatic system include cerebrospinal fluid (CSF), interstitial fluid (ISF), perivenous space (PVS), cerebral vascular, glial cells, and the astrocyte aquaporin 4 (AQP4)-controlled water channels (Liu et al., 2022). The glymphatic system and waste clearance process in the rodent brain comprise three steps: (1) CSF flows from the subarachnoid and cisternal spaces into the brain via PVS, (2) CSF exchanges with interstitial fluid, assisted by AQP4 (Red dots) positioned on the end-foot processes of perivascular astrocyte; and (3) The CSF flow into the brain pushes the motion of ISF and interstitial solute (IS) (Black dots) through the extracellular space to PVS. Perivenous fluid and solutes then exits the brain and enters into the systemic circulation (Figure 5.2) (Presta et al., 2018).

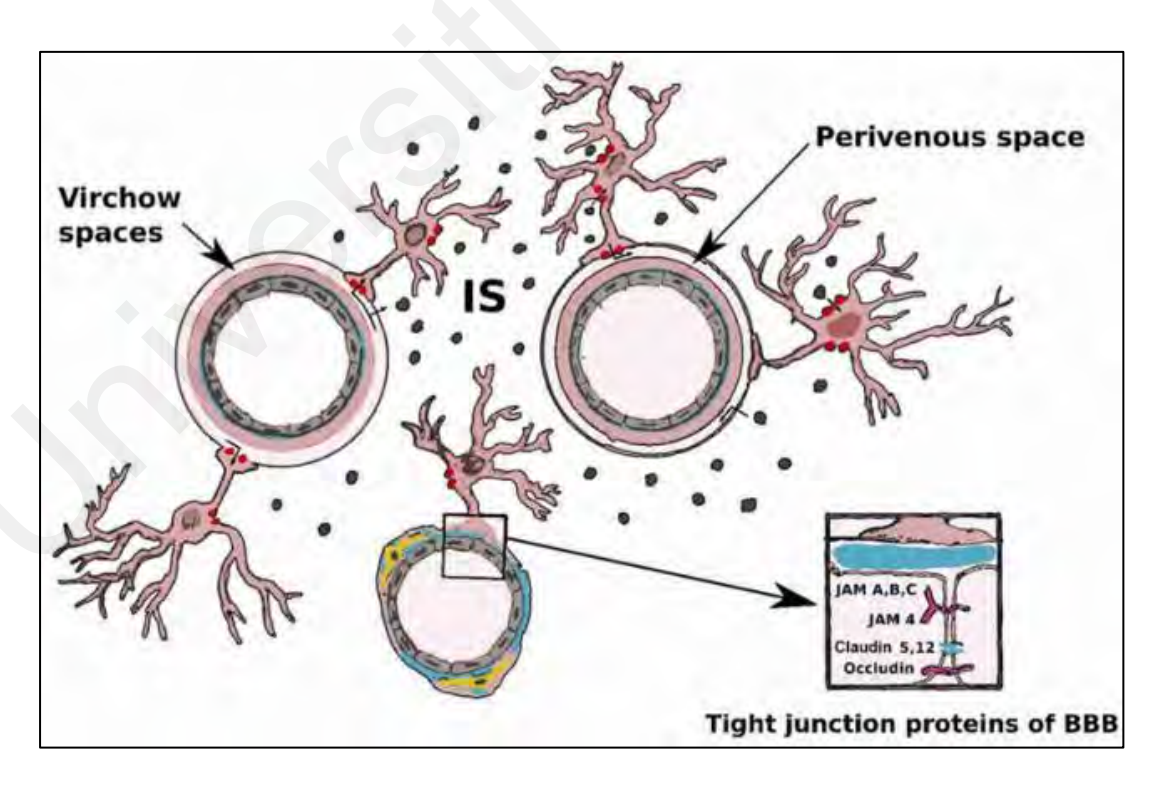


Figure 5.3: Glymphatic system and blood-brain barrier. Taken from Presta et al., (2018)

The glymphatic system and the BBB are presumably complementary systems (Daneman & Prat, 2022). Inflammation may cause impairments to both the BBB and glymphatic system. Alterations in BBB affects the AQP4 channels-expressing astrocytes, which consequently induces glymphatic dysfunction (Liu et al., 2022). As the barrier is impaired, neurotoxins can freely pass through, thus leads to excitotoxicity and neuronal death. NS and its bioactive component have manifested anti-inflammatory properties by reducing the levels of inflammatory mediators such as NO, TNF-α, interleukin (IL)-6, IL-1β, IL-1and inducible nitric oxide synthase (iNOS) (Balbaa et al., 2017; Cobourne-Duval et al., 2016). In addition, NS also has neuroprotective properties against neurodegeneration. Absence of densely stained nucleus, reduced shrunken nerve cells, less degenerative changes in cytoplasm and nucleus of cells, and reduced histopathological changes in tissues demonstrates antineurodegenerative effects of NS (Gökce et al., 2016; Gülşen et al., 2016; Ince et al., 2013; Kanter, 2008a, 2008b). Amyloid precursor protein (APP), a gene associated with AD, have been proven to be downregulated with NS and TQ treatments (Balbaa et al., 2017; Butt et al., 2018).

According to the aforementioned studies, NS protects the nervous system through several mechanisms. Besides having anti-inflammatory properties, NS protects via its potent antioxidant property, followed by maintenance of the mitochondrion membrane potential in cells. The anti-apoptosis property of NS also play a significant role and prominent contribution in protecting the nervous system.

Most evidence on the neuroprotective effects of NS reported in recent studies is mainly attributed to its antioxidant property. ROS include free radicals that are generated during aerobic respiration, a crucial process in living organisms. Free radicals include superoxide anion (O₂-), peroxides, hydroxyl radicals (OH-), and H₂O₂ (Lobo et al., 2010). Among the

most potent instigators of ROS is beta amyloid (Aβ) (Manoharan et al., 2016) making lipid peroxidation among the main cause of ROS generation in brain (Gülşen et al., 2016; Khader & Eckl, 2014). Pre-treatment with TQ in rats inhibited the reduction of several antioxidant enzymes and diminished lipid peroxidation activity in brain (Khader & Eckl, 2014). This is most probably due to the abundant phenolic compounds in NS which includes TQ, p-cymene, carvacrol, and thymol (Khazdair et al., 2019). Phenolic compounds in NS act as reducing agents, free radical scavengers, and metal ion chelators, which substantially contribute to its antioxidant capabilities (Amirullah et al., 2018).

Mitochondria is one of the primary sources of ROS, besides the plasma membrane and cytosol (Manoharan et al., 2016). Mitochondrial membrane potential results from redox transformations and is crucial in cellular energy generation via the activities of Krebs cycle. Disruption of this membrane potential leads to release of cytochrome C into the cytosol which later affects cell viability, inducing cell apoptosis (Zorova et al., 2018). Previous studies proved that NS and its bioactive constituent TQ can maintain mitochondrial membrane potential in cells (Firdaus et al., 2018, 2019b; Ullah et al., 2012).

Apoptosis is the process of programmed cell death. It is an essential component required to maintain a functional immune system, cell development, and chemical-induced cell death. However, inappropriate apoptosis is another leading factor of neurodegenerative diseases. Activation of caspase proteins, DNA cleavage, and tumor necrosis factor (TNF) expressions are among the mechanisms of apoptosis (Elmore, 2007). NS presented anti-apoptotic capacity by reducing caspase-3 and caspase-9 activation (Fouad et al., 2018; Gökce et al., 2016; Tabeshpour et al., 2019), degree of DNA fragmentation (Firdaus et al., 2019), and TNF production (Kassab & El-Hennamy, 2017).

5.5 Limitations and suggestions for future studies

There are limited studies investigating the protective properties of NSS, NSO and TQ on toluene treated mice from the aspects covered by the present study: recognition memory performance, brain morphology, and morphometric properties especially on somatic development of neurons. Thus, the gap being addressed by the present study. However, based on the findings, future studies could improve the limitations faced.

5.5.1 NS supplementations

Present study was done on mice using three different forms of NS supplementations which are the seeds, oil, and its bioactive constituent TQ. Further studies are needed to elucidate the exact mechanism of actions of the three different NS forms, to determine the most effective form of supplementation in exerting neuroprotective properties.

5.5.2 Toluene administration in animals

Occupational and household exposure to toluene in humans are commonly through inhalation, in a constant exchange of gas environment and in various durations from minutes to hours. This makes it difficult to mimic in experimental animals. This explains why the concentration chosen in the present study, administered via intraperitoneal injection, is lower than most of the other toluene studies. In addition, the preparation of an exposure chamber with injection ports and pre-set atmospheric pressure and temperature for this single study is considerably costly. Several studies have reported that intraperitoneal administration of toluene produces similar behavioural symptoms as inhalation (Win-Shwe et al., 2012). In addition, intraperitoneal injections have been widely applied in animal studies involving inhalants, specifically toluene inhalation (Chan et al., 2012; Hsieh et al., 2020; Lee et al.,

2020; Wu et al., 2018). Therefore, intraperitoneal administration of toluene was conducted in the present study.

However, for future studies, inhalation might still be a better methodology in terms of its similarity with real-world human exposure, as compared to intraperitoneal injection. Since humans are exposed to toluene mainly via the respiratory tract, intraperitoneal injection is considered as a poor model (Yoon et al., 2016). According to Kim et al. (2020), the pharmacokinetics and metabolic rates of toluene via intraperitoneal injection differs from inhalation, hence the brain concentrations and neurobehavioural effects between the two routes of administration are more likely to be different as well.

5.5.3 Novel object recognition (NOR) behavioural test

As stated earlier, NOR test is routinely used in assessing non-spatial memory of rodents. The test exploits the innate preference of rodents towards novelty, hence any slight difference in external factors such as background noise and light intensity may easily influence the performance of mice. Besides that, ICR mice are an outbred population, therefore, variability in terms of their behaviour may occur (Hånell & Marklund, 2014). For instance, a few of the mice in the present study showed higher anxiety-like behaviour as compared to the rest.

In addition, differences in the analysis of novel object preference in between studies have been noted. Some studies use the difference score (DS), which is the difference in exploration times between familiar and novel objects, while others use DS over total exploration time of both objects as the novel preference parameter. Therefore, it is difficult to directly compare the DI between various studies. To date, no studies have been conducted to consider how the different discrimination indices may be related (Akkerman et al., 2012).

Recognition memory performance of mice showed no significant differences between the toluene only group and the NS treatment groups. Animal experimentations require standardized conditions of the laboratory environments, test procedures, and physical equipment to reduce factors that might affects animals' physiology and behaviour that ultimately might also affect the research outcomes (Akhtar, 2015). The present study was conducted in a clean and spacious animal facility with controlled room temperature and humidity, but it was open to other users as well. Hence, mild background noise was unavoidable. In future studies, it would be best to have a specific behavioural testing room where external factors that influence behavioural performance can be controlled.

5.5.4 Histology

Histological procedures for brain tissue samples of the TOL-TQ group were not conducted in a continuous manner (as stated in Chapter 3). After intracardiac perfusion and animal dissection, the brain samples of the TOL-TQ group were preserved in alcohol solution for quite a period of time due to the Covid-19 pandemic that hit the world in March 2020. Prolonged dehydration may result in cell shrinkage (Carson & Hladik, 2009); thus, results in the morphometric analysis of the pyramidal neurons might have been affected but standardized through whole specimens studied.

Histological findings in the present study showed no significant differences in brain morphology and neuronal morphometry between the groups. Neuronal cells were stained using the Nissl staining and microscopic evaluation was done under light microscopy. Nissl stain is used to visualize Nissl substance that has high amount of ribosomal RNA that attracts the dye, thus making the neurons appear dark blue and cytoplasm mottled (Gurina & Symms, 2021). The appearance of cytoplasm, nuclei, and plasma membrane of neurons could be

analysed. However, the results obtained could further be supported by secondary stain or by immunohistochemistry for a protein of interest, such as marker of cellular damage, cell death, or cell response to damage (Wang et al., 2018). Furthermore, the actual mechanism that underlies changes in morphology of the neuronal soma in terms of their size and shape could be studied using cytoskeleton markers focusing on actin filaments, intermediate filaments, and microtubules.

5.5.5 Morphometric analysis

Morphometric analysis of the neuronal soma in the present study was conducted by manually tracing individual cells using the ImageJ software, which is challenging and time-consuming. Morphometric analysis of neuronal soma is highly subjective since there is no definite boundaries between soma and the origin of its dendrites and axon. An automatic soma segmentation method on defining the neuronal soma morphology using a three-dimensional virtualization technique enables a clearer visualization of the morphological changes in cell bodies between the treated groups (Luengo-Sanchez et al., 2015). Another interesting method that could be employed is a novel high-throughput neuronal morphology analysis framework (ANMAF) where convolutional neural networks (CNN) were used for automatic contour of the somatic area of neurons in brain slices (Tong et al., 2021).

CHAPTER 6: CONCLUSION

The study was carried out for 14 days to examine the neuroprotective effect of *Nigella sativa* (NS) supplementations: seeds (NSS), oil (NSO), and its main bioactive compound thymoquinone (TQ), against neurotoxicant toluene (TOL) administration on male ICR mice. Aspects being investigated included recognition memory performance, brain morphological changes, and somatic morphometric changes of the hippocampal pyramidal neurons. Research objectives of the present study were fulfilled, and it was observed that:

- 1. Although not statistically significant, NS improved recognition memory in the novel object recognition (NOR) test as the TOL-NSS, TOL-NSO, and TOL-TQ groups showed higher discrimination index and higher percentage of novel object preference than the TOL group, reflecting neuroprotective effects of NS supplementations against toluene.
- 2. All specific treatments did not affect the gross morphology of mice brain as no significant differences were observed in the weight, length, and width of mice brain among the treatment groups.
- 3. Both NS and toluene treatments did not significantly affect the soma size and shape of the CA1 pyramidal neurons. However, evidence of larger somatic size of CA1 pyramidal neurons could be seen in the TOL-NSS, TOL-NSO, and TOL-TQ groups than the TOL group, indicated by the higher value of somatic area and somatic perimeter. No significant differences could be observed in somatic aspect ratio, somatic roundness, somatic circularity, and somatic solidity of the neurons in all groups. These findings lead to the prediction that NS has neuroprotective effects to counter the negative effects of toluene treatment, by improving the size and preserving the shape of neuronal soma.

REFERENCES

- Abd Hamid, H. H., Jumah, N. S., Talib Latif, M., & Kannan, N. (2017). BTEXs in indoor and outdoor air samples: Source apportionment and health risk assessment of benzene. *Journal of Environmental Science and Public Health*, 01(01), 49–56.
- Abdel-salam, O. M. E., El-shamarka, M. E., Hassan, N. S., & Dalia, M. (2021). Effect of piracetam on brain oxidative stress and tissue damage following toluene exposure in rats. *International Journal of Halal Research*, 3(1), 8–23.
- Abdel-salam, O. M. E., Sleem, A. A., Khadrawy, Y. A., & Morsy, F. A. (2020). Prevention of toluene-induced brain neurodegeneration by atropine and neostigmine. *Journal of Basic Pharmacology and Toxicology*, 4(1), 1–9.
- Abdel-Zaher, A. O., Farghaly, H. S. M., Farrag, M. M. Y., Abdel-Rahman, M. S., & Abdel-Wahab, B. A. (2017). A potential mechanism for the ameliorative effect of thymoquinone on pentylenetetrazole-induced kindling and cognitive impairments in mice. *Biomedicine and Pharmacotherapy*, 88, 553–561.
- Abdel-Zaher, A. O., Mostafa, M. G., Farghly, H. M., Hamdy, M. M., Omran, G. A., & Al-Shaibani, N. K. M. (2013). Inhibition of brain oxidative stress and inducible nitric oxide synthase expression by thymoquinone attenuates the development of morphine tolerance and dependence in mice. *European Journal of Pharmacology*, 702(1–3), 62–70.
- Abouee-Mehrizi, A., Rasoulzadeh, Y., Mesgari-Abbasi, M., Mehdipour, A., & Ebrahimi-Kalan, A. (2020). Nephrotoxic effects caused by co-exposure to noise and toluene in New Zealand white rabbits: A biochemical and histopathological study. *Life Sciences*, 259, Article#118254.
- Abulfadl, Y. S., El-Maraghy, N. N., Ahmed, A. A. E., Nofal, S., Abdel-Mottaleb, Y., & Badary, O. A. (2018). Thymoquinone alleviates the experimentally induced Alzheimer's disease inflammation by modulation of TLRs signaling. *Human and Experimental Toxicology*, 37(10), 1092–1104.
- Abulfadl, Yasmin S., El-Maraghy, N. N., Ahmed, A. A. E., Nofal, S., & Badary, O. A. (2018). Protective effects of thymoquinone on D-galactose and aluminum chloride induced neurotoxicity in rats: biochemical, histological and behavioral changes. *Neurological Research*, 40(4), 324–333.

- Ahmad, A., Husain, A., Mujeeb, M., Khan, S. A., Najmi, A. K., Siddique, N. A., Damanhouri, Z. A., & Anwar, F. (2013). A review on therapeutic potential of Nigella sativa: A miracle herb. *Asian Pacific Journal of Tropical Biomedicine*, 3(5), 337–352.
- Akhtar, A. (2015). The Flaws and Human Harms of Animal Experimentation. *Cambridge Quarterly of Healthcare Ethics*, 24(4), 407–419.
- Akhtar, M., Maikiyo, A. M., Najmi, A. K., Khanam, R., Mujeeb, M., & Aqil, M. (2013). Neuroprotective effects of chloroform and petroleum ether extracts of Nigella sativa seeds in stroke model of rat. *Journal of Pharmacy and Bioallied Sciences*, 5(2), 119–125.
- Akkerman, S., Blokland, A., Reneerkens, O., van Goethem, N. P., Bollen, E., Gijselaers, H. J. M., Lieben, C. K. J., Steinbusch, H. W. M., & Prickaerts, J. (2012). Object recognition testing: Methodological considerations on exploration and discrimination measures. *Behavioural Brain Research*, 232(2), 335–347.
- Al-Majed, A. A., Al-Omar, F. A., & Nagi, M. N. (2006). Neuroprotective effects of thymoquinone against transient forebrain ischemia in the rat hippocampus. *European Journal of Pharmacology*, 543(1–3), 40–47.
- Alhebshi, A. H., Gotoh, M., & Suzuki, I. (2013). Thymoquinone protects cultured rat primary neurons against amyloid β-induced neurotoxicity. *Biochemical and Biophysical Research Communications*, 433(4), 362–367.
- Alhebshi, A. H., Odawara, A., Gotoh, M., & Suzuki, I. (2014). Thymoquinone protects cultured hippocampal and human induced pluripotent stem cells-derived neurons against α-synuclein-induced synapse damage. *Neuroscience Letters*, 570, 126–131.
- Alhibshi, A. H., Odawara, A., & Suzuki, I. (2019). Neuroprotective efficacy of thymoquinone against amyloid beta-induced neurotoxicity in human induced pluripotent stem cell-derived cholinergic neurons. *Biochemistry and Biophysics Reports*, 17, 122–126.
- Al-Nailey, K. G. (2010). Study of the protective effect of *Nigella sativa* against Cimetidine induced reproductive toxicity in male mice. *Al-Qadisiyah Journal of Veterinary Medicine Sciences*, 9(1), 55-62.
- Alturkistani, H. A., Tashkandi, F. M., & Mohammedsaleh, Z. M. (2015). Histological Stains: A Literature Review and Case Study. *Global Journal of Health Science*, 8(3), 72–79.

- Ameen-Ali, K. E., Easton, A., & Eacott, M. J. (2015). Moving beyond standard procedures to assess spontaneous recognition memory. *Neuroscience and Biobehavioral Reviews*, 53, 37–51.
- Aminu, I., Teslimat, A., Victoria, W., Samson, C., Aboyeji, O., Olatunbosun, O., Sheu-Tijani, S., & Saliu, A. (2019). Nigella sativa oil protected the hippocampus against Acetyl cholinesterase and oxidative dysfunctions-driven impaired working memory in rats. *Bulletin of Faculty of Pharmacy, Cairo University*, 57(1), 25–34.
- Anaeigoudari, A., Norouzi, F., Abareshi, A., Beheshti, F., Aaghaei, A., Shafei, M. N., Gholamnezhad, Z., & Hosseini, M. (2018). Protective effects of Nigella sativa on synaptic plasticity impairment induced by lipopolysaccharide. *Veterinary Research Forum*, 9(1), 27–33.
- Anand, K., & Dhikav, V. (2012). Hippocampus in health and disease: An overview. *Annals of Indian Academy of Neurology*, 15(4), 239–246.
- Apawu, A. K., Mathews, T. A., & Bowen, S. E. (2015). Striatal dopamine dynamics in mice following acute and repeated toluene exposure. *Psychopharmacology*, 232(1), 173–184.
- Armenta-Reséndiz, M., Ríos-Leal, E., Rivera-García, M. T., López-Rubalcava, C., & Cruz, S. L. (2019). Structure-activity study of acute neurobehavioral effects of cyclohexane, benzene, m-xylene, and toluene in rats. *Toxicology and Applied Pharmacology*, 376, 38–45.
- Asrar, B., Khan, I. U., Homberg, J. R., & Haleem, D. J. (2020). Nigella sativa oil ameliorates chronic ethanol induced anxiety and impaired spatial memory by modulating noradrenaline levels. *Pakistan Veterinary Journal*, 40(3), 350–354.
- Ayu, P. S., Tualeka, A. R., Arini, S. Y., Russeng, S. S., Rahmawati, P., Ahsan, A., & Susilowati, I. H. (2020). Relationship between toluene concentration, malondialdehyde (MDA) level and health complaints in workers of Surabaya printing industry. *Indian Journal of Forensic Medicine & Toxicology*, 14(4), 3389-3395.
- Azaizeh, H., Saad, B., Cooper, E., & Said, O. (2010). Traditional Arabic and Islamic medicine, a re-emerging health aid. *Evidence-Based Complementary and Alternative Medicine*, 7(4), 419–424.
- Baghani, A. N., Sorooshian, A., Heydari, M., Sheikhi, R., Golbaz, S., Ashournejad, Q.,

- Kermani, M., Golkhorshidi, F., Barkhordari, A., Jafari, A. J., Delikhoon, M., & Shahsavani, A. (2019). A case study of BTEX characteristics and health effects by major point sources of pollution during winter in Iran. *Environmental Pollution*, 247, 607–617.
- Baghcheghi, Y., Hosseini, M., Beheshti, F., Salmani, H., & Anaeigoudari, A. (2018). Thymoquinone reverses learning and memory impairments and brain tissue oxidative damage in hypothyroid juvenile rats. *Arquivos de Neuro-Psiquiatria*, 76(1), 32–40.
- Balbaa, M., Abdulmalek, S. A., & Khalil, S. (2017). Oxidative stress and expression of insulin signaling proteins in the brain of diabetic rats: Role of *Nigella sativa* oil and antidiabetic drugs. *PLoS ONE*, *12*(5), 1–23.
- Balbaa, M., El-Zeftawy, M., Abdulmalek, S. A., & Shahin, Y. R. (2021). Health-promoting activities of *Nigella sativa* fixed oil. In Fawzy Ramadan M. (Ed.), *Black cumin (Nigella sativa) seeds: Chemistry, Technology, Functionality, and Applications* (pp. 361-379). Cham, Switzerland: Springer.
- Balderas, I., Rodriguez-Ortiz, C. J., & Bermudez-Rattoni, F. (2013). Retrieval and reconsilidation of object recognition memory are independent processes in the perirhinal cortex. *Neuroscience*, 253, 398-405.
- Balderas, I., Morin, J. P., Rodriguez-Ortiz, C. J., & Bermudez-Rattoni, F. (2012). Muscarinic receptors activity in the perirhinal cortex and hippocampus has differential involvement in the formulation of recognition memory. *Neurobiology of Learning and Memory*, 97(4), 418-424.
- Bali, Y. A., Kaikai, N. E., Ba-Mohamed, S. & Bennis, M. (2019). Learning and memory impairments associated to acetylcholinesterase inhibition and oxidative stress following glyphosate based-herbicide exposure in mice. *Toxicology*, 415, 18-25.
- Bargi, R., Asgharzadeh, F., Beheshti, F., Hosseini, M., Sadeghnia, H. R., & Khazaei, M. (2017). The effects of thymoquinone on hippocampal cytokine level, brain oxidative stress status and memory deficits induced by lipopolysaccharide in rats. *Cytokine*, 96(April), 173–184.
- Beheshti, F., Hosseini, M., Shafei, M. N., Soukhtanloo, M., Ghasemi, S., Vafaee, F., & Zarepoor, L. (2017). The effects of Nigella sativa extract on hypothyroidism-associated learning and memory impairment during neonatal and juvenile growth in rats. *Nutritional Neuroscience*, 20(1), 49–59.

- Beheshti, F., Khazaei, M., & Hosseini, M. (2016). Neuropharmacological effects of Nigella sativa. *Avicenna Journal of Phytomedicine*, 6(1), 104–116.
- Ben-Shaul, Y. (2017). OptiMouse: A comprehensive open source program for reliable detection and analysis of mouse body and nose positions. *BMC Biology*, 15(1), 1–22.
- Benavides-Piccione, R., Regalado-Reyes, M., Fernaud-Espinosa, I., Kastanauskaite, A., Tapia-González, S., León-Espinosa, G., Rojo, C., Insausti, R., Segev, I., & Defelipe, J. (2020). Differential Structure of Hippocampal CA1 Pyramidal Neurons in the Human and Mouse. *Cerebral Cortex*, 30(2), 730–752.
- Benveniste, H., Liu, X., Koundal, S., Sanggaard, S., Lee, H., & Wardlaw, J. (2019). The Glymphatic System and Waste Clearance with Brain Aging: A Review. *Gerontology*, 65(2), 106–119.
- Bird, C. M. (2017). The role of the hippocampus in recognition memory. *Cortex*, 93(0), 155–165.
- Braunscheidel, K. M., Okas, M. P., Hoffman, M., Mulholland, P. J., Floresco, S. B., & Woodward, J. J. (2019). The abused inhalant toluene impairs medial prefrontal cortex activity and risk/reward decision-making during a probabilistic discounting task. *Journal of Neuroscience*, 39(46), 9207–9220.
- Brucker, N., do Nascimento, S. N., Bernardini, L., Charão, M. F., & Garcia, S. C. (2020). Biomarkers of exposure, effect, and susceptibility in occupational exposure to traffic-related air pollution: A review. *Journal of Applied Toxicology*, *December 2019*, 1–15.
- Burry, M., Guizzetti, M., Oberdoerster, J., & Costa, L. G. (2003). Developmental neurotoxicity of toluene: In vivo and in vitro effects on astroglial cells. *Developmental Neuroscience*, 25(1), 14–19.
- Butt, U. J., Shah, S. A. A., Ahmed, T., & Zahid, S. (2018). Protective effects of: *Nigella sativa* L. seed extract on lead induced neurotoxicity during development and early life in mouse models. *Toxicology Research*, 7(1), 32–40.
- Callan, S. P., Hannigan, J. H., & Bowen, S. E. (2017). Prenatal toluene exposure impairs performance in the Morris Water Maze in adolescent rats. *Neuroscience*, *342*, 180–187.

- Callan, S. P., Kott, J. M., Cleary, J. P., McCarthy, M. K., Baltes, B. B., & Bowen, S. E. (2016). Changes in developmental body weight as a function of toluene exposure: A meta-analysis of animal studies. *Human and Experimental Toxicology*, 35(4), 341–352.
- Camina, E., & Güell, F. (2017). The neuroanatomical, neurophysiological and psychological basis of memory: Current models and their origins. *Frontiers in Pharmacology*, 8, Article#438.
- Chan, M., Chung, S., Stoker, A. K., Markou, A., & Chen, H. (2012). Sarcosine attenuates toluene-induced motor incoordination, memory impairment, and hypothermia but not brain stimulation reward enhancement in mice. *Toxicology and Applied Pharmacology*, 265(2), 158–165.
- Cheema, M. A. R., Nawaz, S., Gul, S., Salman, T., Naqvi, S., Dar, A., & Haleem, D. J. (2018). Neurochemical and behavioral effects of *Nigella sativa* and *Olea europaea* oil in rats. *Nutritional Neuroscience*, 21(3), 185–194.
- Chew, S., Kolosowska, N., Saveleva, L., Malm, T., & Kanninen, K. M. (2020). Impairment of mitochondrial function by particulate matter: Implications for the brain. *Neurochemistry International*, 135, Article#104694.
- Clos, M., Bunzeck, N., & Sommer, T. (2018). Dopamine is a double-edged sword: Dopaminergic modulation enhances memory retrieval performance but impairs metacognition. *Neuropsychopharmacology*, 44(3), 555-563.
- Cobourne-Duval, M. K., Taka, E., Mendonca, P., Bauer, D., & Soliman, K. F. A. (2016). The Antioxidant Effects of Thymoquinone in Activated BV-2 Murine Microglial Cells. *Neurochemical Research*, 41(12), 3227–3238.
- Cohen, A., Morin, J.-P., Vazdarjanova, A., Stackman Jr, R. W., Jr, C. DA, Jr, S. R., Cinalli Jr, D. A., Cohen, S. J., & Guthrie, K. (2020). Object recognition memory: Distinct yet complementary roles of the mouse CA1 and perirhinal cortex. *Frontiers in Molecular Neuroscience*, 13, Article#527543.
- Cohen, S. J., Munchow, A. H., Rios, L. M., Zhang, G., Ásgeirsdóttir, H. N., & Stackman, R. W. (2013b). The rodent hippocampus is essential for nonspatial object memory. *Current Biology*, 23(17), 1685–1690.
- Cohen, S. J., & Stackman, R. W. (2015). Assessing rodent hippocampal involvement in the novel object recognition task: A review. *Behavioural Brain Research*, 285, 105–117.

- Costa, L. G., Cole, T. B., Dao, K., Chang, Y. C., Coburn, J., & Garrick, J. M. (2020). Effects of air pollution on the nervous system and its possible role in neurodevelopmental and neurodegenerative disorders. *Pharmacology and Therapeutics*, 210, Article#107523.
- Costa, L. G., Cole, T. B., Dao, K., Chang, Y. C., & Garrick, J. M. (2019). Developmental impact of air pollution on brain function. *Neurochemistry International*, 131, Article#104580.
- Cowan, N., Brain, P., & Author, R. (2008). What are the differences between long-term, short-term, and working memory? NIH Public Access Author Manuscript. *Progress in Brain Research*, 169, 323–338.
- Crowley, R., Bendor, D., & Javadi, A. H. (2019). A review of neurobiological factors underlying the selective enhancement of memory at encoding, consolidation, and retrieval. *Progress in Neurobiology*, 179, Article#101615.
- Cruz, S. L., Armenta-Reséndiz, M., Carranza-Aguilar, C. J., & Galván, E. J. (2020). Minocycline prevents neuronal hyperexcitability and neuroinflammation in medial prefrontal cortex, as well as memory impairment caused by repeated toluene inhalation in adolescent rats. *Toxicology and Applied Pharmacology*, 395, Article#114980.
- Cruz, S. L., Rivera-García, M. T., & Woodward, J. J. (2014). Review of toluene actions: Clinical evidence, animal studies, and molecular targets. *Journal of Drug and Alcohol Research*, 3, 1–8.
- Cruz, S. L., Torres-Flores, M., & Galván, E. J. (2019). Repeated toluene exposure alters the synaptic transmission of layer 5 medial prefrontal cortex. *Neurotoxicology and Teratology*, 73(235), 9–14.
- Daneman, R., & Prat, A. (2022). The Blood-Brain Barrier. *Cold Spring Harbor Perspectives in Biology*, 7(1), Article#a020412.
- Dekeyzer, S., De Kock, I., Nikoubashman, O., Vanden Bossche, S., Van Eetvelde, R., De Groote, J., Acou, M., Wiesmann, M., Deblaere, K., & Achten, E. (2017). "Unforgettable" A pictorial essay on anatomy and pathology of the hippocampus. *Insights into Imaging*, 8(2), 199–212.
- Demir, M., Cicek, M., Eser, N., Yoldaş, A., & Sisman, T. (2017). Effects of acute toluene toxicity on different regions of rabbit brain. *Analytical Cellular Pathology*, 2017,

- Denninger, J K, Smith, B. M., & Kirby, E. D. (2018). Novel object recognition and object location behavioral testing in mice on a budget. *Journal of Visualized Experiment*, 141, Article#58593.
- Denninger, Jiyeon K, Smith, B. M., & Kirby, E. D. (2019). Testing in mice on a budget. Journal of Visual Ized Experiments, 20(141), 1–20.
- Dere, E., Huston, J. P., & De Souza Silva, M. A. (2007). The pharmacology, neuroanatomy and neurogenetics of one-trial object recognition in rodents. *Neuroscience and Biobehavioral Reviews*, 31(5), 673-704.
- Dick, A. L. W., Zhao, Q., Crossin, R., Baker-Andresen, D., Li, X., Edson, J., Roeh, S., Marshall, V., Bredy, T. W., Lawrence, A. J., & Duncan, J. R. (2021). Adolescent chronic intermittent toluene inhalation dynamically regulates the transcriptome and neuronal methylome within the rat medial prefrontal cortex. *Addiction Biology*, 26(3), 1–11.
- Dolzhikov, A. A., Tverskoi, A. V., Bobyntsev, I. I., Kriukov, A. A., & Belykh, A. E. (2015). Morphometric study of hippocampal neurons in chronic immobilization stress. *Medicine And Pharmacy Series*, 1(4), 62–65.
- Du, Z., Mo, J., Zhang, Y., & Xu, Q. (2014). Benzene, toluene and xylenes in newly renovated homes and associated health risk in Guangzhou, China. *Building and Environment*, 72, 75–81.
- Duncan, J. R., Dick, A. L. W., Egan, G., Kolbe, S., Gavrilescu, M., Wright, D., Lubman, D. I., & Lawrence, A. J. (2012). Adolescent toluene inhalation in rats affects white matter maturation with the potential for recovery following abstinence. *PLoS ONE*, 7(9), 1–12.
- Edokpolo, B., Yu, Q. J., & Connell, D. (2014). Health risk assessment of ambient air concentrations of benzene, toluene and Xylene (BTX) in service station environments. *International Journal of Environmental Research and Public Health*, 11(6), 6354–6374.
- Ehsanifar, M., Jafari, A. J., Nikzad, H., Zavareh, M. S., Atlasi, M. A., Mohammadi, H., & Tameh, A. A. (2019). Prenatal exposure to diesel exhaust particles causes anxiety, spatial memory disorders with alters expression of hippocampal pro-inflammatory cytokines and NMDA receptor subunits in adult male mice offspring. *Ecotoxicology and Environmental Safety*, 176(March), 34–41.

- Ekor, M. (2014). The growing use of herbal medicines: Issues relating to adverse reactions and challenges in monitoring safety. *Frontiers in Neurology*, 4(January), 1–10.
- El-Marasy, S. A., El-Shenawy, S. M., El-Khatib, A. S., El-Shabrawy, O. A., & Kenawy, S. A. (2012). Effect of *Nigella sativa* and wheat germ oils on scopolamine-induced memory impairment in rats. *Bulletin of Faculty of Pharmacy, Cairo University*, 50(2), 81–88.
- El-Naggar, T., Gómez-Serranillos, M. P., Palomino, O. M., Arce, C., & Carretero, M. E. (2010). *Nigella sativa* L. seed extract modulates the neurotransmitter amino acids release in cultured neurons in vitro. *Journal of Biomedicine and Biotechnology*, 2010, 1-8.
- El-Safti, F.-N. A., El-Kholoy, W., El-Mehi, A., & Selima, R. (2017). A comparative study on the effect of aging on the hippocampal CA1 area of male albino rat. *Menoufia Medical Journal*, 30(4), 1079-1084.
- Elmore, S. (2007). Apoptosis: A review of programmed cell death. *Toxicologic Pathology*, 35(4), 495–516.
- Elshama, S. S., Shehab, G. M. G., El-Kenawy, A. E., Osman, H. E. H., & Farag, M. M. (2013). Role of *Nigella Sativa* Seeds on modulation testicular toxicity of colchicine repeated use in adult albino rats. *Life Science Journal*, 10(4), 1629–1639.
- Essawy Prof., A. E., Abdel-Moneim, A. M., Khayyat, L. I., & Elzergy, A. A. (2012). *Nigella sativa* seeds protect against hepatotoxicity and dyslipidemia induced by carbon tetrachloride in mice. *Journal of Applied Pharmaceutical Science*, 2(10), 021–025.
- Fahmy, H. M., Noor, N. A., Mohammed, F. F., Elsayed, A. A., & Radwan, N. M. (2014). Nigella sativa as an anti-inflammatory and promising remyelinating agent in the cortex and hippocampus of experimental autoimmune encephalomyelitis-induced rats. *The Journal of Basic and Applied Zoology*, 67(5), 182–195.
- Famitafreshi, H., & Karimian, M. (2018). Social state influences memory in novel object recognition test through oxidative stress balance in male rats. *The Open Pharmacology Journal*, 8(1), 1–9.
- Fanoudi, S., Alavi, M. S., Hosseini, M., & Sadeghnia, H. R. (2019). *Nigella sativa* and thymoquinone attenuate oxidative stress and cognitive impairment following cerebral hypoperfusion in rats. *Metabolic Brain Disease*, 34(4), 1001–1010.

- Feigin, V. L., Krishnamurthi, R. V., Theadom, A. M., Abajobir, A. A., Mishra, S. R., Ahmed, M. B., Abate, K. H., Mengistie, M. A., Wakayo, T., Abd-Allah, F., Abdulle, A. M., Abera, S. F., Mohammed, K. E., Abyu, G. Y., Asgedom, S. W., Atey, T. M., Betsu, B. D., Mezgebe, H. B., Tuem, K. B., ... Zaki, M. E. (2017). Global, regional, and national burden of neurological disorders during 1990–2015: A systematic analysis for the Global Burden of Disease Study 2015. *The Lancet Neurology*, 16(11), 877–897.
- Fiasal Zaher, M., Abdelfattah Bendary, M., Saeed Abd El-Aziz, G., & Shaker Ali, A. (2019). Potential protective role of thymoquinone on experimentally-induced Alzheimer rats. *Journal of Pharmaceutical Research International*, 31(June), 1–18.
- Firdaus, F., Zafeer, M. F., Ahmad, M., & Afzal, M. (2018). Anxiolytic and anti-inflammatory role of thymoquinone in arsenic-induced hippocampal toxicity in Wistar rats. *Heliyon*, 4(6), Article#e00650.
- Firdaus, F., Zafeer, M. F., Anis, E., Ahmad, F., Hossain, M. M., Ali, A., & Afzal, M. (2019). Evaluation of phyto-medicinal efficacy of thymoquinone against Arsenic induced mitochondrial dysfunction and cytotoxicity in SH-SY5Y cells. *Phytomedicine*, *54*, 224–230.
- Fouad, I. A., Sharaf, N. M., Abdelghany, R. M., & El Sayed, N. S. E. D. (2018). Neuromodulatory effect of thymoquinone in attenuating glutamate-mediated neurotoxicity targeting the amyloidogenic and apoptotic pathways. *Frontiers in Neurology*, 9, 1–12.
- Freas, C. A., Roth, T. C., Ladage, L. D., & Pravosudov, V. V. (2013). Hippocampal neuron soma size is associated with population differences in winter climate severity in foodcaching chickadees. *Functional Ecology*, 27(6), 1341–1349.
- García-Lázaro, H. G., Ramirez-Carmona, R., Lara-Romero, R., & Roldan-Valadez, E. (2012). Neuroanatomy of episodic and semantic memory in humans: A brief review of neuroimaging studies. *Neurology India*, 60(6), 613–617.
- Gökce, E. C., Kahveci, R., Gökce, A., Cemil, B., Aksoy, N., Sargon, M. F., Kisa, Ü., Erdoğan, B., Güvenç, Y., Alagöz, F., & Kahveci, O. (2016). Neuroprotective effects of thymoquinone against spinal cord ischemia-reperfusion injury by attenuation of inflammation, oxidative stress, and apoptosis. *Journal of Neurosurgery: Spine*, 24(6), 949–959.
- Gülşen, I., Ak, H., Çölçimen, N., Alp, H. H., Akyol, M. E., Demir, I., Atalay, T., Balahrollu, R., & Ralbetli, M. (2016). Neuroprotective effects of thymoquinone on the hippocampus

- Gupta, S. R., Palmer, C. A., Curé, J. K., Balos, L. L., Lincoff, N. S., & Kline, L. B. (2011). Toluene optic neurotoxicity: Magnetic resonance imaging and pathologic features. *Human Pathology*, 42(2), 295–298.
- Hales, J. B., Broadbent, N. J., Velu, P. D., Squire, L. R., & Clark, R. E. (2015). Hippocampus, perirhinal cortex, and complex visual discriminations in rats and humans. *Learning and Memory*, 22(2), 83–91.
- Hamdan, A. M., Al-Gayyar, M. M., Shams, M. E. E., Alshaman, U. S., Prabahar, K., Bagalagel, A., Diri, R., Noor, A. O., & Almasri, D. (2019). Thymoquinone therapy remediates elevated brain tissue inflammatory mediators induced by chronic administration of food preservatives. *Scientific Reports*, 9(1), 1–11.
- Hamdy, N. M., & Taha, R. A. (2009). Effects of nigella sativa oil and thymoquinone on oxidative stress and neuropathy in streptozotocin-induced diabetic rats. *Pharmacology*, 84(3), 127–134.
- Hamid, H. A., Hazman, M. H. M., Nadzir, M. S. M., Uning, R., Latif, M. T., & Kannan, N. (2019). Anthropogenic and biogenic volatile organic compounds and ozone formation potential in ambient air of Kuala Lumpur, Malaysia. *IOP Conference Series:* Earth and Environmental Science, 228(1), 0–8.
- Hånell, A., & Marklund, N. (2014). Structured evaluation of rodent behavioral tests used in drug discovery research. *Frontiers in Behavioral Neuroscience*, 8, 1–13.
- Hassanein, K. M. A., & El-Amir, Y. O. (2017). Protective effects of thymoquinone and avenanthramides on titanium dioxide nanoparticles induced toxicity in Sprague-Dawley rats. *Pathology Research and Practice*, 213(1), 13–22.
- Hobbenaghi, R., Javanbakht, J., Sadeghzadeh, S., Kheradmand, D., Abdi, F. S., Jaberi, M. H., Mohammadiyan, M. R., Khadivar, F., & Mollaei, Y. (2014). Neuroprotective effects of Nigella sativa extract on cell death in hippocampal neurons following experimental global cerebral ischemia-reperfusion injury in rats. *Journal of the Neurological Sciences*, 337(1–2), 74–79.
- Hopf, N. B., Kirkeleit, J., Bråtveit, M., Succop, P., Talaska, G., & Moen, B. E. (2012). Evaluation of exposure biomarkers in offshore workers exposed to low benzene and toluene concentrations. *International Archives of Occupational and Environmental*

- Hossain, M. S., Sharfaraz, A., Dutta, A., Ahsan, A., Masud, M. A., Ahmed, I. A., Goh, B. H., Urbi, Z., Sarker, M. M. R., & Ming, L. C. (2021). A review of ethnobotany, phytochemistry, antimicrobial pharmacology and toxicology of *Nigella sativa* L. *Biomedicine and Pharmacotherapy*, 143(2021), Article#112182.
- Hsieh, C. P., Chen, H., Chan, M. H., Chen, L., & Chen, H. H. (2020). N,N-dimethylglycine prevents toluene-induced impairment in recognition memory and synaptic plasticity in mice. *Toxicology*, 446(2020), Article#152613.
- Huerta-Rivas, A., López-Rubalcava, C., Sánchez-Serrano, S. L., Valdez-Tapia, M., Lamas, M., & Cruz, S. L. (2012). Toluene impairs learning and memory, has antinociceptive effects, and modifies histone acetylation in the dentate gyrus of adolescent and adult rats. *Pharmacology Biochemistry and Behavior*, 102(1), 48–57.
- Hussien, N. I., Elawady, M. A., Elmaghrabi, M. M., & Muhammad, M. H. (2020). Impact of thymoquinone on memory deficit-associated with global cerebral ischemia-reperfusion injury in rats: Possible role of PPAR-. *American Journal of Biomedical Sciences*, *September 2019*, 77–90.
- Imam, M., Adamu, A., Muhammad, U., & Yusha'u, Y. (2017). *Nigella sativa* (black seed) extract improves spatial learning frequency of platform crossing. *Bayero Journal of Pure and Applied Sciences*, 10(2), 111–114.
- Ince, S., Kucukkurt, I., Demirel, H. H., Turkmen, R., Zemheri, F., & Akbel, E. (2013). The role of thymoquinone as antioxidant protection on oxidative stress induced by imidacloprid in male and female Swiss albino mice. *Toxicological and Environmental Chemistry*, 95(2), 318–329.
- Ismail, N., Ismail, M., Azmi, N. H., Abu Bakar, M. F., Basri, H., & Abdullah, M. A. (2016). Modulation of hydrogen peroxide-induced oxidative stress in human neuronal cells by thymoquinone-rich fraction and thymoquinone via transcriptomic regulation of antioxidant and apoptotic signaling genes. *Oxidative Medicine and Cellular Longevity*, 2016, Article#2528935.
- Ismail, N., Ismail, M., Mazlan, M., Latiff, L. A., Imam, M. U., Iqbal, S., Azmi, N. H., Ghafar, S. A. A., & Chan, K. W. (2013). Thymoquinone prevents β-amyloid neurotoxicity in primary cultured cerebellar granule neurons. *Cellular and Molecular Neurobiology*, 33(8), 1159–1169.

- Jackson, S. J., Andrews, N., Ball, D., Bellantuono, I., Gray, J., Hachoumi, L., Holmes, A., Latcham, J., Petrie, A., Potter, P., Rice, A., Ritchie, A., Stewart, M., Strepka, C., Yeoman, M., & Chapman, K. (2017). Does age matter? The impact of rodent age on study outcomes. *Laboratory Animals*, *51*(2), 160–169.
- Jeneson, A., Kirwan, C. B., Hopkins, R. O., Wixted, J. T., & Squire, L. R. (2010). Recognition memory and the hippocampus: A test of the hippocampal contribution to recollection and familiarity. *Learning & Memory (Cold Spring Harbor, N.Y.)*, 17(1), 63–70.
- Jianguang, C., & Dazhong, Y. (2011). Malondialdehyde decreased the capability of learning and spatial memory, impaired the ultra-microstructure of the hippocampal CA1 area in SD rats. *Proceedings 2011 International Conference on Human Health and Biomedical Engineering, HHBE 2011*, 371–377.
- Kalueff, A. V., Keisala, T., Minasyan, A., Kuuslahti, M., & Tuohimaa, P. (2006). Temporal stability of novelty exploration in mice exposed to different open field tests. *Behavioural Processes*, 72(1), 104–112.
- Kantachai, P., Kaewkaen, P., & Janthakhin, Y. (2020). The analysis of toluene concentrations affecting learning and long-term memory of mice and workers who long-term exposed to low-level of toluene. *Research Methodology and Cognitive Science*, 17(2), 69-82.
- Kanter, M. (2008a). *Nigella sativa* and derived thymoquinone prevents hippocampal neurodegeneration after chronic toluene exposure in rats. *Neurochemical Research*, 33(3), 579–588.
- Kanter, M. (2008b). Protective effects of *Nigella sativa* on the neuronal injury in frontal cortex and brain stem after chronic toluene exposure. *Neurochemical Research*, 33(11), 2241–2249.
- Kao, H. W., Pare, L., Kim, R., & Hasso, A. N. (2014). Toxic leukoencephalopathy with atypical MRI features following a lacquer thinner fire. *Journal of Clinical Neuroscience*, 21(5), 878–880.
- Kassab, R. B., & El-Hennamy, R. E. (2017). The role of thymoquinone as a potent antioxidant in ameliorating the neurotoxic effect of sodium arsenate in female rat. *Egyptian Journal of Basic and Applied Sciences*, 4(3), 160–167.
- Kern, J. K., Geier, D. A., Homme, K. G., King, P. G., Bjørklund, G., Chirumbolo, S., &

- Geier, M. R. (2017). Developmental neurotoxicants and the vulnerable male brain: A systematic review of suspected neurotoxicants that disproportionally affect males. *Acta Neurobiologiae Experimentalis*, 77(4), 269–296.
- Khalife, K. H., & Lupidi, G. (2007). Nonenzymatic reduction of thymoquinone in physiological conditions. *Free Radical Research*, 41(2), 153–161.
- Khan, M. S., Gohar, A., Abbas, G., Mahmood, W., Rauf, K., & Sewell, R. D. E. (2015). Thymoquinone inhibition of acquisition and expression of alcohol-induced behavioral sensitization. *Phytotherapy Research*, 29(10), 1610–1615.
- Khazdair, M. R., Anaeigoudari, A., Hashemzehi, M., & Mohebbati, R. (2019). Neuroprotective potency of some spice herbs, a literature review. *Journal of Traditional and Complementary Medicine*, 9(2), 98–105.
- Kim, J. M., Kim, D. H., Lee, Y., Park, S. J., & Ryu, J. H. (2014). Distinct roles of the hippocampus and perirhinal cortex in GABAA receptor blockade-induced enhancement of object recognition memory. *Brain Research*, 1552, 17–25.
- Kinnavane, L., Albasser, M. M., & Aggleton, J. P. (2015). Advances in the behavioural testing and network imaging of rodent recognition memory. *Behavioural Brain Research*, 285, 67–78.
- Kodavanti, P. R. S., Royland, J. E., Moore-Smith, D. A., Besas, J., Richards, J. E., Beasley, T. E., Evansky, P., & Bushnell, P. J. (2015). Acute and subchronic toxicity of inhaled toluene in male Long-Evans rats: Oxidative stress markers in brain. *NeuroToxicology*, 51, 10–19.
- Kodavanti, P. R. S., Royland, J. E., Richards, J. E., Besas, J., & MacPhail, R. C. (2011). Toluene effects on oxidative stress in brain regions of young-adult, middle-age, and senescent Brown Norway rats. *Toxicology and Applied Pharmacology*, 256(3), 386–398.
- Laio, T. Y., Chen, C. C., Tsou, H. H., Liu, T. Y., & Wang, H. T. (2019). Acute and chronic exposure of toluene induces genotoxicity in different regions of the brain in normal and allergic mouse models. *Neurotoxicity Research*, 36(4), 669–678.
- Latif, M. T., Abd Hamid, H. H., Ahamad, F., Khan, M. F., Mohd Nadzir, M. S., Othman, M., Sahani, M., Abdul Wahab, M. I., Mohamad, N., Uning, R., Poh, S. C., Fadzil, M. F., Sentian, J., & Tahir, N. M. (2019). BTEX compositions and its potential health impacts

- Lee, M. Y., Lin, B. F., Chan, M. H., & Chen, H. H. (2020). Increased behavioral and neuronal responses to a hallucinogenic drug after adolescent toluene exposure in mice: Effects of antipsychotic treatment. *Toxicology*, 445(64), Article#152602.
- Leger, M., Quiedeville, A., Bouet, V., Haelewyn, B., Boulouard, M., Schumann-Bard, P., & Freret, T. (2013). Object recognition test in mice. *Nature Protocols*, 8(12), 2531–2537.
- Levcik, D., Nekovarova, T., Antosova, E., Stuchlik, A., & Klement, D. (2018). The role of the hippocampus in object discrimination based on visual features. *Neurobiology of Learning and Memory*, 155, 127–135.
- Lin, B. F., Ou, M. C., Chung, S. S., Pang, C. Y., & Chen, H. H. (2010). Adolescent toluene exposure produces enduring social and cognitive deficits in mice: An animal model of solvent-induced psychosis. *World Journal of Biological Psychiatry*, 11(6), 792–802.
- Liu, Jiachen, Guo, Y., Zhang, C., Zeng, Y., Luo, Y., & Wang, G. (2022). Clearance systems in the brain: From structure to function. *Frontiers in Cellular Neuroscience*, 15, 1-12.
- Liu, Jinping, Chang, L., Song, Y., Li, H., & Wu, Y. (2019). The role of NMDA receptors in Alzheimer's disease. *Frontiers in Neuroscience*, 13, 1–22.
- Lobo, V., Patil, A., Phatak, A., & Chandra, N. (2010). Free radicals, antioxidants and functional foods: Impact on human health. *Pharmacognosy Reviews*, 4(8), 118–126.
- Lotfi, M., & Satarian, L. (2021). Thymoquinone improved nonylphenol-induced memory deficit and neurotoxicity through its antioxidant and neuroprotective effects. *Research Square*, 1–25.
- Lu, C., Dong, L., Lv, J., Wang, Y., Fan, B., Wang, F., & Liu, X. (2018). 20(S)-protopanaxadiol (PPD) alleviates scopolamine-induced memory impairment via regulation of cholinergic and antioxidant systems, and expression of Egr-1, c-Fos and c-Jun in mice. *Chemico-Biological Interactions*, 279, 64–72.
- Luengo-Sanchez, S., Bielza, C., Benavides-Piccione, R., Fernaud-Espinosa, I., Defelipe, J., & Larrañaga, P. (2015). A univocal definition of the neuronal soma morphology using gaussian mixture models. *Frontiers in Neuroanatomy*, *9*, 1–11.

- Lueptow, L. M. (2017a). Novel object recognition test for the investigation of learning and memory in mice. *Journal of Visualized Experiments*, 2017(126), 1–9.
- Magee, J. C., & Cook, E. P. (2000). Somatic EPSP amplitude is independent of synapse location in hippocampal pyramidal neurons. *Nature Neuroscience*, *3*(9), 895–903.
- Manoharan, S., Guillemin, G. J., Abiramasundari, R. S., Essa, M. M., Akbar, M., & Akbar, M. D. (2016). The role of reactive oxygen species in the pathogenesis of Alzheimer's disease, Parkinson's disease, and Huntington's disease: A mini review. *Oxidative Medicine and Cellular Longevity*, 2016, Article#8590578.
- Marchetto, M. C. N., Carromeu, C., Acab, A., Yu, D., Yeo, G. W., Mu, Y., Chen, G., Gage, F. H., & Muotri, A. R. (2010). A model for neural development and treatment of rett syndrome using human induced pluripotent stem cells. *Cell*, *143*(4), 527–539.
- Marganda, S., & Ashar, T. (2018). Occupational risk factors associated with perceived central nervous system disorder among printing industry workers in Medan. In 4th International Conference on Public Health 2018, Surakarta, Indonesia, August 2018 (p.96). Sebelas Maret University.
- Mehri, S., Shahi, M., Razavi, B. M., Hassani, F. V., & Hosseinzadeh, H. (2014). Neuroprotective effect of thymoquinone in acrylamideinduced neurotoxicity in Wistar rats. *Iranian Journal of Basic Medical Sciences*, 17(12), 1007–1011.
- Meira, T., Leroy, F., Buss, E. W., Oliva, A., Park, J., & Siegelbaum, S. A. (2018). A hippocampal circuit linking dorsal CA2 to ventral CA1 critical for social memory dynamics. *Nature Communications*, 9(1), 1–14.
- Meitzen, J., Pflepsen, K. R., Stern, C. M., Meisel, R. L., & Mermelstein, P. G. (2011). Measurements of neuron soma size and density in rat dorsal striatum, nucleus accumbens core and nucleus accumbens shell: Differences between striatal region and brain hemisphere, but not sex. *Neuroscience Letters*, 487(2), 177–181.
- Mesa-Gresa, P., Pérez-Martinez, A., & Redolat, R. (2013). Environmental enrichment improves novel object recognition and enhances agonistic behavior in male mice. *Aggressive Behavior*, 39(4), 269–279.
- Meydan, S., Altas, M., Nacar, A., Ozturk, O. H., Tas, U., Zararsiz, I., & Sarsilmaz, M. (2012). The protective effects of omega-3 fatty acid against toluene-induced neurotoxicity in prefrontal cortex of rats. *Human and Experimental Toxicology*, 31(11), 1179–1185.

- Moawad, R. S., Abd El Fattah, E. R., & Alsemeh, A. (2021). Deleterious effect of toluene on rat cerebrum cortex and the exert effect of resveratrol: Histological, immunohistochemical and ultrastructural study. The *Egyptian Journal of Histology*, 44(3), 855-872.
- Mohamadin, A. M., Sheikh, B., Abd El-Aal, A. A., Elberry, A. A., & Al-Abbasi, F. A. (2010). Protective effects of *Nigella sativa* oil on propoxur-induced toxicity and oxidative stress in rat brain regions. *Pesticide Biochemistry and Physiology*, 98(1), 128–134.
- Montes, S., Solís-Guillén, R. del C., García-Jácome, D., & Páez-Martínez, N. (2017). Environmental enrichment reverses memory impairment induced by toluene in mice. *Neurotoxicology and Teratology*, 61, 7-16.
- Morillas, E., Gómez-Chacón, B., & Gallo, M. (2017). Flavor and object recognition memory impairment induced by excitotoxic lesions of the perirhinal cortex. *Neurobiology of Learning and Memory*, 144, 230–234.
- Moro, A. M., Brucker, N., Charão, M., Bulcão, R., Freitas, F., Baierle, M., Nascimento, S., Valentini, J., Cassini, C., Salvador, M., Linden, R., Thiesen, F., Buffon, A., Moresco, R., & Garcia, S. C. (2012). Evaluation of genotoxicity and oxidative damage in painters exposed to low levels of toluene. *Mutation Research Genetic Toxicology and Environmental Mutagenesis*, 746(1), 42–48.
- Mugwagwa, A. T., Gadaga, L. L., Pote, W., & Tagwireyi, D. (2015). Antiamnesif effects of a hydroethanolic extract of Crinum macowanii on scopolamine-induced memory impairment in mice. *Journal of Neurodegenerative Diseases*, 2015, 1-9.
- Murase, S., Poser, S. W., Joseph, J., & Mckay, R. D. (2011). p53 controls neuronal death in the CA3 region of the newborn mouse hippocampus. *European Journal of Neuroscience*, 34(3), 374–381.
- Nitulescu, G. M., Van De Venter, M., Nitulescu, G., Ungurianu, A., Juzenas, P., Peng, Q., Olaru, O. T., Grădinaru, D., Tsatsakis, A., Tsoukalas, D., Spandidos, D. A., & Margina, D. (2018). The Akt pathway in oncology therapy and beyond (Review). *International Journal of Oncology*, 53(6), 2319–2331.
- Páez-Martínez, N., Pellicer, F., González-Trujano, M. E., & Cruz-López, B. (2020). Environmental enrichment reduces behavioural sensitization in mice previously exposed to toluene: The role of D1 receptors. *Behavioural Brain Research*, 390, Article#112624.

- Paramo, B., Bachmann, S. O., Davies, A. M., Baudouin, S. J., & Martinez-Garay, I. (2021). Neuregulin-4 is required for maintaining soma size of pyramidal neurons in the motor cortex. *ENeuro*, 8(1), 1–12.
- Pascual, R., Aedo, L., Meneses, J. C., Vergara, D., Reyes, Á., & Bustamante, C. (2010). Solvent inhalation (toluene and n-hexane) during the brain growth spurt impairs the maturation of frontal, parietal and occipital cerebrocortical neurons in rats. *International Journal of Developmental Neuroscience*, 28(6), 491–495.
- Peinado, M. A., Quesada, A., Pedrosa, J. A., Martinez, M., Esteban, F. J., Del Moral, M. L., & Peinado, J. M. (1997). Light microscopic quantification of morphological changes during aging in neurons and glia of the rat parietal cortex. *Anatomical Record*, 247(3), 420–425.
- Presta, I., Vismara, M., Novellino, F., Donato, A., Zaffino, P., Scali, E., Pirrone, K. C., Spadea, M. F., Malara, N., & Donato, G. (2018). Innate immunity cells and the neurovascular unit. *International Journal of Molecular Sciences*, 19(12), 1–26.
- R. Kannan, S. P. I. and J. H. (2019). Acetylcholinesterase and growth inhibitory effects various grades of *N. sativa* oils. *International Journal of Pharmaceutical Sciences and Research*, 10(1), 245–250.
- Radad, K., Hassanein, K., Al-Shraim, M., Moldzio, R., & Rausch, W. D. (2014). Thymoquinone ameliorates lead-induced brain damage in Sprague Dawley rats. *Experimental and Toxicologic Pathology*, 66(1), 13–17.
- Rahim Yacob, A., Zainalibdin, M. R., & Said, N. (2012). Detection of vapour metabolites of glue sniffer's urine using head space gas chromatography mass spectrometry. *Journal of Drug Metabolism & Toxicology*, 02(03), 3–6.
- Rangasamy, S., Olfers, S., Gerald, B., Hilbert, A., Svejda, S., & Narayanan, V. (2016). Reduced neuronal size and mTOR pathway activity in the Mecp2 A140V Rett syndrome mouse model. *F1000Research*, 5(0), 1–13.
- Raslau, F. D., Klein, A. P., Ulmer, J. L., Mathews, V., & Mark, L. P. (2014). Memory part 1: Overview. *American Journal of Neuroradiology*, *35*(11), 2058–2060.
- Raslau, F. D., Mark, I. T., Klein, A. P., Ulmer, J. L., Mathews, V., & Mark, L. P. (2015). Memory part 2: The role of the medial temporal lobe. *American Journal of Neuroradiology*, 36(5), 846–849.

- Reger, M. L., Hovda, D. A., & Giza, C. C. (2009). Ontogeny of rat recognition memory measured by the novel object recognition task. *Developmental Psychobiology*, 51(8), 672–678.
- Sahak, M. K. A., Kabir, N., Abbas, G., Draman, S., Hashim, N. H., & Hasan Adli, D. S. (2016). The role of *Nigella sativa* and its active constituents in learning and memory. *Evidence-Based Complementary and Alternative Medicine*, 2016, Article#6075679.
- Sahak, M. K. A., Mohamed, A. M., Hashim, N. H., & Hasan Adli, D. S. (2013). *Nigella sativa* oil enhances the spatial working memory performance of rats on a Radial Arm Maze. *Evidence-Based Compkementary and Alternative Medisine*, 2013, Article#180598.
- Sahindokuyucu-Kocasarı, F., Erdemli-Kose, S. B., Erol, Z., & Garlı, S. (2021). The protective effect of p-coumaric acid on toluene-induced hepatotoxicity, nephrotoxicity and neurotoxicity in rats. *Revista Colombiana de Ciencia Animal RECIA*, 13(1), Article#e843.
- Saleh, H. A., Abd El-Aziz, G. S., Mustafa, H. N., El-Fark, M., Mal, A., Aburas, M., & Deifalla, A. H. (2019). Thymoquinone ameliorates oxidative damage and histopathological changes of developing brain neurotoxicity. *Journal of Histotechnology*, 42(3), 116–127.
- Salem, R. R., & Kelada, M. N. B. (2020). A biochemichal and ultrastructural study on the effect of toluene on the pars distalis of anterior pituitary glands of adult male albino rats. *Egyptian Journal of Histology*, 43(3), 948–959.
- Sarkhosh, M., Hossein, A., Reza, M., & Fakhri, Y. (2012). Indoor contaminants from hardcopy devices: Characteristics of VOCs in photocopy centers. *Atmospheric Environment*, 63, 307–312.
- Sathe, S., Chan, X., Jin, J., Bernitt, E., Döbereiner, H.-G., & Yim, E. (2017). Correlation and comparison of cortical and hippocampal neural progenitor morphology and differentiation through the use of micro- and nano-topographies. *Journal of Functional Biomaterials*, 8(35), 1-19.
- Schreiber, J. A., Schepmann, D., Frehland, B., Thum, S., Datunashvili, M., Budde, T., Hollmann, M., Strutz-Seebohm, N., Wünsch, B., & Seebohm, G. (2019). A common mechanism allows selective targeting of GluN2B subunit-containing N-methyl-D-aspartate receptors. *Communications Biology*, 2(1), 1-14.

- Sedaghat, R., Roghani, M., & Khalili, M. (2014). Neuroprotective effect of thymoquinone, the *Nigella sativa* bioactive compound, in 6-hydroxydopamine-induced hemiparkinsonian rat model. *Iranian Journal of Pharmaceutical Research*, 13(1), 227–234.
- Seo, H. S., Yang, M., Song, M. S., Kim, J. S., Kim, S. H., Kim, J. C., Kim, H., Shin, T., Wang, H., & Moon, C. (2010). Toluene inhibits hippocampal neurogenesis in adult mice. *Pharmacology Biochemistry and Behavior*, 94(4), 588–594.
- Seo, S., & Kim, J. (2018). An aggravated return-to-work case of organic solvent induced chronic toxic encephalopathy. *Annals of Occupational and Environmental Medicine*, 30(1), 1–6.
- Shaffie, N., & Shabana, M. E. (2019). Role of citicoline as a protective agent on toluene-induced toxicity in rats. *Journal of The Arab Society for Medical Research*, 14(1), 14–24.
- Shahroudi, M. J., Mehri, S., & Hosseinzadeh, H. (2017). Anti-aging effect of *Nigella sativa* fixed oil on d-galactose-induced aging in mice. *Journal of Pharmacopuncture*, 20(1), 29–35.
- Soares, M. V., Charão, M. F., Jacques, M. T., dos Santos, A. L. A., Luchese, C., Pinton, S., & Ávila, D. S. (2020). Airborne toluene exposure causes germline apoptosis and neuronal damage that promotes neurobehavioural changes in *Caenorhabditis elegans*. *Environmental Pollution*, 256, Article#113406.
- Tabeshpour, J., Mehri, S., Abnous, K., & Hosseinzadeh, H. (2019). Neuroprotective effects of thymoquinone in acrylamide-induced peripheral nervous system toxicity through MAPKinase and apoptosis pathways in rat. *Neurochemical Research*, 44(5), 1101–1112.
- Tahmasebi, S., Oryan, S., Mohajerani, H. R., Akbari, N., & Palizvan, M. R. (2020). Probiotics and *Nigella sativa* extract supplementation improved behavioral and electrophysiological effects of PTZ-induced chemical kindling in rats. *Epilepsy and Behavior*, 104, Article#106897.
- Takehara-Nishiuchi, K. (2021). Neurobiology of systems memory consolidation. *European Journal of Neuroscience*, 54(8), 6850–6863.
- Tanimizu, T., Kenney, J. W., Okano, E., Kadoma, K., Frankland, P. W., & Kida, S. (2017). Functional connectivity of multiple brain regions required for the consolidation of social

- Tanimizu, T., Kono, K., & Kida, S. (2018). Brain networks activated to form object recognition memory. *Brain Research Bulletin*, 141, 27–34.
- Taqui, R., Debnath, M., Ahmed, S., & Ghosh, A. (2022). Advances on plant extracts and phytocompounds with acetylcholinesterase inhibition activity for possible treatment of Alzheimer's disease. *Phytomedicine Plus*, 2(1), Article#100184.
- Thetkathuek, A., Jaidee, W., Saowakhontha, S., & Ekburanawat, W. (2015). Neuropsychological symptoms among workers exposed to toluene and xylene in two paint manufacturing factories in Eastern Thailand. *Advances in Preventive Medicine*, 2015, 1–10.
- Toktam, M., Mahmood, H., Reza, K., Mohammad, S., & Ziba, R. (2011). The acetylcholine esterase activity inhibition as a possible mechanism for beneficial effects of *Nigella sativa* on memory. *Clinical Biochemistry*, 44(13), Article#S349.
- Tong, L., Langton, R., Glykys, J., & Baek, S. (2021). ANMAF: an automated neuronal morphology analysis framework using convolutional neural networks. *Scientific Reports*, 11(1), 1–12.
- Tsiola, A., Hamzei-Sichani, F., Peterlin, Z., & Yuste, R. (2003). Quantitative morphologic classification of layer 5 neurons from mouse primary visual cortex. *Journal of Comparative Neurology*, 461(4), 415–428.
- Tualeka, A. R., Wibrata, D. A., Ilmi, B., Ahsan, A., & Rahmawati, P. (2019). Association between toluene inhalation exposure and demography towards risk of neurotoxic: A cross-sectional study at plastic sack industry workers in Indonesia. *Global Journal of Health Science*, 11(2), 20-27.
- Ullah, I., Ullah, N., Naseer, M. I., Lee, H. Y., & Kim, M. O. K. (2012). Neuroprotection with metformin and thymoquinone against ethanol-induced apoptotic neurodegeneration in prenatal rat cortical neurons. *BMC Neuroscience*, 13, 1-11.
- Umukoro, S., Apara, M., Ben-Azu, B., Ajayi, A. M., & Aderibigbe, A. O. (2021). Neurobehavioral effects of prolonged exposure to solid air freshener in mice. *Iranian Journal of Toxicology*, 13(3), 45–51.

- Üstün, R., Oğuz, E. K., Şeker, A., & Korkaya, H. (2018). Thymoquinone prevents cisplatin neurotoxicity in primary DRG neurons. *NeuroToxicology*, 69, 68–76.
- Vafaee, F., Hosseini, M., Hassanzadeh, Z., Edalatmanesh, M. A., Sadeghnia, H. R., Seghatoleslam, M., Mousavi, S. M., Amani, A., & Shafei, M. N. (2015). The effects of *Nigella sativa* hydro-alcoholic extract on memory and brain tissues oxidative damage after repeated seizures in rats. *Iranian Journal of Pharmaceutical Research*, 14(2), 547–557.
- Vago, D. R., Wallenstein, G. V., & Morris, L. S. (2014). Hippocampus. *Encyclopedia of the Neurological Sciences*, 2, 566–570.
- Van Hooste, W. L. C. (2017). Myoclonic seizure prior to diagnosis of chronic toxic encephalopathy: A case report. *Journal of Medical Case Reports*, 11(1), 1-4.
- Vogel-Ciernia, A., & Wood, M. A. (2014). Examining object location and object recognition in mice. *Current Protocols in Neuroscience*, 69(1), 8-31.
- Von Euler, M., Pham, T. M., Hillefors, M., Bjelke, B., Henriksson, B., & Von Euler, G. (2000). Inhalation of low concentrations of toluene induces persistent effects on a learning retention task, beam-walk performance, and cerebrocortical size in the rat. *Experimental Neurology*, 163(1), 1–8.
- Wang, A. (2017). Air Toxics Hot Spots Program Toluene Reference Exposure Levels. December. Retrieved on 20 August 2018 from https://oehha.ca.gov/media/downloads/crnr/publicreviewdrafttoluene120117.pdf.
- Wang, F., Fangfang, Z., Guo, X., Chen, W., Yao, W., Liu, H., Lyu, C., Zhang, Y., & Fan, C. (2018). Effects of volatile organic compounds and carbon monoxide mixtures on learning and memory, oxidative stress, and monoamine neurotransmitters in the brains of mice. *Toxicology and Industrial Health*, 34(3), 178–187.
- Wang, F., Li, C., Liu, W., & Jin, Y. (2014). Potential mechanisms of neurobehavioral disturbances in mice caused by sub-chronic exposure to low-dose VOCs. *Inhalation Toxicology*, 26(4), 250–258.
- Werder, E. J., Engel, L. S., Blair, A., Kwok, R. K., McGrath, J. A., & Sandler, D. P. (2019). Blood BTEX levels and neurologic symptoms in Gulf states residents. *Environmental Research*, 175, 100–107.

- Wible, C. G. (2013). Hippocampal physiology, structure and function and the neuroscience of schizophrenia: A unified account of declarative memory deficits, working memory deficits and schizophrenic symptoms. *Behavioral Sciences*, 3(2), 298–315.
- Win-Shwe, T. T., Kunugita, N., Yoshida, Y., Nakajima, D., Tsukahara, S., & Fujimaki, H. (2012). Differential mRNA expression of neuroimmune markers in the hippocampus of infant mice following toluene exposure during brain developmental period. *Journal of Applied Toxicology*, 32(2), 126–134.
- Win-Shwe, T. T. & Fujimaki, H. (2012). Acute administration of toluene affects memory retention in novel object recognition test and memory function related gene expression in mice. *Journal of Applied Toxicology*, 32(4), 300–304.
- Win-Shwe, Tin Tin, Fujimaki, H., Arashidani, K., & Kunugita, N. (2013). Indoor volatile organic compounds and chemical sensitivity reactions. *Clinical and Developmental Immunology*, 2013, Article#623812.
- World Health Organization. (2021). WHO global air quality guidelines. *Coastal And Estuarine Processes*, 1–360.
- Wu, C. Y., Tsai, Y. L., Hsieh, C. P., Wang, T. C., Chan, M. H., & Chen, H. H. (2018). Attenuation of toluene-induced brain stimulation reward enhancement and behavioral disturbances by N-acetylcysteine in mice. *Toxicology*, 408(June), 39–45.
- Yamasaki. (2014). 基因的改变NIH Public Access. Bone, 23(1), 1-7.
- Yasar, S., Yildirim, E., Koklu, M., Gursoy, E., Celik, M., & Yuksel, U. C. (2016). A case of reversible cardiomyopathy associated with acute toluene exposure. *Turkish Journal of Emergency Medicine*, 16(3), 123–125.
- Yavari, F., van Thriel, C., Nitsche, M. A., & Kuo, M. F. (2018). Effect of acute exposure to toluene on cortical excitability, neuroplasticity, and motor learning in healthy humans. *Archives of Toxicology*, 92(10), 3149–3162.
- Yi, G. S., Wang, J., Deng, B., & Wei, X. Le. (2017). Morphology controls how hippocampal CA1 pyramidal neuron responds to uniform electric fields: A biophysical modeling study. *Scientific Reports*, 7(1), 1–13.

- Yoon, J. H., Seo, H. S., Lee, J., Moon, C., & Lee, K. (2016). Acute high-level toluene exposure decreases hippocampal neurogenesis in rats. *Toxicology and Industrial Health*, 32(11), 1910–1920.
- You, R., Liu, Y., & Chang, R. C. C. (2019). A behavioral test battery for the repeated assessment of motor skills, mood, and cognition in mice. *Journal of Visualized Experiments*, 2019(145), 1–10.
- Younus, H. (Ed.). (2018). *Molecular and Therapeutic actions of Thymoquinone: Actions of Thymoquinone*. Berlin, Germany: Springer.
- Zorova, L. D., Popkov, V. A., Plotnikov, E. Y., Silachev, D. N., Irina, B., Jankauskas, S. S.,
 Babenko, V. A., Zorov, S. D., Balakireva, V., Juhaszova, M., Sollott, S. J., Zorov, D.
 B., Federation, R., Federation, R., Federation, R., & Federation, R. (2018).
 Mitochondrial membrane potential. *Analytical Biochemistry*, 552, 50-59.